

PREFACE

This master's thesis will complete my education to become a civil engineer in mechanical engineering. This has been a personal goal for the last ten years, and I am proud of myself for completing this goal.

When I chose to write my master's thesis with robotics as the subject, I was pretty nervous. I have only had one subject regarding robotics, and I knew I thought robotics was hard. Last spring, I was a part of the team who made covers for Thorvald, the first robot. I knew a bit about the project, and thought it was really interesting. I've also gotten to know Lars, who I knew really cared for this robot. I was very relieved when I found out that the focus of my thesis would be on design, and practical solutions.

We were a team of four young men writing our theses on the agricultural robot, and in March we went on a trip to Brazil. Here we got to see how big the potential of agricultural robotics is. UMOE is a "Norwegian" farm next to Sao Paulo where they grow sugar canes. With 400 000 square meters of land, autonomous robots could really make a difference. The first thanks will therefore go to Knut, the owner of UMOE, and who showed us how farming is done in such a big scale.

I would like to thank Electro Drives AS and Allweier Präzisionsteile GmbH for good service, and discounted prices. I would like to thank Endre Grøtvik, Rune Stensrud and Øyvind Hansen at Ås VGS for production and experience, and Bjørn Tenge for production and validation of the design. I would also like to thank my fellow master students: Øystein Tårnes Sund, Espen Noren Ovik and Alexander Ghebrehiwot, we have been a good team.

The last persons I would like to thank is my supervisor Prof. Pål Johan From, and his PhD. candidate Lars Grimstad. This thesis could not have been done without proper guidance from you.

Ås

12/5-2016

Marius Austad

ABSTRACT

The main purpose of this thesis is to make the NMBU agricultural robot very modular, and determine new components for the drivetrain and steering. The new robot will be available in four different versions. The most powerful version will have 4WD and 4WS. Two versions will have 2WD. The difference between them is that one will only have propulsion motors and use skid steering, while the other one will have Ackerman steering on the wheels with propulsion. The last version is a three-wheel robot, with steering and propulsion on one wheel. This will be very narrow, and is practical for simple tasks.

Three modules are designed: with propulsion and steering, only propulsion, and a passive module with caster wheels. The casters have not been delivered, so the design of this module is not completed when this thesis is sent to printing.

The principle design of the first robot is used as foundation, and the module with both propulsion and steering is considered the main module. The other modules are based on the design of the main module. The power requirements are calculated after worst case scenario that can be expected. The new propulsion motor is a BLDC with a power of 500 W. Even though it is weaker than the previously used motor, the calculations confirms that it is strong enough for the robot to work in the worst expected conditions. The planetary gearbox is very tough, and can be immersed in 1 m of water due to its IP67 certification. The whole module is designed to be waterproof, and glue is used between parts to prevent water from leaching in to the modules.

The propulsion motor used for steering is the same type as the propulsion motor, only weaker. The motor is flipped upside-down, and a belt transmission is inserted to make the tower lower. As for the steering gearbox, it has been reduced to a one stage planetary gear due to the reduction ratio in the belt drive. The tower construction is very compact.

Light weight is highly prioritized, and aluminum is used as the main material. Components that must be very durable are made in steel. The modules will mainly be assembled by riveting. This technique provides a stable and durable construction.

The design looks very promising, and the finished product will be tested to verify that the modules are ready for the market.

SAMMENDRAG

Hovedmålet med denne oppgaven er å gjøre NMBUs landbruksrobot veldig modulær, og bestemme nye komponenter for drivverk og styring. Den nye roboten vil være tilgjengelig i fire forskjellige versjoner. Den kraftigste versjonen vil ha 4WD og 4WS. To versjoner vil ha 2WD. Forskjellen mellom dem er at den ene bare vil ha fremdriftsmotorer og bruke skidstyring, mens den andre vil ha Ackermanstyring på hjulene med fremdrift. Den siste versjonen er en trehjulsrobot, med styring og fremdrift på ett hjul. Denne vil være meget smal, og er praktisk for enkle oppgaver.

Tre moduler er designet: med framdrift og styring, bare fremdrift, og en passiv modul med handlevognhjul. Handlevognhjulene har ikke blitt levert, slik at designen av denne modulen ikke er helt ferdig når denne oppgaven er sendt til trykking.

Oppsettet på den første robot benyttes som fundament, og modulen med både fremdrift og styring er ansett som hovedmodulen. De andre modulene er basert på utformingen av denne. Motorkravene er beregnet etter verste tenkelige forhold som kan forventes. Den nye fremdriftsmotor er en BLDC med en effekt på 500 W. Selv om det er svakere enn den tidligere brukte motoren, bekrefter beregningene at den er sterk nok til at roboten klarer jobbe i de verste bruksforholdene. Planetgirkassen er veldig tøff, og kan senkes ned i én meter med vann på grunn av sin IP67-sertifisering. Hele modulen er designet for å være vanntett, og lim benyttes mellom delene for å hindre vann fra å piple inn i modulene.

Motoren som brukes til styringen er av samme type som fremdriftsmotoren, bare svakere. Motoren er snudd opp-ned, og en belteoverføring er satt inn for å gjøre tårnet mer kompakt. Styringsgirkassen er det blitt redusert til ett trinns planetgir på grunn av reduksjonsforholdet i fremdriften. Tårnkonstruksjonen er svært kompakt.

Lav vekt er høyt prioritert, og aluminium er brukt som hovedmateriale. Komponenter som må være ekstra slitesterke er laget i stål. Modulene vil hovedsakelig bli satt sammen med nagler. Denne teknikken gir en stabil og varig konstruksjon.

Designen ser veldig lovende ut, og det ferdige produktet vil bli testet for å bekrefte at modulene er klare for markedet.

ABBREVIATIONS

4WD	Four-wheel drive	2WD	Two-wheel drive
4WS	Four-wheel steering	2WS	Two-wheel steering
NMBU	Norwegian University of Life Sciences	TRL	Technology Readiness Level
DC	Direct current	BDC	Brushed DC motor
BLDC	Brushless DC motor	N	North
S	South	FCC	Front Centered Cubic
BCC	Cody Centered Cubic	HCP	Hexagonal-Closed Pack
PCB	Printed Circuit Board	PID	Proportional Integral Derivative
LED	Light Emitting Diode	GND	Ground
CNC	Computer Numeric Control		

LIST OF FIGURES

Figure 1-1: Thorvald, the agricultural robot. Image: Håkon Sverdvik	2
Figure 1-2: The wheel modules for Thorvald II.....	9
Figure 2-1: Ideal performance characteristics for vehicular power plants. Image: Wong	11
Figure 2-2: Performance characteristics of piston engines. Image: Wong.....	12
Figure 2-3: An illustration of a DC motor. Image: HyperPhysics [15].....	13
Figure 2-4: Brushed DC motor. Image: ON Semiconductor.....	14
Figure 2-5: Cross section of a three-phase BLDC motor Image: Microchip [19]	15
Figure 2-6: Torque - speed characteristics of a BLDC motor. Image: Microchip [19]	16
Figure 2-7: Spur gear. Image: Gibbs Gears.....	17
Figure 2-8: Helical gear. Image: Hewitt & Topham	17
Figure 2-9: Herringbone gear. Image: Hewitt & Topham	18
Figure 2-10: Planetary gears. Image: Rohloff	18
Figure 2-11: Frictional belts. Image: Eurasia PH.....	19
Figure 2-12: Timing belts. Image: SDP/SI.....	19
Figure 2-13: Chain wrapped around wheel. Image: Eurasia PH.....	20
Figure 2-14: Stress-strain diagram	21
Figure 2-15: Most common structures of metal	23
Figure 2-16: Rivet before and after driving.....	25
Figure 2-17: Exploded view of an incremental encoder. Image: Sandin	28
Figure 2-18: The layers of a PCB.....	29
Figure 2-19: Terminal block. Image: Phoenix Contacts	29
Figure 3-1: Gradient resistance	31
Figure 3-2: Projection of the front of the robot.....	34
Figure 3-3: Ackerman steering. Image: Wittren 1975 [42].....	35
Figure 3-4: Typical curves based on rubber-tired vehicles on dry concrete. Image: Wittren 1975 [42]	37
Figure 4-1: Example motor and drivetrain combination	40
Figure 4-2: 3Men BL840.....	41
Figure 4-3: Allweier PGR500	42
Figure 4-4: Timing belt. Image: Electro Drives	43

Figure 4-5: Wheel with H-279 tire print	44
Figure 4-6: Simple drawing of the powertrain	45
Figure 4-7: 3Men BL830.....	46
Figure 4-8: Apex Dynamics AB060.....	47
Figure 4-9: Autonics PR12-2DP	49
Figure 4-10: Roboteq FBL2360. Image: Roboteq	50
Figure 4-11: Autonics E-40 hollow-shaft.....	51
Figure 5-1: Circuit diagram of the PCB	55
Figure 5-2: Picture of the PCB	55
Figure 6-1:Exploded view of the propulsion foot	56
Figure 6-2: Adjustments of shaft and motor	57
Figure 6-3: The propulsion module.....	58
Figure 6-4: Exploded views	59
Figure 43: Cross-section of the bearing house	60
Figure 6-6: Modifications done for the propulsion module	61
Figure 6-7: Design plan of the caster module	61
Figure 6-8: ANSYS analysis for situation 1	62
Figure 6-9: ANSYS analysis for situation 2.....	63
Figure 6-10: ANSYS analysis for situation 3.....	64
Figure 7-1: Bending machine	66
Figure 7-2: Plasma-cutter	67
Figure 7-3: Side brack, foot covers and the bent brack.....	67
Figure 7-4: U-beams.....	68
Figure 7-5: Support beam.....	68
Figure 7-6: Compositions to verify the dimensions	69

LIST OF TABLES

Table 1-1: Motor specifications of Thorvald [3].....	3
Table 1-2: Gear specifications of Thorvald [3].....	3
Table 1-3: Comparison of agricultural robots	5
Table 1-4: TRL-scale modified to fit Horizon 2020 [8].....	7
Table 2-1: Compositions and mechanical properties for some common aluminum alloys	24
Table 3-1: Summary of the resistance forces	34
Table 3-2: Parameters that influence the steering power requirements	36
Table 4-1: Evaluation of different gears.....	39
Table 4-2: Evaluation of belts and chain.....	39
Table 4-3: Specifications of 3Men BL840	41
Table 4-4: Specifications of the Allweier PGR 500 gearbox.....	42
Table 4-5: Specifications of timing pulleys	43
Table 4-6: Powertrain data	46
Table 4-7: Specification of the 3Men BL830.....	47
Table 4-8: Specification for the Apex Dynamics AB060	48
Table 5-1: Components for the PCB	53
Table 5-2: The function of the different pins on the D-sub	54

LIST OF FORMULAS

Von Mises criterion

$$\sqrt{\sigma_x^2 + \sigma_y^2 - \sigma_x\sigma_y + 3\tau_{xy}^2} \quad ((2.1))$$

Gradient resistance

$$F_g = mg \cdot \sin(\alpha) \quad ((3.1))$$

Acceleration torque

$$M_A = \alpha_A \left(I_A + \frac{I_B}{(i_{A \rightarrow B})^2 \eta_{A \rightarrow B}} + \frac{I_C + \frac{m}{n_w} r_w^2}{(i_{A \rightarrow C})^2 \eta_{A \rightarrow C}} \right) \quad (3.2)$$

Drag force

$$F_D = \frac{1}{2} C_D A \rho v^2 \quad (3.3)$$

Rolling resistance

$$F_r = C_{rr} N \quad (3.4)$$

Kingpin steering torque

$$T = Wf \sqrt{\frac{I_0}{A_0} + e^2} \quad (3.5)$$

Simplification

$$\frac{I_A}{A} = \frac{\pi D^4}{\frac{\pi D^2}{16}} = \frac{D^2}{8} \quad (3.6)$$

Simplified steering torque

$$T = Wf \sqrt{\frac{D^2}{8}} \quad (3.7)$$

Moment of inertia of cylinder

$$I_{cyl} = \frac{1}{2} m_{cyl} r_{cyl}^2 \quad (4.1)$$

Moment of inertia of thin disc

$$I_{thindisc} = \frac{m_{td} (r_{td})^2}{2} \quad (4.2)$$

Table of Contents

1	Introduction	1
1.1	Background.....	1
1.2	Existing Concepts	2
1.2.1	Thorvald	2
1.2.2	Other agricultural robots	3
1.3	The Thorvald-Project.....	6
1.4	Technology Readiness Level.....	7
1.5	Scope of the Thesis.....	8
2	Theory	11
2.1	Motors and Transmissions.....	11
2.1.1	Internal Combustion Engine.....	11
2.1.2	Electric Motors	13
2.2	Transmission.....	16
2.2.1	Gears.....	16
2.2.2	Belt	18
2.2.3	Chain	20
2.3	Materials	20
2.3.1	Metals	22
2.4	Assembly Technique	24
2.4.1	Adhesives	24
2.4.2	Coatings.....	25
2.4.3	Bolts and Rivets	25
2.4.4	Welding	26
2.4.5	Fittings.....	26
2.5	Controlling the Robot	26
2.5.1	Motor Controller	26
2.5.2	Encoders	27
2.6	Printed Circuit Board.....	29
2.6.1	Components for the PCB.....	29
3	Power Requirements	31

3.1	Propulsion.....	31
3.1.1	Climbing.....	31
3.1.2	Acceleration	31
3.1.3	Drag Forces	32
3.1.4	Rolling Resistance.....	33
3.1.5	Minimum power requirements	33
3.2	Steering.....	35
4	Selection of Components, Materials and Assembly Technique.....	38
4.1	Motors and Transmissions.....	38
4.1.1	Motor.....	38
4.1.2	Drivetrain	38
4.1.3	Propulsion Components	40
4.1.4	Timing belts.....	43
4.1.5	Wheels.....	43
4.1.6	Verification of Propulsion Components.....	44
4.1.7	Steering Components	46
4.1.8	Timing belt	48
4.1.9	Inductive sensor.....	48
4.1.10	Verification of Steering Components.....	49
4.1.11	Motor controller	49
4.1.12	Encoder.....	50
4.1.13	Caster wheel	51
4.2	Materials and Assembly Technique	51
4.2.1	Materials.....	51
4.2.2	Assembly technique	52
5	Control and Connections.....	53
6	Design of the Modules	56
6.1	Propulsion Foot.....	56
6.2	Tower.....	58
6.3	Propulsion module.....	60
6.4	Caster Module.....	61
6.5	Verification of Loads.....	61

6.5.1	ANSYS.....	61
6.5.2	Roller Bearings.....	65
7	Production of the Robot	66
8	Discussion	70
9	Conclusion.....	72
9.1	Further Work	72
9.2	Goal Evaluation	72
10	References	73
11	Vedlegg	1

This page is intentionally left blank

1 INTRODUCTION

1.1 BACKGROUND

Two years ago, a team of four students designed and built Thorvald, an agricultural robot. Their main goal was to reduce the amount of energy consumed in traditional farming with the arguments that the development was heading in the wrong direction. The farmers will always be interested in covering more area in less time, until now, the only solution has been bigger machines with bigger equipment. The negative repercussions surpass the positive by far. Even though the farmers are able to increase their production, they waste a lot of energy, pollute the environment, and damage the soil. The big bad wolf is the soil compaction, which reduces the soils capacity of growth. This happens because of the pressure from the heavy machines, which again makes the soil dens and reduces the soils ability to take in nutrition. In farming as it is today, a lot of resources are used to fix soil that has been exposed to compaction. An article published in “LandbrugsAvisen” says that 90% of the energy used on the soil, are used to fix damages caused by heavy machinery [1]. Some agricultural machines reduce their ground pressure by adding more axles, or using tracks instead of wheels, but this makes the construction more complex, and reduces the machines mobility.

Another issue they wanted to solve, was the amount of fertilizer and pesticides used in agriculture. Many of the modern machines uses to much of these resources, which is unnecessary waste, and very unhealthy for the crops. The pesticides, when over-used, gives the crops unnatural growth. Also, humans use products from these farms on a daily basis, so this can have some dangerous side-effects if not dealt with.

To solve these problems, they made Thorvald, a lightweight robot. The main principle while designing the robot was low weight to reduce compaction of the soil. The idea is basically that you have more than one lightweight robot that can work day and night (a more thorough review of the robot will be done in the next chapter).

An average tractor weighs approximately 4.5 tons[2]. This is thirty times more than the prototype they made, which weighs about 150 kg. All though this is without any tools mounted the difference is huge, and will reduce the ground pressure considerably. The robot will be able to rotate on the spot, a huge benefit when it comes to maneuvering in tight areas.

The prototype was indeed a success, but it was not perfect. The next version shall take modularity even further, by being able to have steering and propulsion on as many wheels as desired. As many components as possible should be identical, so production can be done very efficient. The frame of the robot will be upgraded so that it can be more stable against horizontal forces, and have a better system for shock absorbing.

Our goal is to make this robot ready for the market.

1.2 EXISTING CONCEPTS

1.2.1 Thorvald

This is the first agricultural robot built at NMBU, and our robot will be based on this prototype. The frame of Thorvald has the shape of the letter “U” with a wheel on each of its corners, and a storage box on each side. The electric system (batteries, computer, controller, etc.) is stored in the boxes, and there is a water-proof touch-screen on the left box. The finished prototype is shown in Figure 1-1.

The robot is made to do one task at a time, by using interchangeable tools. These tools can easily be changed, due to the U-shape of the frame. Today it is only one tool available, a precision seeding-machine, but other high-precision tools will be manufactured. Because of this modularity, the robot can be used to other things than agriculture, you just need the right tool. An example of this, is Espen Oviks master’s thesis, he is going to make a prototype of a demining tool for the robot.



Figure 1-1: Thorvald, the agricultural robot. Image: Håkon Sverdvik

Thorvald has four wheels, which all have propulsion motors, as well as steering motors. This makes it able to drive in rough terrain and rotate on the spot. All of the motors used are electric 48 VDC-motors. The specifications of the motors are listed in Table 1-1.

Table 1-1: Motor specifications of Thorvald [3]

	3Men BL823-A02	JVL MAC141
Rated output	600 W	134 W
Nominal speed	4400 rpm	2700 rpm
Continuous torque	1.32 Nm	0.48 Nm
Length	112.5 mm	172 mm
Weight	3.5 kg	1.1 kg

Table 1-2 shows specifications of the hub gears. Because of the low weight of the robot, we don't need a lot of power to move the robot. It is dimensioned to withstand a load of 150kg in addition to its own weight of 150 kg [4].

Table 1-2: Gear specifications of Thorvald [3]

	AL110	AB060
Number of stages	2	2
Nominal output torque	140 Nm	55 Nm
Continuous input speed	3000 rpm	5000 rpm
Max radial load	6500 N	1530 N
Max axial load	3250 N	765 N
Efficiency	≥94 %	≥94 %
Weight	4.1 kg	1.5 kg

1.2.2 Other agricultural robots

Currently, there are several types of agricultural robots being developed, so there is no doubt that agricultural robotics has a future. In the following paragraphs I will give a short review of other agricultural robots getting ready for the market. The specifications of the robots will be compared in

Thorvald	AgBot II	Ladybird	BoniRob
----------	----------	----------	---------

Application	Modular	Weed, fertilizing, seeding	Gather information	Modular
Project type	Research	Commercial	Research	Research
Speed	5 km/h	10 km/h	-	13 km/h
Weight	150 kg + 150 kg	-	-	800 kg
Length x width	1.2 m x 1.5 m	3 m x 2 m	-	Length: 75-200 cm
Ground clearance	50 cm	-	-	40-80 cm
Main material	Steel and aluminum	-	-	Steel
Drive	4WD	2WD	4WD	4 WD
Steering system	4WS Ackerman	Skid	4WS Ackerman	4WS Ackerman
Suspension	Passive	Shock absorbers	Passive	Passive

At Queensland University of Technology, they have developed the AgBot II, which is probably the agricultural robot with most recognition in the media. With 2WD, the AgBot uses the same motors for both steering and propulsion. The front wheels can be operated at different speeds, and which will make the robot rotate. The rear wheels are passive, and will therefore adjust their rotation automatically.



(a) AgBot II, Image: Queensland University of Technology

(b) Ladybird, Image: The University of Sydney



(c) BoniRob [5]

The Ladybird, a research product managed by the University of Sydney, is a solar powered robot specialized in monitoring the fields and providing information. It is equipped with many different sensors so that it can build a very detailed 3D-map of the farm. Since it is a research platform, it also has other sensors that the developers think will be useful in future precision agriculture [6].

The BoniRob is a robot developed by Amazonen-Werke, a German manufacturer of agricultural machines. It has 4WD and 4WS, and is modular.

In Table 1-3, the different robots are compared by specs. To find information about the different robots was very hard. Therefore, some key features, like motor power, and gear ratio could not be found.

Table 1-3: Comparison of agricultural robots

	Thorvald	AgBot II	Ladybird	BoniRob
Application	Modular	Weed, fertilizing, seeding	Gather information	Modular
Project type	Research	Commercial	Research	Research
Speed	5 km/h	10 km/h	-	13 km/h

Weight	150 kg + 150 kg	-	-	800 kg
Length x width	1.2 m x 1.5 m	3 m x 2 m	-	Length: 75-200 cm
Ground clearance	50 cm	-	-	40-80 cm
Main material	Steel and aluminum	-	-	Steel
Drive	4WD	2WD	4WD	4 WD
Steering system	4WS Ackerman	Skid	4WS Ackerman	4WS Ackerman
Suspension	Passive	Shock absorbers	Passive	Passive

1.3 THE THORVALD-PROJECT

The first theses on the Thorvald-project was written in 2014, and made the ground bricks of this project started by Pål Johan From. It is going to be made an autonomous agricultural robot that runs on electricity, and can perform many different tasks. By using high precision interchangeable tools, the weight can be hold at a minimum, and all the necessary tasks cans be done one at a time. These tools will be changed without manual labor; Thorvald will be all autonomous. As well as changing tools it will also be able to charge the batteries by “knowing” when to drive to the charging station.

By choosing electricity as power source, power will be distributed to all the components from the main batteries, and no other power supply will be needed. If any of the tools need external power, they can be connected to the batteries. The robot will contain the most usual sensors, so the tools don’t have more sensors mounted than needed. By equipping the robot with some kind of navigations system, it can navigate by itself, and it will be able to work 24 hours a day, seven days a week, with minimal supervision.

Modularity will be a very big part of the design of the new robot. In addition to the interchangeable tools, the frame can be resized, and different wheel modules can be used. By offering different wheel modules it can be decided which of the wheels that shall have steering and/or propulsion. The customer can thereby customize their robot to fit their specific demands.

Naturally, a lot of the above are long-term goals of this project, and we have no chance of completing all of it this semester. Therefore, this semester is considered a smaller project focusing on some of the short-term goals.

When this semester is over, it will have been designed a new platform for agricultural robotics, the Thorvald II. The following robots will be built using the Thorvald II platform:

- Lincoln University has ordered one robot
- Vollebekk has ordered a robot with an integrated sprayer
- One robot will be built for NMBU, for further research
- Three wheel Thorvald for NMBU

The robot made for Vollebekk need to be taller than the standard Thorvald II, and will therefore have a tall module for increasing the height. In Ås there is a stereotype of the local student, and they are called Thorvald and Tora. To keep adding some local hallmarks, the tall module will be called the Tora-module.

This year's team consists of me, Øystein Tårnes Sund, Alexander Ghebrehiwot and Espen Noreng Ovik. Øystein and I are going to make the platform; Øystein will make the frame and the battery case, and I will make the wheel modules and the power analysis. Alexander is responsible of the sprayer for Vollebekk. Espen is working for FFI, investigating the possibility of using Thorvald II as a deminer.

Goal for the project: Design and start the production of four agricultural robots, with a working sprayer and a deminer.

1.4 TECHNOLOGY READINESS LEVEL

In the 1970's NASA developed the TRL-scale (Technology readiness level), as a more effective assessment of new technologies [7]. Stan Sadin developed the scale with seven steps, but in 1990 two more steps were added. With a total of nine steps, the scale gained acceptance across industry and government. Around 2005, this scale was used to define the readiness of technology throughout the international space development community. Other development communities were also in need of a tool that could properly evaluate research results, and the scale is today used by other communities as well. When the scale is used by other than space communities, it is often modified to match specific criteria.

Horizon 2020 is the biggest research and development program ever in EU [7], which hopefully will secure Europe's competitiveness on a global basis. In a period of seven years, this program has nearly €80 billion available for funding. With a major focus on science, industrial leadership and how to handle societal challenges, a TRL-scale has been made in order to judge with this in mind. This scale can be seen in Table 1-4.

Table 1-4: TRL-scale modified to fit Horizon 2020 [8]

TRL 1	Basic principles observed
TRL 2	Technology concept formulated

TRL 3	Experimental proof of concept
TRL 4	Technology validated in lab
TRL 5	Technology validated in relevant environment
TRL 6	Technology demonstrated in relevant environment
TRL 7	System prototype demonstration in relevant environment
TRL 8	System complete and qualified
TRL 9	Actual system proven in operational environment

Some of the stages in the TRL-scale is pretty similar, so the product can be hard to place on the right stage. In the summer of 2015, the project reached a point where they used the first prototype with a precision sawing machine on a nearby field. Since the final system is supposed to be more modular than the prototype used at the time, this qualifies as TRL 6, but not all the way up to stage 7.

To get the project to the grade of TRL 9, we need a complete modular frame, with tools, that has been properly tested in operational environment.

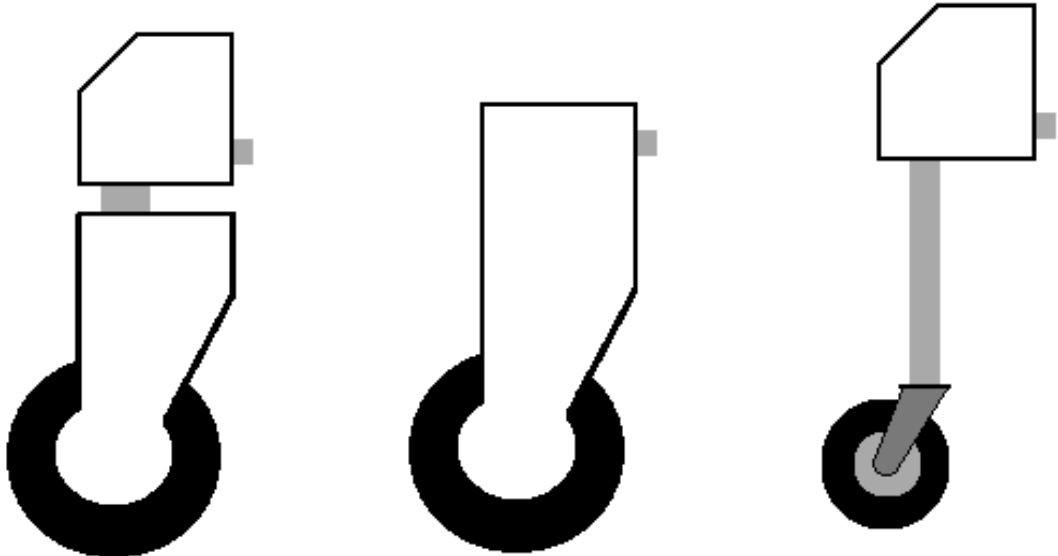
1.5 SCOPE OF THE THESIS

The purpose of this thesis is to design the wheel modules for Thorvald II, and determine which components that is best suited for our demands.

The robot will be designed for four different versions. Four robots will be built, but only two of them will be identical. Both the robot for NMBU, and the robot ordered by Lincoln University will have 4WS and 4WD. The robot ordered by Vollebekk will only work on a flat field with a light sprayer installed. This have to be made differently than the other two Because it only requires propulsion on two of the wheels, the weight can be reduced, which is ideal for the soil. A three-wheel Thorvald will also be made. This can be used for simple applications with sensors and surveillance. By designing the robot for modularity, customers can have their robot produced to fulfill their needs. This is a huge advantage in the marked, as well as for the customers and the soil. As seen in the drawings in Figure 1-2, the design of the new modules will be based on the set-up used in the prototype that was made in 2014. One module will have both propulsion and steering motor. This is the same kind of layout as on the prototype, and will be considered the main module. This is because both the robot for NMBU, and the university in Lincoln will have four of these modules. The second module only has a propulsion motor, so it will not be able to rotate. This module can be paired with a caster-wheel module that has passive steering. When these two modules are paired, the robot will have a kind of skid steering, where the two propulsion modules operate with different speeds to make the robot turn.

It will be done calculations to determine how much power we need from the motors used for both steering and propulsion, and they need to be combined with suitable gears that can withstand the static loads of the robot. These parts needs to be well integrated to the design, to avoid them taking unnecessary loads.

The concept of the first robot will form the basis of the main module, but the focus of this thesis will be to make the design more practical. The modules of the prototype are heavy and oversized. They should be as lightweight and narrow as possible, but need to withstand the loads applied by the frame. The final design must take into account the materials that are going to be used. Different materials have different characteristics, and thereby needs a different approach to the principle of design.



(a) Propulsion and steering (b) Propulsion motor (c) Caster wheel

Figure 1-2: The wheel modules for Thorvald II

Components needs to be selected so that the robot will work with the existing software and communication protocols, or else the robot can't be controlled with demanded precision.

As for production, choice of components and design must be done to reduce time. The time schedule is very tight, and a low amount of different parts is desired. This will contribute to making the production and composition effective, the robot will also be easy to maintain in the future.

The finished module design is intended to meet the demands of the grade 9 on the TRL-scale. Unfortunately, this thesis has to be delivered by May 15th, and the robot won't be ready for testing until June 1th.

Goal for the thesis: Design three different wheel modules for the agricultural robot, Thorvald II, and start the production. After additional testing, the finished modules shall achieve the grade of 9 in the TRL-scale.

2 THEORY

As this thesis is part of a big project, the theory section will focus on the most crucial points. Many of these things were selected two years ago, and this builds on the foundations of the master's thesis of Lars Grimstad [3] and Fredrik Blomberg [4].

2.1 MOTORS AND TRANSMISSIONS

When determining the performance of a vehicle, there are two limiting factors; the traction between the wheel and the surface, and the maximum torque provided by the motor/transmission on board of the vehicle. The smaller of these two factors will decide the potential of the vehicle [9]. As seen in Figure 2-1, the desired power plant will provide large amount of torque at low speeds when the robot is accelerating or climbing. A short introduction of different motors and transmission will be given in the next chapters.

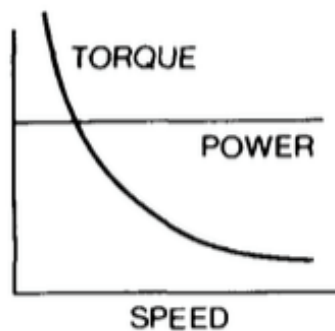
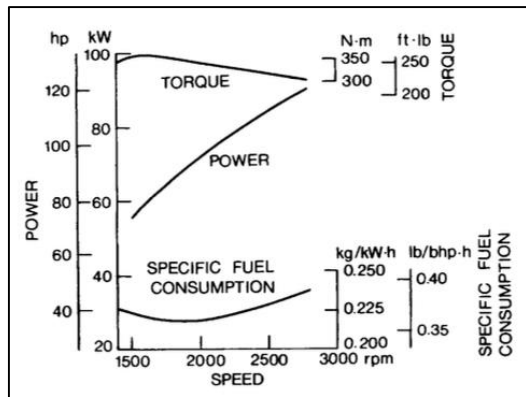


Figure 2-1: Ideal performance characteristics for vehicular power plants. Image: Wong

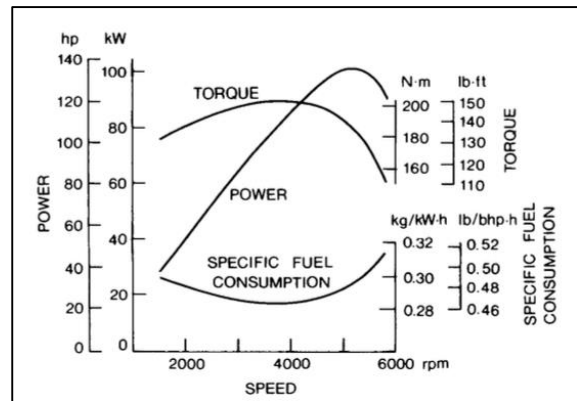
2.1.1 Internal Combustion Engine

Usually, the term internal combustion engine is associated with an engine with intermittent combustion, such as the two-stroke and four-stroke piston engines. There also are internal combustions engines with continuous combustion; for instance jet engines and most rocket engines [10]. All internal combustion engines have in common that they burn fuel internally, and transforms the energy to mechanical energy.

Figure 2-2: Performance characteristics of piston engines. Image: Wong



(a) Diesel engine



(b) Gasoline engine

Piston engines are by far the most common engine used in vehicles. This includes automobiles, motorcycles, trains etc. The most common fuels used for these vehicles are gasoline and diesel. In agricultural machines, piston engines running on diesel is mostly used for both large and small machines.

By comparing the graphs shown in Figure 2-1 and Figure 2-2, the conclusion is that the performance of the piston engines are far from the preferred performance. If the engine is supposed to be used directly for propulsion, it requires a multi-step gearbox or a continuously variable transmission. In the later years there has been a growing interest in protecting the environment and reducing the fuel consumption. A transmission with a continuously variable reduction ratio enables the engine to run over a wide range of speed, while operating under the most economical conditions, therefore this solution is gaining popularity. Either way, both of these two solutions will make an in-gear solution impossible to implement in our robot.

Good combustion quality, together with maximum engine torque are reached at intermediate engine speed. As the speed is increasing further, the power output increases with it, but the torque is decreasing. As the power output reaches its maximum value, the torque will start decreasing more rapidly which will make the power output decrease. Therefore, the maximum speed of a vehicle engine is usually set right above the speed of the maximum power output.

The efficiency of a typical combustion engine is approximately 25 %, which is very poor, and over 60 % of these losses are due to engine thermal losses [11]. In addition to this, the combustion process produces toxic gases and particles, and most of the fuels are made of non-renewable sources.

As the concern for the climate changes and future oil supply increases, the interest for alternative fuel for the combustion engines also increase. Biofuel can be made all emission-free, such as ethanol, methanol and biodiesel made from feedstocks (soybean, palms, sunflower etc.) [12]. Combustion engines needs to be altered so that it can run on pure bio-fuel. Sadly, the bio-fuels often is blended with regular fossil fuels so unaltered combustion engines can run on them.

2.1.2 Electric Motors

An electric motor converts electrical energy into mechanical energy, and are very versatile. Electric motors can be found with ratings less than 0.5 W [13], while others exceed 100 megawatts[14]. They can be found in everything from small toys and watches, to cars, trains and factories.

The two main types of electric motors are powered by direct current or alternate current. Electric DC motors ability to run on batteries makes them very suitable for mobile applications. In the following explanation, only DC motors will be taken into account. A DC motor consists of two parts, a rotor (the rotating part) and a stator (the stationary part).

When you run an electric current through a coil of wires, a magnetic field is created around it, which can interact with the magnetic field of a permanent magnet. Magnets with the opposite polarization are attracted to each other, while magnets with the same polarization are repelled. As illustrated in Figure 2-3, the coil appears as two parallel windings with current flowing in opposite direction. Since there is a north- and a south pole, it will start to rotate until the north pole on the rotor aligns with the south pole on the stator. In the illustration figure the coil is the rotor, and the magnet is the stator. The coil has to be connected to a commutator, two halves of metal which reverses the current in the coil each half-turn. When the current changes its direction, naturally, the poles in the stator also change. Now, the poles that previously were attracted to each other, are repelling each other, and the rotor will continue to rotate.

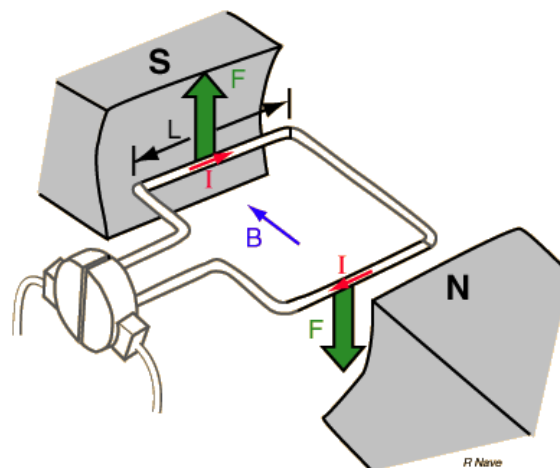


Figure 2-3: An illustration of a DC motor. Image: HyperPhysics [15]

The rotation should be as continuously as possible, and for that reason there are more than one coil in most of the DC motors. To change the polarization of the winding at the right time, the commutator needs information about which of the windings that are supposed to be energized. The commutation was originally done mechanically (brushed DC motor), but the increased availability of semi-conductors has made electronic switching of the current more common (brushless DC motor).

Brushed DC motor

The BDC motor is the simplest edition of the DC motor, and because of its early development, it still is a very popular electric motor. Carbon is the most common material used for the brushes, this is to stand against friction where they are pushed against the commutator, which is fixed on the rotor. Each of the coils are connected to two conductive segments of the commutator. The brushes are two spring-loaded metal pieces that conducts power from the DC power supply to the coils, and thereby creates a magnetic field. The position of the brushes is responsible for changing the magnetic field so that it always is opposite to the magnetic field, which is provided by the permanent magnet in the stator. This is causing the rotation of the rotor.

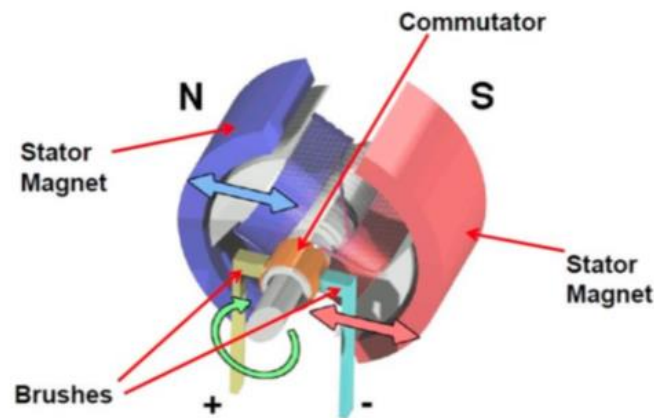


Figure 2-4: Brushed DC motor. Image: ON Semiconductor

Shown in Figure 2-4 is a BDC motor, with arrows pointing out the parts mentioned above. In general, the BDC motor is an affordable motor that don't require complex drive electronics, but the lifetime is limited. Since the brushes is in direct contact with the commutator they will wear down, and the motor needs maintenance. A brushed motor is also significantly larger than a brushless motor.

The information about the BDC motor, and electric motors in general are gotten from the following references: [16], [17], [18]

Brushless DC motor

In BLDC motors, the permanent magnet is positioned at the rotor, and the coils are driven by transistors. Alternatively, the motor shaft can be driven by a fixed core of the armature coils, with the permanent magnets revolving around it. Either way, the coils are stationary and the brushes aren't necessary.

Instead of a mechanical commutator, such as on the BDC motor, the BLDC motor uses a transistor to continuously change the phase of the stator coils to keep the rotor spinning. While the BDC motor's speed is determined by the voltage applied, the BLDC's speed is determined by the frequency at which the transistor operates.

The BLDC motor is available with 1-, 2-, and 3 phases; the single-phase motor are used for low-power applications, two-phase are used for application of medium power. Three-phase BLDC are used for high-power applications, and are much better suited for driving and steering. Therefore, single- and double-phased BLDC will not be taken into account.

The rotor is a permanent magnet with two to eight pole pairs. Ferrite was traditionally used in the permanent magnets, but as the technology has advanced, rare earth magnets are also often used. Magnets made of ferrite is less expensive, but the alloy material has higher magnetic density and improves the size-to-weight ratio. The rotor can be compressed to a smaller size, and still provide the same torque.

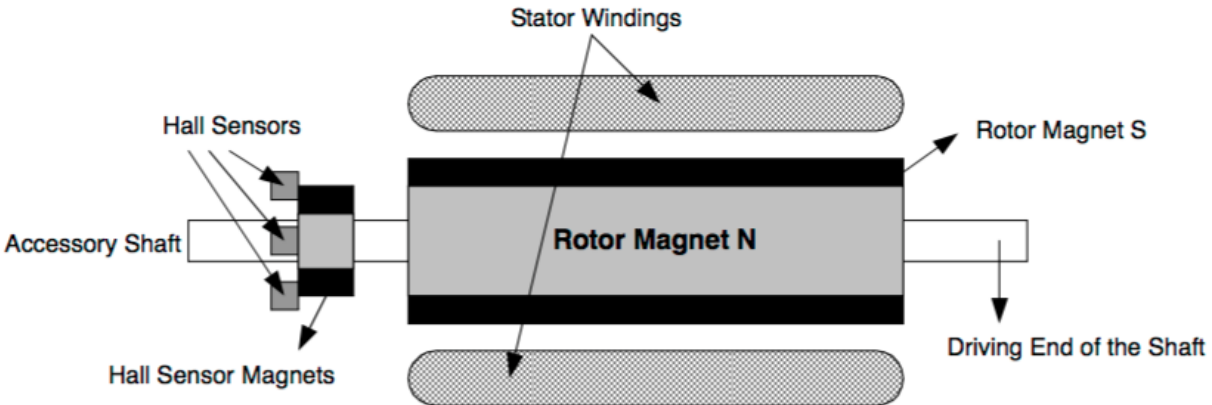


Figure 2-5: Cross section of a three-phase BLDC motor Image: Microchip [19]

Most three-phase motors have three stator windings connected in star fashion, and each of them are distributed over the stator periphery to form an even amount of poles. The stator windings have to be energized in the right sequence for the motor to rotate, and therefore, the stator-position has to be known at all time. By embedding Hall effect sensors into the stator, the position can be mapped. Whenever a magnetic pole passer near a Hall sensor, they give a high (N) or low (S) signal, indicating which pole is passing. The sequence of commutation is determined by using three Hall sensors with a phase shift of 60° or 120° to each other. To get this alignment correct can be difficult, and some motors have dedicated Hall effect magnets on the rotor to simplify this process.

A cross section of a BLDC motor can be seen in Figure 2-5 with some essential components pointet out.

As seen in the characteristics diagram in Figure 2-6, the BLDC motor has two references of both speed and torque. During continuous operations, the motor can be loaded up to the rated torque, which can be kept constant for a speed range up to the rated speed. For short periods of time, higher torque can be achieved, but with a lower speed. Also the speed can be run higher, with the bi-effect of dropping torque.

For additional information about the BLDC motor, see references: [18], [19]

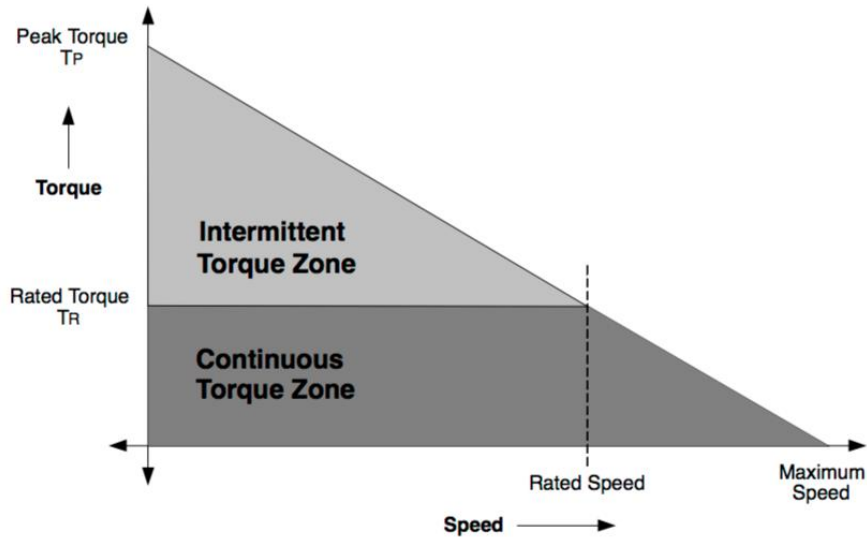


Figure 2-6: Torque - speed characteristics of a BLDC motor. Image: Microchip [19]

2.2 TRANSMISSION

Transmission is a device mounted between a power source and a specific application for the purpose of getting a good adaption between them. Most transmissions functions as rotary speed changers, with constant- or variable ratio of the output speed to the input speed. Since the agricultural robot will have low range in speed, this thesis will focus on transmissions with constant ratio [20].

2.2.1 Gears

Gears are used to transmit power/motion between two shafts by meshing toothed wheels without slipping. In a pair of wheels, the smaller one is called “pinion” and the larger one is called “gear”. When the power input is at the pinion, it results in a step down drive where the output speed decreases, and the torque increases. With the opposite set up we get a step up drive. High efficiency and quiet operation can be achieved, but requires high precision in the shape of the teeth and the distance between the wheels.

Spur gears

Spur gears, seen in Figure 2-7, are the most common type of gears. The shafts are parallel and in the same plane. The teeth are cut straight and parallel with the axis of the shaft. Because of the design, spur gears produce a large amount of stress on the teeth, and they make a lot of sound. Therefore, they are mostly used at low to moderate speeds.



Figure 2-7: Spur gear. Image: Gibbs Gears

Helical gear

Helical gears, as seen in Figure 2-8, are similar to spur gears, but the teeth are cut with an angle relative to the shaft axis. Helical teeth have increased length of contact, which makes them stronger and less noisy compared to spur gears. Due to the angled cuts, there will occur sideways forces, which reduces the efficiency slightly. They are normally used at high speeds.



Figure 2-8: Helical gear. Image: Hewitt & Topham

Herringbone gear

Herringbone gear, also called double helical gear, can be seen in Figure 2-9. These gears give the same advantages as helical gears, but eliminates the sideways force on the mounting shafts. Because of the shape, herringbone gears are more difficult to manufacture and are more expensive than regular helical gears. They are well suited for heavy loads at medium to high speeds.

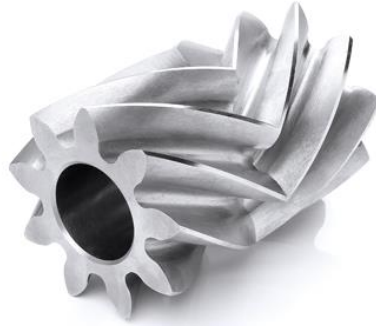


Figure 2-9: Herringbone gear. Image: Hewitt & Topham

Planetary gears

A planetary- or epicyclic transmission system, normally consists of three coaxial elements. A central pivoted sun gear, an outer ring gear and planet gears rotating in between these. The layout of a planetary gear is shown in Figure 2-10. The main advantage of this system is its ability to transfer high torques with high efficiency and a compact design. This is because the loads are distributed over multiple planet gears.

The planetary gear seen in the figure has two sun gears. One of them has to be fixed for the system to work as a transmission, while the other drives the planet gears. This set up allows the planetary system do operate with three different configurations, including 1:1 where both sun gears are fixed.

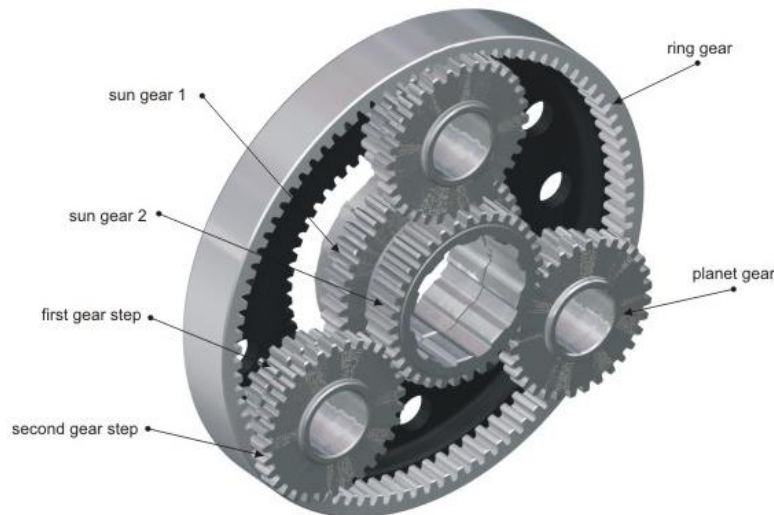


Figure 2-10: Planetary gears. Image: Rohloff

For more information about gears, see references: [21], [22], [23], [24], [25]

2.2.2 Belt

Belts are used to transmit power between two shafts by using rotating pulleys. If the pulleys have different sizing, we get a ratio in the speed of the two shafts. Belt drives are very useful in

applications where layout flexibility is important, because you can place components in more advantageous locations and still achieve the same efficiency.

Based completely on friction, we have three main types of belt drives: flat belts, V-belts and circular belts. These are shown in Figure 2-11. Of these, only the V-belt can be used for the agricultural robot; the flat belt can't handle a great amount of power, and the circular belt are best suited for pulleys more than eight meters apart [26].

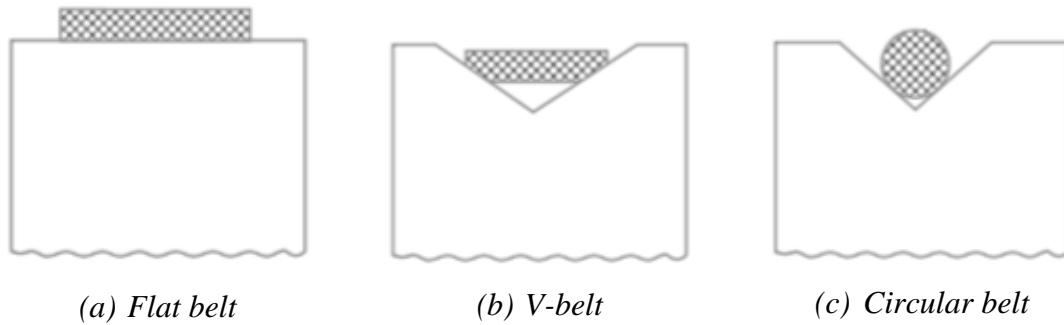
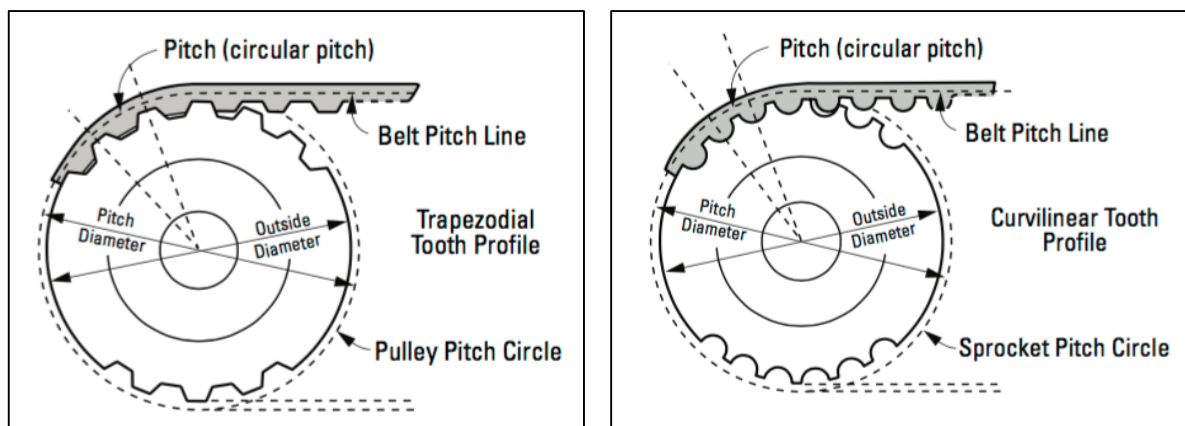


Figure 2-11: Frictional belts. Image: Eurasia PH

A fourth alternative is the timing belt, a belt with teeth. A transmission with timing belts has no slip, and there is no relative motion between the two elements in mesh. The required tension is significantly lower than with regular belts, which gives very small bearing loads.

Different teeth profiles are shown in Figure 2-12. The most common tooth profile is trapezoidal which is similar to the teeth on spur gears. In the later years the curvilinear tooth profile has superseded the trapezoidal, because the area of contact is larger and the unit pressure is lower. Since the teeth design makes loads on the belt so small compared to other belts, it can be narrower [27].



(a) Trapezoidal tooth profile

(b) Curvilinear tooth profile

Figure 2-12: Timing belts. Image: SDP/SI

More information about belts can be found in references: [26], [27]

2.2.3 Chain

Chain drives are made of a number of rigid links which are hinged together by pin joints in order to provide the necessary flexibility. The wheels have projecting teeth, and are known as sprockets, they can be seen along with the chain in Figure 2-13. The sprockets are constrained with the chains to move together without any slip. Chain drive is suited for applications with velocities of maximum 25 m/s and power up to 10 kW, with an efficiency up to 98 %.

Compared to belt drive, the chains will be narrower since they are made of metal, and it can transmit more power. The disadvantages of using chains, is that the productions costs are relatively high, it has a low tolerance for dirt, and needs maintenance, especially lubrication.

The principles of chain drive can be seen in Figure 2-13, and more information about chain drive can be found in reference: [26].

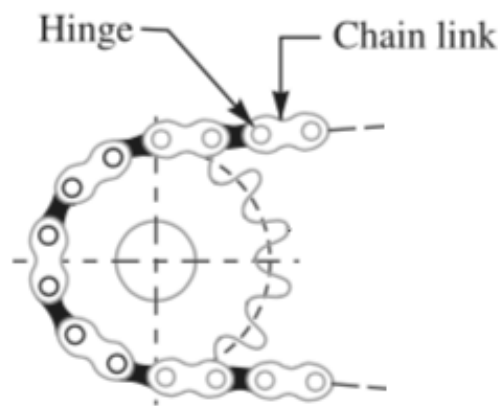


Figure 2-13: Chain wrapped around wheel. Image: Eurasia PH

2.3 MATERIALS

Solid materials are mainly grouped in three categories: metals, ceramics and polymers. This is based primarily on atomic structure and chemical makeup, so most materials fall into one specific group. Since the robot mainly consists of metal, this group will be the focus of this thesis. For information about polymers and organic materials, see reference: [4].

Modulus of elasticity

The modulus of elasticity, also known as Young's modulus, describes a materials stiffness and ability to resist elastic deformations when exposed to compressive- or tensile stress. The greater the modulus, the stiffer the material, or the smaller the strain that results from the stress. For metal, the typical value of this modulus ranges between 45 GPa, for magnesium, and 407 GPa, for tungsten. The values for steel and aluminum are respectively 207 GPa and 69 GPa.

The modulus of elasticity of a certain material is determined by plotting a stress versus strain diagram. The slope of the curve corresponds to the modulus of elasticity. The modulus is an important parameter used for calculating elastic deflection.

Yield strength (R_e)

Most structures are designed to ensure that only elastic deformation occurs when stress is applied, a component that has been plastically deformed may not function as intended. It is desirable to know the stress level at which the plastic deformation, or yielding, begins.

The yield strength of a material is the lowest amount of stress that results in plastic deformation, which is shown as the yield point in Figure 2-14. The unit for yield stress is MPa.

Tensile strength (R_m)

After a material starts to yield, the internal stress increases to a maximum before it decreases to the point of fracture. The tensile strength is the maximum stress that can be sustained by a structure in tension; fracture will result if this stress is applied and maintained. This is visualized in Figure 2-14

Tensile strength has a wide range from 50 MPa for an aluminum to as high as 3000 MPa for high strength steels.

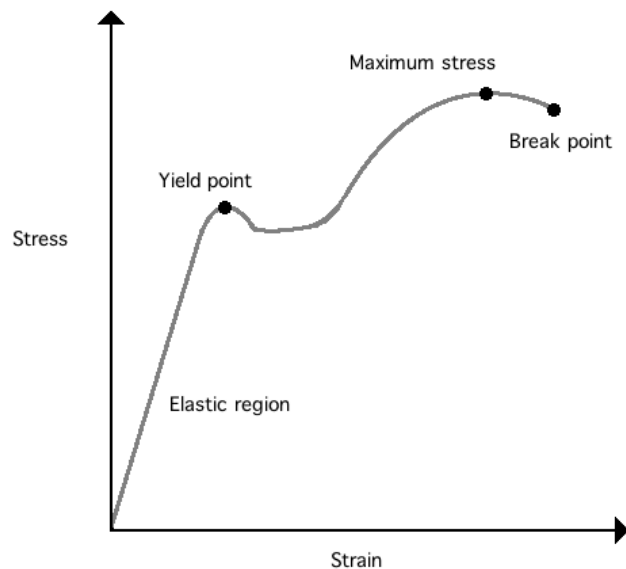


Figure 2-14: Stress-strain diagram

When the strength of a material is cited for design purposes, the yield strength is used. By the time stress corresponding to the tensile strength has been applied, the material has usually experienced so much plastic deformation that it is completely useless.

For more information about material properties, see reference: [28].

Equivalent stress (σ_{eq})

When materials are under the influence of multi-axis loads, we need to combine the stresses to one equivalent stress which can be compared to the yield- or tensile strength. This equivalent stress is hypothetical and in one direction. Von Mises criterion is described in equation (2.1).

Von Mises criterion is the most realistic theory regarding ductile materials as steel, aluminum and copper [29].

$$\sigma_{eq} = \sqrt{\sigma_x^2 + \sigma_y^2 - \sigma_x\sigma_y + 3\tau_{xy}^2} \quad (2.1)$$

where:

σ_{eq} is the equivalent stress

σ_x is the x-component of stress

σ_y is the y-component of stress

τ_{xy} is the shear stress

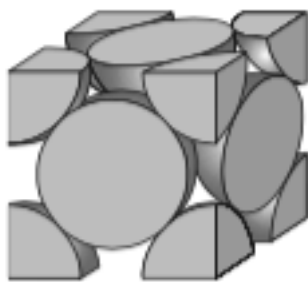
2.3.1 Metals

Materials in this group are composed of at least one metallic element, such as iron, aluminum, copper, etc. and often small amounts of nonmetallic elements, such as carbon, nitrogen and oxygen. Compared to polymers and ceramics, metals are relatively dense. Due to its characteristics, metal is used for a wide range of structural applications. These materials are strong, stiff, ductile and resistant to fracture, which makes them very versatile.

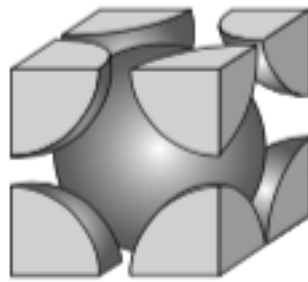
Solid materials can be classified according to the regularity with which atoms or ions are arranged with respect to one another. A crystalline material is one in which the atoms are positioned in a repeating or periodic array over large atomic distances. All metals form crystalline structures under normal conditions. When describing crystal structures, it is often convenient to subdivide the structure into unit cells. Unit cells are parallelepipeds that represents the symmetry of the crystal structure, wherein all the atoms positions can be generated by projecting the unit cell.

Three types of crystal structures are found in the most common metals: face-centered cubic, body-centered cubic, and hexagonal close-packed. These can be seen in Figure 2-15.

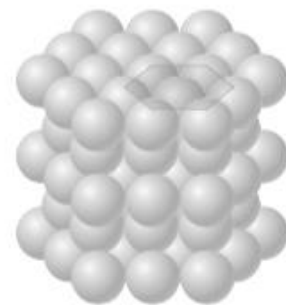
Face-centered cubic crystal structure is a common structure amongst metals, where the unit cell is a cube with atoms located at each of the corners and the centers of all the cubic faces. FCC structure is typical for soft metals such as: copper, aluminum and gold.



(a) FCC structure



(b) BCC structure



(c) HCP structure

Figure 2-15: Most common structures of metal

Body-centered cubic crystal structure is also a common structure amongst metal which also has a cubic cell with atoms located at each of the corners. Unlike the FCC structure, the BCC structure has a single atom at the cubic center. This structure is typical for harder materials such as: chromium, iron and tungsten.

The last common type of crystal structure amongst metals is *Hexagonal close-packed crystal structure*, where the unit cell is hexagonal. The top and bottom faces consists of six atoms forming a hexagon surrounding a single atom in the center. A middle plane provides three atoms to the unit cell. HCP structure can be found in cadmium, cobalt and others.

Alloys

A metal consisting of only one type of atom is impossible to achieve; there will always be impurity. In the most common metals, impurity atoms have been added intentionally to give the material specific characteristics. Alloying is often used to improve the mechanical strength and resistant against corrosion.

Alloys are often grouped into two classes: ferrous and nonferrous. Ferrous alloys, with iron as the principle constituent, include steel and cast irons. Alloys that are not iron based are nonferrous.

Ferrous alloys are produced in larger quantities than other metal types, and are especially important as construction materials. It is three main reasons for the popularity of this type of alloys: Iron-containing compounds are easily found within the earth's crust, metallic iron and steel alloys can be produced economically and with simple fabrication techniques. They are also exceptionally versatile, and can be modified to meet a wide range of mechanical and physical demands. The main disadvantages with ferrous alloys is their high density, vulnerability to corrosion, and low electrical conductivity.

Steels are iron-carbon alloys that may contain concentrations of other alloying elements. Some of the common steels are classified according to their concentration of carbon: low-, medium-, and high-carbon steels, but the content of carbon is usually less than 1.0 %. Low-carbon steels generally contain less than 0.25 % C, and are relatively soft and weak. Their strengths are outstanding ductility and toughness, and they are easily worked with. Typical applications for low-carbon steel is structural shapes and sheets used in pipelines, bridges etc. Medium-carbon steels contain concentrations of 0.25 – 0.60 % C. By heat-treating the material, they become stronger than the low-carbon steels, but at a sacrifice of ductility and toughness. High-carbon steels usually have a concentration of 0.60 – 1.4 % C, and are the hardest, strongest and least ductile of the carbon steels. They are extremely wear resistant and capable of holding a sharp cutting edge. These steels are very suitable as cutting tools and dies for forming and shaping materials, as well as knives, razors and high-strength wires.

As a nonferrous alloy, *aluminum* is often combined with copper, silicon, magnesium, manganese, and zinc, it can also be cold worked to enhance the mechanical strength. Both of these methods tend to reduce the resistance to corrosion. Aluminum is known for its low

density, which is only a third compared to steel. It also has high electrical- and thermal conductivity, and good resistance to corrosion in some common environments. The crystal structure of aluminum is FCC, so the ductility is remained even at very low temperatures.

Table 2-1: Compositions and mechanical properties for some common aluminum alloys

Aluminum Association Number	Composition [%]	Tensile strength [MPa]	Yield Strength [MPa]	Ductility [mm]
1100	0.12 Cu	90	35	35-40
5052	2.5 Mg, 0.25 Cr	230	195	12-18
6061	1.0 Mg, 0.6 Si, 0.3 Cu, 0.2 Cr	240	145	22-25
7075	5.6 Zn, 2.5 Mg, 1.6 Cu, 0.23 Cr	570	505	11
356.0	7.0 Si, 0.3 Mg	228	163	3.5

Aluminum is generally classified as cast or wrought, and both are designated by a number with four digits that indicates the impurities of the material. For cast iron, a decimal point is located between the last two digits. A selection of aluminum alloys are listed in Table 2-1, along with their composition and mechanical properties. The cast iron listed in the table, 356.0, is a relatively strong cast alloy, but still it does not come close to the mechanical properties of the 7075 wrought alloy.

If more information about steel, aluminum or other materials is desired, see reference: [28]

2.4 ASSEMBLY TECHNIQUE

2.4.1 Adhesives

An adhesive is a material used to bond together two solid materials (adherends). Adhesives can be used to combine several sorts of materials, such as metals, ceramics, polymers, composites, skins and even more. This technique is used for a great amount of applications, especially in aerospace, automotive, and construction industries, packing, and some household goods.

It is important to choose the right kind of adhesive for the considered application, such as what type of materials are going to be bonded, should the bond be temporary or permanent, the temperature the adhesive is going to be exposed to, and the processing conditions.

The advantages offered by adhesive bonding is light weight, ability to join dissimilar materials and thin components, more fatigue resistance, and lower manufacturing costs. This technique is well suited when components need to be positioned with high precision, and the process needs to be fast.

The main limitation of using adhesives is how it behaves with temperature changes. Polymers only maintain their mechanical toughness at relatively low temperatures, and the strength decreases rapidly as the temperature increases. Some polymers can be used continuously with a temperature of 300°C, but that is the maximum of what is available today.

2.4.2 Coatings

Coatings are applied to the surface of materials as protection from the environment against corrosive or worse reaction, provide electrical insulation, or to simply improve the components appearance. Often, the coatings are organic, such as paint, enamel, and lacquer. Other common coating are latexes, which is not organic, but a stable suspension of small insoluble polymer particles dispersed in water. These have become more popular because of their low amount of organic solvents.

2.4.3 Bolts and Rivets

The main advantage with bolts, is that they are not permanent. In fact, they are very easy to remove, and can be used almost everywhere. The fact that anyone can use it, you don't need any special education, makes it very versatile. It is used in everything from furniture, automobiles, buildings, to small toys and electric tools.

In the metrical system, it is usual to size the bolts according to the ISO 68-1 standard [30], where the bolts are named with the letter M, followed by the size of the bolt (M12 = 12mm diameter). To determine the right dimension of the bolt, it has to be controlled to interception in the bolt, pressure on the hole edge, tearing in the main material, and plastic deformation of the materials cross-section.

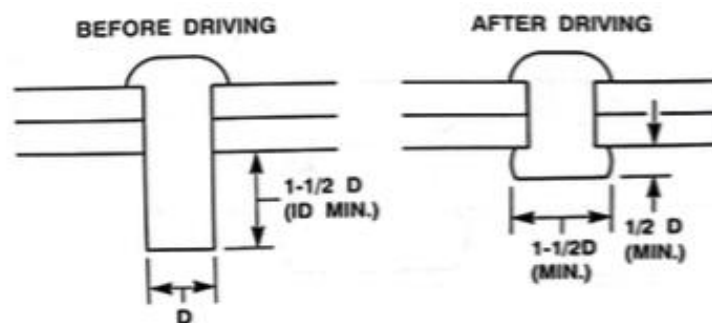


Figure 2-16: Rivet before and after driving

Riveting is very popular for bonding aircraft skins, and make a tight and effective joint. Riveting and bolting share many of the same principles, but unlike bolting, riveting is permanent. The rivet is placed in the holes of the materials to be joint, and driven flat on one of the sides. The principle of driving a rivet can be seen in Figure 2-16. If a smooth surface is desired, flush rivets can be used in countersunk holes.

2.4.4 Welding

When two materials are joint by welding, they are melted together to form a single piece. Different welding methods exist, but the most common are arc and gas welding. They need a filler material, which is heated to a temperature that causes the main materials to melt; upon solidification, the filler materials become a fusion joint between the work pieces.

A region close to the weld may have experienced microstructural and property alterations; this area is called the affected zone, and is a big drawback in welding.

- If the work piece was previously cold worked, the heat-affected zone can experience recrystallization and grain growth, which results in reduced strength, hardness, and toughness. Because of this reason, aluminum is not well suited for welding.
- During the cooling of the weld, stresses may form in this region that weaken the joint.

Welding can be a very good technique. By using well suited materials, the heat-affected zone can grow stronger. Regardless, welding should be done by a properly qualified person.

2.4.5 Fittings

Materials expands and shrinks when exposed to change in temperature. By heating one component, it can be strung on another component that is cooled down. When the temperatures approaches room temperature, it results in an interference fit. This can also be achieved without the heat treatment, but in a smaller scale where only force is used to fit the components to each other.

By using this technique, only the components to be joint are needed, no extra material. The biggest downside is that corrosion can occur if the fitting is too loose.

For more information about assembly techniques, see references:[28], [31], [32], [33]

2.5 CONTROLLING THE ROBOT

2.5.1 Motor Controller

The motor controller is used to provide necessary information to the motor. With a manually controlled machine the user uses feedback from the application to decide whether to reduce, increase or keep the supplied power. For instance, when a car is driven, the speedometer gives feedback to the driver, who then can adjust the amount of throttle to achieve the desired speed.

With an autonomous robot, this task is done by the motor controller. An open-loop controller doesn't get any feedback from the sensors, but tries to predict the required power output. More common is the closed-loop controller, which uses the feedback to adjust the provided power. The feedback is critical for the motor controller to function intentionally. Different conditions will make the motor behave differently to the same input. Therefore, the motor controller has to adjust the motor input by using information from different sensors monitoring the output shaft. The sensors relevant in this thesis are encoders, which will be explained in the next

sections, and Hall effect sensor, which is explained in 2.1.2. First, the PID controller will be presented, this is the most common of the controller for closed-loop applications.

PID controller

The difference between the process-variable and the desired set-point is measured, and then the controller modifies the the input to minimize the difference. The PID motor controller uses three constant parameters to control the motor: proportional, integral and derivative. The integral part multiplies the measured difference with a gain value, the integral part gathers information about previously differences, and the derivative part tries to predict the future difference based on the current change rate. I other word, they deal with the present, the past, and the future.

For more information about controllers, see reference: [34]

2.5.2 Encoders

Rotary encoders are electromechanical transducers that convert shaft rotation into output pulses. These pulses can be counted to measure the revolutions of the shaft, or the shaft angle. By sensing a number of positions per revolution the encoder provides the motor controller with information about rate and positioning. The number of counts an encoder can make is called points per revolutions, and the speed of an encoder is measured in counts per second.

The most popular types of encoders are incremental encoders and absolute encoders.

Incremental encoders

These type of encoders contains a glass or plastic code disk rotating between an internal light source (usually LED), a mask and a photodetector assembly. The code disk is incremental and contains a pattern of equally spaced non-transparent and transparent segments that radiate out from its center. Light from the LED passing through the code disk and mask is “chopped” as the shaft rotates. As the light hits the photodetector assembly, it outputs high or low signals. These parts can be seen in Figure 2-17.

A second photodetector can be added 90° out of phase to the first one, and the direction of rotation can be determined. If the pulses in channel 1 lead those in channel 2, the shaft rotates clockwise. If the pulses in channel 1 lag those in channel 2, the direction is counter-clockwise. This is the most common type of incremental encoders, and are called incremental quadrature encoders.

Incremental encoders only provide information about the motion of the shaft, and not the actual position. Because of this, a motor using incremental encoders for feedback have to find a known reference at every start-up. To find this reference, an inductive sensor is necessary.

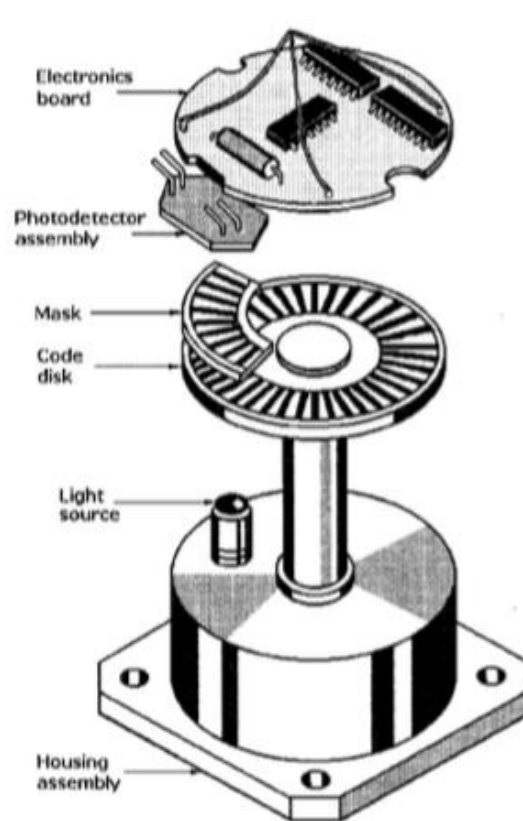


Figure 2-17: Exploded view of an incremental encoder. Image: Sandin

Absolute encoder

An absolute encoder contains multiple photodetectors and light sources, and a code disk with up to 20 tracks of segmented patterns arranged as annular rings. Contrary to an incremental encoder, the code disk in an absolute encoder provides a binary output that defines each shaft angle, an absolute measurement. This type of encoder is similar to the incremental encoder, but LED approaches a photodetector for each track.

Since the encoder gives the absolute measurement of the position, the usually provide information for only one revolution. Multi-turn absolute encoders uses several single-turn encoders with reduction gears. The first encoder returns the orientation of the shaft, while the next count the number of revolutions the first encoder has completed.

The main advantage with an absolute encoder is that the code disk retains the last known position of the encoder shaft when it stops moving. Thereby, the homing procedure at start-up is unnecessary.

Information about encoders are gather from reference: [35]

2.6 PRINTED CIRCUIT BOARD

A PCB is a board with lines and pads that connects points together. On the board, it is traces that allows signals and power to be routed between components and their connectors. Solder is both used as an adhesive, to mount the components, and to make the electrical connections in the PCB. The board is constructed with different layers, seen in Figure 2-18.



Figure 2-18: The layers of a PCB

The substrate is usually made of fiberglass with the grade FR4. This solid material provides the board with rigidity and stiffness. The next layer is a laminated copper foil. Usually the PCB has two layers of copper, but it can be as few as one or as many as 16, sometimes even more. On top of the copper lies the soldermask and gives the color to the board, usually green. The soldermask insulates the copper traces to avoid contact with metal, solder or other conductive components. The last layer is a silk screen, which is used to apply letters, numbers or other symbols.

Each of the components that is supposed to be on the PCB have footprints. The board need to have drill holes that fits these footprints, or else, the components can't get installed. Components can also get soldered onto pads, which is a portion of exposed metal on the surface of the board.

For more information about PCBs see [36]

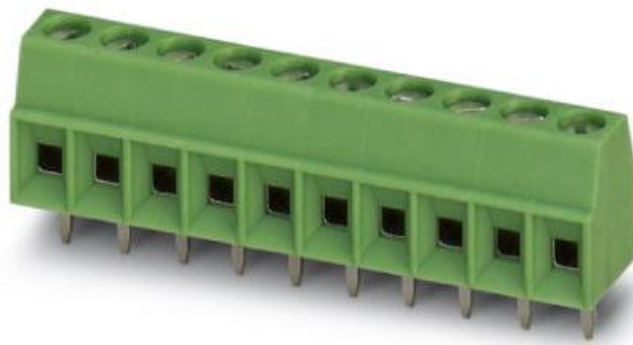


Figure 2-19: Terminal block. Image: Phoenix Contacts

2.6.1 Components for the PCB

Resistors are one of the most common components used on a PCB, and reduces the current flowing in the traces. It can be used to control the amount of current flowing through the components. [37]

A *transistor* can be seen as a switch controlled by an electric signal. By supplying the transistor with a voltage of 0.7 V, a much higher voltage is allowed to pass through. Transistors can work

in three stages: transistor on, where the current flows freely, transistor off, where the current flow is stopped, or linear flow control, where the flow rate is somewhere between fully open and fully closed. A transistor can be seen as variable, adjustable resistor [38].

Terminal blocks are used to connect wires to the PCB. They are available in different sizes, and a high amount of terminals. If a compact solution is desired, they also are available with two floors. A terminal block is shown in Figure 2-19

A *converter* is a little device that can convert signals, for instance 48 V DC to 12 V DC.

3 POWER REQUIREMENTS

Thorvald II can be produced in three different combinations, where the toughest edition will be the combination with 4WD. In this chapter the power requirements for both steering and propulsion will be calculated, with emphasis on the 4WD version.

Today, there is not many agricultural robots, so it is difficult to estimate the required power with high accuracy. Even though Thorvald I has had a peaceful life until now, some tests have shown that it is capable of withstanding the loads it is dimensioned for. This indicates that the method used to calculate the power requirements gives a decent estimate.

3.1 PROPULSION

The robot need to cope with climbing and acceleration. In addition to this, it also has to withstand the drag forces and rolling resistance.

3.1.1 Climbing

The robot needs to be capable of driving up hills. When it does, the weight can be seen as two components: one parallel to the surface, and one perpendicular. The parallel force will try to pull the robot down the hill, a gradient resistance. In equation (3.1), sine of the hill angle is multiplied with the vehicle weight. This results in the force trying to pull the vehicle down.

$$F_g = mg \cdot \sin(\alpha) \quad (3.1)$$

where:

F_g is the gradient resistanse

m is the vehicles mass

g is the gravitational constant with a value of 9.81 m/s^2

α is the hill angle

How the forces are applied to the vehicle can be seen in Figure 3-1.

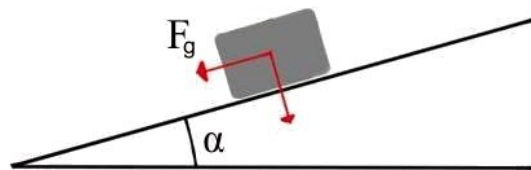


Figure 3-1: Gradient resistance

3.1.2 Acceleration

For a motor to accelerate, it needs torque equal to the desired angular acceleration multiplied with the mass moment of inertia of the motor. In this case, the motor will be connected to a

powertrain and the moment of inertia must therefore be calculated for each of the components with respect to the motor.

To obtain the mass moment of inertia for the vehicle with respect to the motor shaft, the mass must be divided by the number of wheels with propulsion, and then multiplied with the squared radius of the wheel. The equivalent moment of inertia is calculated with respect to the motor shaft. All of these put together results in Equation (3.2), which describes the how the acceleration torque is calculated.

$$M_A = \alpha_A \left(I_A + \frac{I_B}{(i_{A \rightarrow B})^2 \eta_{A \rightarrow B}} + \frac{I_C + \frac{m}{n_w} r_w^2}{(i_{A \rightarrow C})^2 \eta_{A \rightarrow C}} \right) \quad (3.2)$$

where:

M_A is the acceleration torque of shaft A

α_A is the angular acceleration of shaft A

I is the moment of inertia of each shaft

i is the gear ratio of each shaft

η is the efficiency between each transmission stage

m is the vehicles mass

r_w is the radius of the wheels

n_w number of wheels

3.1.3 Drag Forces

When a vehicle is driving, the air that flows around the body will generate air resistance, or drag force. The magnitude of this force increases with the squared speed of the air relative to the vehicle. For high speed applications, this force can have a huge negative impact on the efficiency of the process. For low speed application, drag forces from wind can reduce the efficiency more than the vehicles speed.

Different vehicles have different shapes, and logically they behave different when exposed to flowing air. A drag coefficient describes the vehicles ability to cut through the air. By testing the vehicle in a wind tunnel, a precise drag coefficient for that particular shape can be determined.

Of course, the density of the fluid needs to be taken into account. Normally, this fluid is air, but in other applications it can be other fluids. The final factor in this calculation is the area of the vehicles projection where the wind impact, usually the front of the vehicle. The drag force on a vehicle is calculated with equation (3.3).

$$F_D = \frac{1}{2} C_D A \rho v^2 \quad (3.3)$$

where:

F_D is the drag force

C_D is the drag coefficient

A is the area of the vehicles projection

ρ is the density of the fluid

v is the speed of the fluid relative to the vehicle

3.1.4 Rolling Resistance

When a body rolls on a surface, there is a force resisting the motion of the body. When the weight of a vehicle is applied to a wheel, the wheel will be deformed. All of the energy consumed by this deformation is not recovered when the pressure is removed. The consequence of this energy loss is a force resisting the movement of the vehicle. This force, the rolling resistance, is calculated by multiplying the normal force on the tire, from the ground, with a coefficient. The value of the coefficient depends on the type of the tire and the foundation the vehicle drives on.

$$F_r = C_{rr} N \quad (3.4)$$

where:

F_r is the rolling resistance force

C_{rr} is the resistance coefficient

N is the normal force

3.1.5 Minimum power requirements

The terrain in agriculture varies from big flat stretches of land, to small hilly fields. The agricultural robot, of course has to be capable of working on variable terrain. This makes it hard to calculate the power requirements, since it depends on the robot's module set up, and which tool is functioning.

The propulsion motor has to be strong enough for the robot to overcome the forces from rolling, gradient, and air resistance with maximum load. The following calculation are done with "worst-case scenario" in terms of continuous loads and incline:

- Incline: 10°
- Weight: 400 kg
- Wind speed: 15 m/s
- Vehicle speed: 5 km/h

With these factors in mind, and the gravitational acceleration, g , set to 9.81 m/s², equation (3.1) results in a gradient resistance of 681.4 N.

The rolling resistance coefficient is calculated to 0.04, which is for tractor tires on wet earth road [39]. The online calculator used to estimate the rolling resistance coefficient is developed by using information from Wong [9]. Equation (3.4) results in a rolling resistance of 157 N.

To estimate an area of the robot’s projection, the contours of the first agricultural robot is manipulated to show lower towers, since this will be applied in Thorvald II. The frame is also made thicker, to compensate for a tool. The projection is shown in Figure 3-2, with an area of 0.64 m².

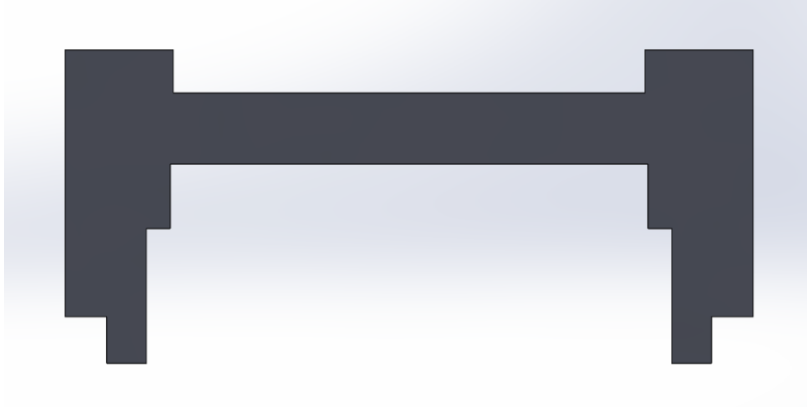


Figure 3-2: Projection of the front of the robot

The density of air is set to 1.293 kg/m³ [40], and the speed of the air relative to the vehicle is 16.5 m/s. The drag coefficient is set to 0.5, which is similar to an off-road vehicle [40]. By entering these values in equation (3.3) the result is a drag force of 56.3 N.

Table 3-1: Summary of the resistance forces

F _g , gradient resistance	681.4 N
F _r , rolling resistance	157 N
F _D , air resistance	56.3 N
Total resistance	894.7 N

The torque needed for acceleration can’t be calculated until the drivetrain is determined, and will therefore be used as confirmation after the components have been selected.

When the robot is driving with a speed of 5 km/h it has to generate:

$$\begin{aligned}
 P &= F \times v \\
 P &= 894.7 \text{ N} \times 1.38 \text{ m/s} \\
 P &= 1234.7 \text{ W}
 \end{aligned}$$

The power transmitted by each wheel have to be:

$$\frac{1234.7 \text{ W}}{4} = 308.7 \text{ W}$$

The robot will drive in rough and slippery terrain, and it will most likely lose traction on one of the wheels. With traction on only three of the four wheels, the power transmitted by each motor have to be:

$$\frac{1234.7 W}{3} = 411.36$$

The components must be selected with this in mind, and the combination should provide at least this amount of power.

3.2 STEERING

There are numerous parameters that influence the power requirements of steering. The parameters listed by Liljedahl et al. [41] can be seen in Table 3-2. Some of the parameters can be visualized in Figure 3-3.

When the traditional car is steering, they only have to generate enough torque to overcome the friction between the tire and the surface. An agricultural robot is a vehicle made for off-road driving, which means the torque has to be strong enough to get rid of mud if the wheel digs into the ground.

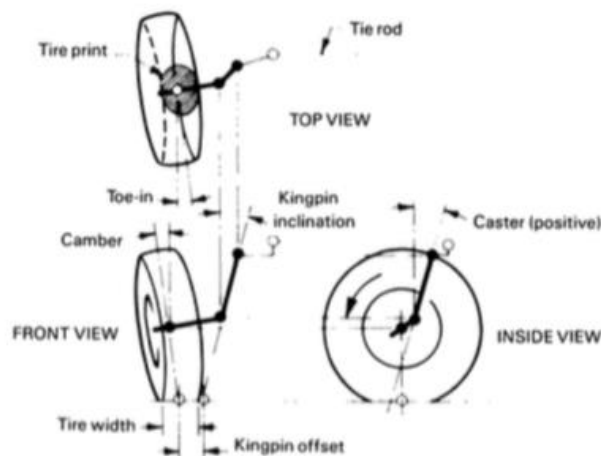


Figure 3-3: Ackerman steering. Image: Wittren 1975 [42]

The best suited condition for calculating maximum power requirements when using Ackerman steering, is when the tractor is stationary on dry, clean concrete. The heaviest steering loads normally take place in this condition [41]. On tractors, and agricultural robots, tire load is the most significant variable effecting the power requirements. Thorvald II will be able to use tools with a weight of 200 kg, which is more than the base-weight of the robot.

Table 3-2:Parameters that influence the steering power requirements

Tire loading
Road surface and soil conditions
Tire inflation pressures
Tire sizes and tread patterns
Kingpin inclination
Caster angle
Camber angle
Kingpin offset or scrub radius
Toe-in and toe-out
Tread settings
Travel speeds
Steering rates
System efficiency
Front-end type
Tractive and braking forces
Chassis type

The required kingpin torque to turn the wheel can be calculated using equation (3.5).

$$T = Wf \sqrt{\frac{I_0}{A_0} + e^2} \quad (3.5)$$

where:

T is the kingpin steering torque

W is the wheel load

f is the friction coefficient

I_0 is the polar moment of inertia of tire print

A_0 is the tire print area

E is the kingpin offset

Equation (3.5) assumes that the pressure from the tire print is uniform. Thorvald II will have wider tires than the first version. Standard tire dimensions indicate that 6.5” is a good alternative. If the precise tire print is unknown, a simplification can be done by considering the tire print as a circle with diameter equal to the width of the tire:

$$\frac{I_A}{A} = \frac{\frac{\pi D^4}{32}}{\frac{\pi D^2}{16}} = \frac{D^2}{8} \quad (3.6)$$

Since the modules with propulsion will have a kingpin-offset of zero, this component can be neglected. By inserting equation (3.6) in equation (3.5) the equation for steering torque can be written as:

$$T = Wf \sqrt{\frac{D^2}{8}} \quad (3.7)$$

In figure Figure 3-4 (a) is a curve that states the friction coefficient for a vehicle with no kingpin offset can be set to 0.7. In Figure 3-4 (b) it is shown that there exist an optimal kingpin offset for a minimum value of torque, however, higher offsets contribute to misleading shock loads further into the system. Therefore, a smaller kingpin offset, or center-point steering, are better suited for heavy loaded application in loose soil.

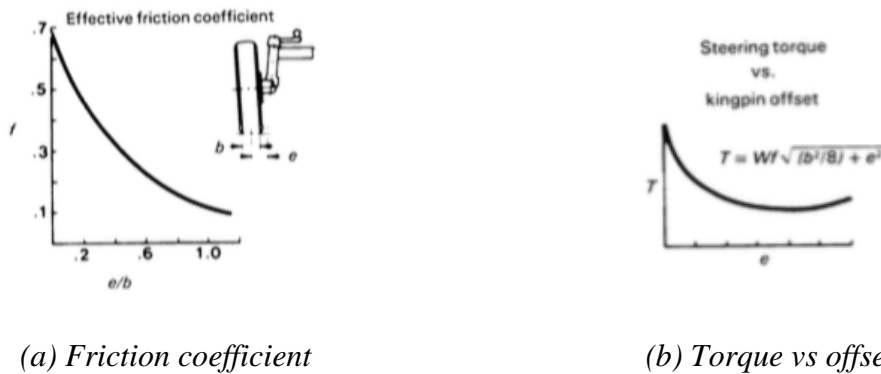


Figure 3-4: Typical curves based on rubber-tired vehicles on dry concrete. Image: Wittren 1975 [42]

The maximum steering torque is calculated using equation (3.7):

$$T = \frac{400kg \times 9.81 \text{ m/s}^2}{4} \times 0.7 \sqrt{\frac{(0.165 \text{ m})^2}{8}} = 40 \text{ Nm}$$

The steering motor has to provide a minimum torque of at least 40 Nm.

4 SELECTION OF COMPONENTS, MATERIALS AND ASSEMBLY TECHNIQUE

4.1 MOTORS AND TRANSMISSIONS

4.1.1 Motor

This project has a fairly short deadline, so it is natural to keep building on the groundwork done on Thorvald I. Electric motors running on batteries is a solution we have experience with from when the first robot was built. Since the new version will be very modular, each of the modules need its own system of motors and transmissions.

Unlike the combustion engine, the electric motor generates a lot of torque at low speeds, which is desirable according to the graph in Figure 2-1. The electric motor itself won't offer enough torque, and is thereby in need of a transmission. Fortunately, the speed can be varied with a motor controller, and the transmission only need one step. A BLDC motor will be used, due to the positive experience from the first robot. Even though it is more expensive, and need a more complex controller than the brushed motor, the advantages compensate for these two drawbacks. The brushless motors are still smaller, more efficient, and require less maintenance.

4.1.2 Drivetrain

The different alternatives are evaluated with the decision-matrix method, invented by Stuart Pugh. Different advantages and drawbacks are compared, and given points to make a classified selection [43]. This is only meant to give a good indication of the advantages and drawbacks of the different alternatives, and the results of the table will be evaluated before the final decision is made.

The drivetrain will be evaluated by the following criteria:

- Size – Compact size is preferable
- Efficiency – High effectivity is desired
- Price – Low price is always a benefit
- Durability – The components should be tough

Some criteria are more important than others; they will therefore be emphasized with different impact. We are interested in the best possible solution, so the price will have a fairly low value of 10 %. All of the possible solutions are properly tested in other applications, and are probably durable enough. Even though it is an important factor, durability will only have a value of 20%. Size and effectivity are the most important factors, and will therefore have a value of 35 % each.

Table 4-1: Evaluation of different gears

		Planetary gear		Spur gear		Helical gear		Herringbone gear	
Size	35 %	4	1.4	3	1.05	3	1.05	2	0.7
Efficiency	35 %	5	1.75	4	1.4	3	1.05	4	1.4
Price	10 %	2	0.2	4	0.4	4	0.4	2	0.2
Durability	20 %	4	0.8	4	0.8	5	1	5	1
Sum	100%	4.15		3.65		3.5		3.3	

Different gears are compared in Table 4-1, and as expected, size and efficiency are the deciding factors. The planetary gears are very efficient and compact compared to the other alternatives, and there will be no problem mounting it inside the wheel to obtain a narrow design of the module. It has more components than the other alternatives, and thereby it is a slightly higher risk of shortcoming. It also is more expensive than the the other gears, but it is still the preferable choice.

Table 4-2: Evaluation of belts and chain

		V-belt		Timing belt		Chain	
Size	35 %	4	1.4	4	1.4	4	1.4
Efficiency	35 %	3	1.05	5	1.75	5	1.75
Price	10 %	5	0.5	4	0.4	2	0.2
Durability	20 %	3	0.6	3	0.6	2	0.4
Sum	100%	3.45		4.15		3.75	

In Table 4-2, two different types of belt transmission and one transmission with chain are evaluated. All the alternatives are compact in size, as long as the wheels can be close together. The V-belt is considered less effective than the other alternatives because of the risk of slip. It is crucial that the transmission don't slip when used for steering. The chain is considered less durable than the others, even though it is made of a metal all the way. The reason for this assessment is the low tolerance of dirt and mud. In an agricultural robot all components must function intentionally, even in bad weather. The timing belt is as efficient as chain, but require more precision during the installation. Because of the bevels, there is no need for sensors to measure the speed, and adjust for slippage. Still, it is the better choice. The conclusion is that the timing belt and the planetary gear are the best alternatives.

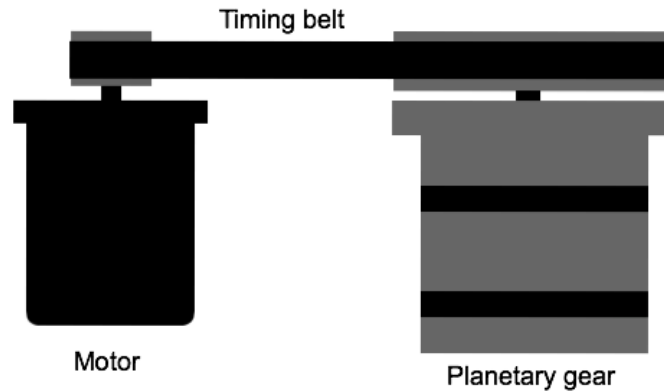


Figure 4-1: Example motor and drivetrain combination

To acquire a narrow construction, the gears will be mounted inside the wheel. However, the required reduction ratio for a BLDC-motor cannot be obtained with a single stage planetary gearbox. Rather than having two-stage planetary gears, which would make the module wider, a timing belt with a reduction ratio is used to combine the motor with the gearbox. This is showed in Figure 4-1. By using this method, the planetary gear can be positioned inside the wheel, providing a low center of gravity, while the lighter motor can be positioned outside of the wheel, and still be very efficient.

4.1.3 Propulsion Components

Electro Drives AS provided a lot of parts with good discounts during the process of building Thorvald I, and will also be included in the development of Thorvald II. For the propulsion, they provided motor and timing belts with pulleys.

Motor – 3Men BL840

3Men is a Taiwanese company that is specialized in electric motors and drivers. Propulsion motor from 3men was also used on the first robot, with positive results. The new motor has a little less power than the one used in Thorvald I, but generates more torque. The specifications of the motor can be seen in Table 4-3, and a picture can be seen in Figure 4-2.



(a) Regular view of the motor



(b) Side-view to see the modified shaft

Figure 4-2: 3Men BL840

The motor comes with integrated Hall sensors, but the encoder has to be bought separately. In Figure 4-2 b, it is shown that the motors have a modification where the shaft is longer. This is done for a hollow-bore encoder to be mounted on the backside.

Table 4-3: Specifications of 3Men BL840

Voltage	48 V
Speed	3000 rpm
Power	500 W
Continuous torque	1.57 Nm
Continuous current	12.8 A
Length	112.5 mm
Weight	3.5 kg

Planetary gears – Allweier PGR500

Allweier are specialists in machinery and compact solutions, and contacted us to see if we were interested in some of their products. The specification of the PGR500 gearbox are listed in Table 4-4, and a picture can be seen in Figure 4-3.

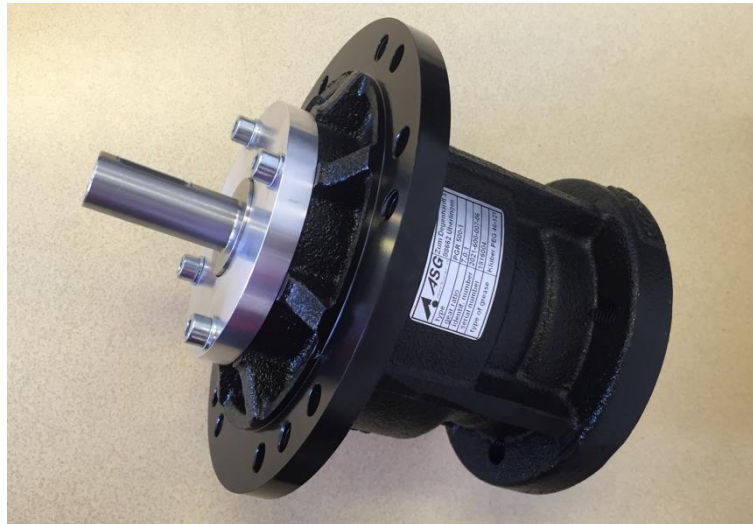


Figure 4-3: Allweier PGR500

The gearbox, consisting of spur gears, will be mounted directly in some modified wheels to make the module very narrow. A flange on each gearbox will be used to bolt it to the module, so the gearboxes have to bear the load of the whole robot frame. Allweier also provided the gearbox with an adapter making it possible to install the belt pulley directly on the gearbox.

Table 4-4: Specifications of the Allweier PGR 500 gearbox.

Number of stages	1
Gear ratio	7
Nominal output torque	160 Nm
Peak torque	500 Nm
Output acceleration torque	450 Nm
Nominal speed	3000 rpm
Maximum speed	6000 rpm
Protection class	IP67
Efficiency	96 %
Maximum radial load	7000 N
Maximum axial load	2500 N
Weight	7.3 kg

The PGR500 gears is really tough, and capable of loads up to 7000 N. With static conditions and a robot of 400 kg, we will have the following safety factor:

$$\frac{7000 \text{ N/kg}}{9.81 \text{ N} \times \frac{400 \text{ kg}}{4}} = 7.13$$

This is a high safety factor. When the robot is subjected to shocks during field operations, this should make the gears more than capable of resisting the shocks.

4.1.4 Timing belts

The timing belt between the motor and the gearbox will have a reduction ratio of 1:6, this will give a total reduction ratio of 42. The belt is made of polyurethane, and the design is illustrated in Figure 4-4.

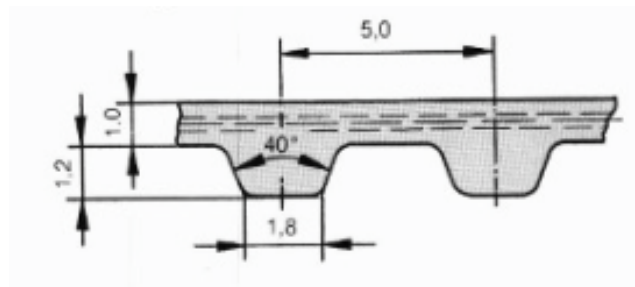


Figure 4-4: Timing belt. Image: Electro Drives

The pulleys are made of aluminum, and the essential specifications are listed in Table 4-5 [44].

Table 4-5: Specifications of timing pulleys

D	15.05	94.65
Number of teeth	10	60
Weight	12g	307 g

4.1.5 Wheels

Early in the design process Røwdehjul was contacted regarding wheels. They were really helpful during the design of Thorvald I, and had a great contribution this time as well. Different sizes were inspected, and a H-279 tire print was selected. This has a diameter of 401 mm, and a width of 165 mm [45]. The wheel can be seen in Figure 4-5.

The PGR-500 gears don't originally fit, so the wheels have to be modified. A new flange has to be made, that fits the gears. A spacer will be fixed to the original flange, and the new flange will be welded on with the spacer as templet. This will provide the desired offset on the wheels.



Figure 4-5: Wheel with H-279 tire print

4.1.6 Verification of Propulsion Components

The efficiency of a timing belt is usually greater than 95% [27], and will therefore be set to 0.95 for the following calculations. To estimate the required torque per motor at constant speed, the combined friction force (from chapter 3.1.5) will be multiplied with the wheel radius, and divided by the number of wheel with ground contact, and each of the reduction ratios efficiency.

$$M = \frac{894.7 \text{ N} \times 0.2\text{m}}{3 \times 0.96 \times 0.95 \times (7 \times 6)} = 1.56 \text{ Nm}$$

By dividing the required wheel power by the the total efficiency of the reduction ratios.

$$P_A = \frac{411.3}{0.96 \times 0.95} = 451 \text{ W}$$

Before the rest of the calculations can be done, the moment of inertia of the different shafts, shown in Figure 4-6, have to be determined.

The moment of inertia of the PGR500 gearbox is not listed in the datasheet. In the calculations the moment of inertia, the Apex Dynamics PL120 is used, and the value is set to 2.2×10^{-4} . The shaft has a diameter of 19 mm, which is the same as the PGR500 gearbox. The moment of inertia of the pulleys are calculated with equation (4.1), and for the wheel with equation (4.2). the weight of the wheel is approximately 4.5 kg.

$$I_{cyl} = \frac{1}{2} m_{cyl} r_{cyl}^2 \quad (4.1)$$

where:

I_{cyl} is the moment of inertia of the cylinder

m_{cyl} is the mass of the cylinder

r_{cyl} is the radius of the cylinder

$$I_{td} = \frac{m_{td} r_{td}^2}{2} \quad (4.2)$$

where:

I_{td} is the moment of inertia of the thin disc

m_{td} is the mass of the thin disc

r_{td} is the radius of the thin disc

The shafts need to be defined before the calculations can proceed.

Shaft A: The motor and the smaller pulley

Shaft B: The big pulley and the gearbox

Shaft C: The wheel

The different moment of inertia, gear ratios and efficiencies are listed in Table 4-6.

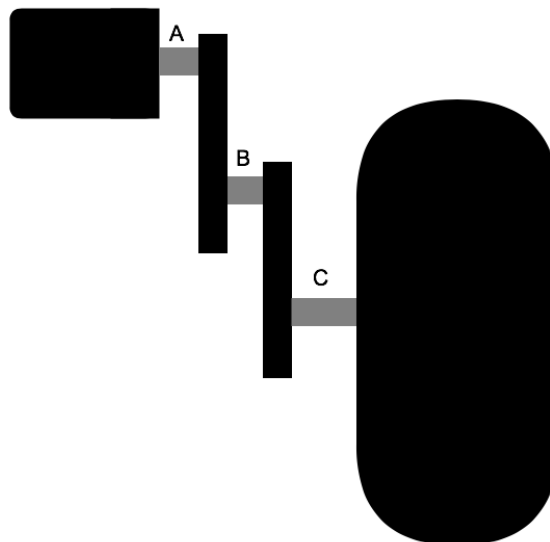


Figure 4-6: Simple drawing of the powertrain

The robot should have an acceleration of approximately 0.5 m/s^2 , so that the maximum speed will be achieved in under three seconds. With a wheel radius of 0.20 m , the angular acceleration of the motor shaft will be:

$$\alpha_A = \frac{0.49 \text{ m/s}^2 \times 6 \times 7}{0.20 \text{ m}} = 102.9 \text{ s}^{-2}$$

By inserting the required values in equation (3.2), we get an acceleration torque of 0.38 Nm per motor.

Table 4-6: Powertrain data

I_A	$2.98 \times 10^{-4} \text{ kg} \times \text{cm}^2$
I_B	$5.64 \times 10^{-4} \text{ kg} \times \text{cm}^2$
I_C	$0.09 \text{ kg} \times \text{cm}^2$
$i_{A \rightarrow B}$	6
$i_{B \rightarrow C}$	7
$\eta_{A \rightarrow B}$	0.95
$\eta_{B \rightarrow C}$	0.96

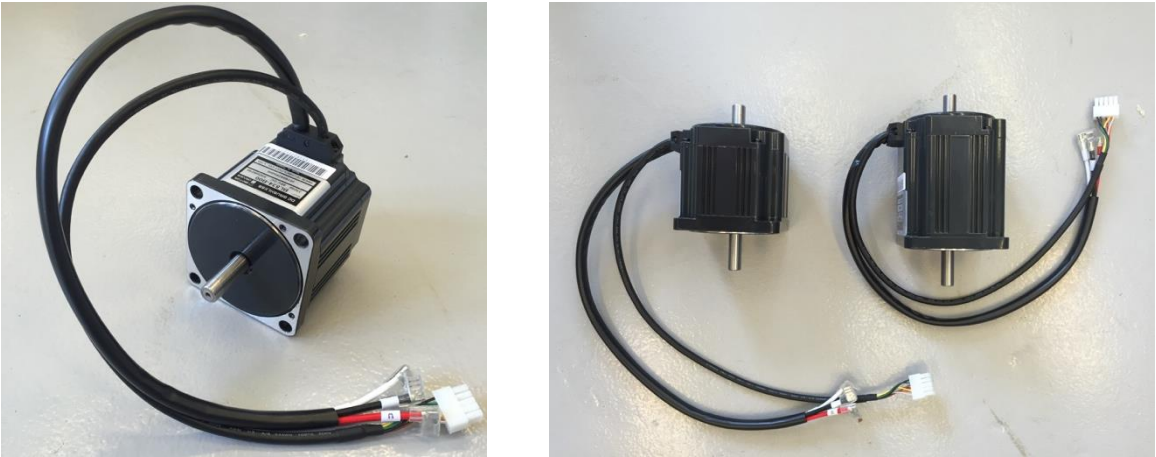
The rated continuous torque on the motor is 1.57 Nm. By the calculations above, the motor is strong enough to attain the requirements. With this set up, the maximum speed of the robot will be:

$$\frac{3000 \text{ rpm}}{42} \times \frac{\pi}{30} \times 0.2 \text{ m} \times 3.6 = 5.4 \text{ m/s}$$

4.1.7 Steering Components

Motor – 3Men BL830

The motor is shown in Figure 4-7, and the specifications of the motor are shown in Table 4-7.



(a) Regular view of the motor

(b) Size comparison of the two motors

Figure 4-7: 3Men BL830

This is the same kind of motor used for the propulsion, only a bit smaller both in size and power. A comparison of the steering motor and the propulsion motor is shown in Figure 4-7 b. Like the propulsion motor, this motor also has the shaft modification to fit a hollow-bore encoder.

Table 4-7: Specification of the 3Men BL830

Voltage	48 V
Speed	3000 rpm
Power	350 W
Continuous torque	1.10 Nm
Continuous current	16 A
Length	87.5 mm
Weight	2.5 kg

Planetary gears – Apex Dynamics AB060

The Apex Dynamics AB060 gearbox were provided by Electro Drives, and can be seen in Figure 4-8. The key specifications are listed in Table 4-8. This is a very efficient gearbox, and it is much lighter the the PGR-gears, which makes it well suited for the steering.

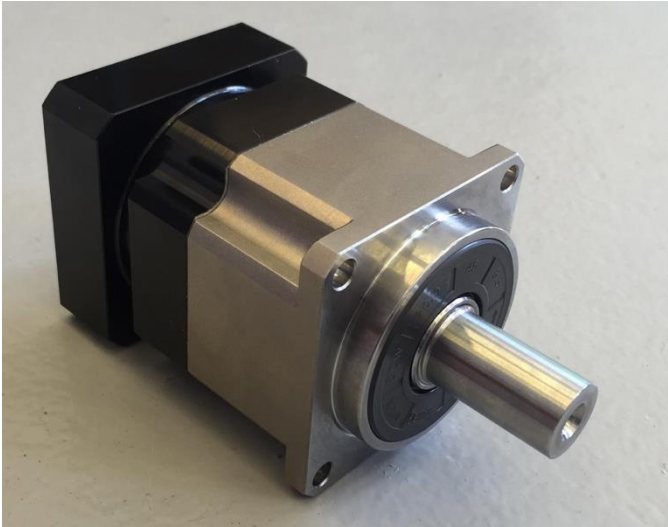


Figure 4-8: Apex Dynamics AB060

Unlike the Allweier gears, these are made up of helical gears.

Table 4-8: Specification for the Apex Dynamics AB060

Number of stages	1
Gear ratio	10
Nominal output torque	40 Nm
Peak torque	120 Nm
Nominal speed	5000 rpm
Maximum speed	10000 rpm
Protection class	IP65
Efficiency	97 %
Maximum radial load	1530 N
Maximum axial load	765 N
Weight	1.3 kg
Mass moment of inertia	0.13 kg•cm ²

4.1.8 Timing belt

The timing belt and timing pulleys used for the steering is the same kind as used for the propulsion. The reduction ratio is 1:5, where the smaller wheel has a diameter of 15.05 mm, and the bigger wheel has a diameter of 75.55 mm.

4.1.9 Inductive sensor

For the homing process, an inductive sensor is needed to get a reference point. Autonics PR12-2DP is selected.

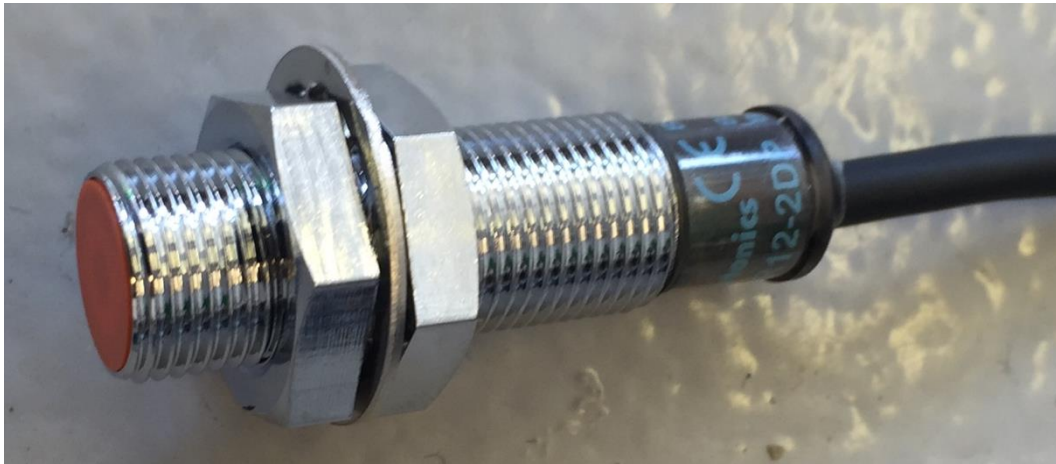


Figure 4-9: Autonics PR12-2DP

4.1.10 Verification of Steering Components

By multiplying the torque and reduction ratio listed in Table 4-7 and Table 4-8 with the efficiencies, the result is the torque provided rotating the wheel.

$$1.1 Nm \times 5 \times 10 \times 0.98 \times 0.97 = 52.3 Nm$$

As specified by the calculations done in chapter 3.2, the torque generated is sufficient for the wheel to rotate in the toughest conditions.

This value is higher than the nominal torque output of the gearbox, and for short periods of time, the motor is able to generate three times this amount of torque. Even though this power will surpass the emergency stop torque of the gearbox, a software limit should be added. If the torque exceeds 60 Nm, there probably is a mistake and the robot should be shut down for safety reasons. Even during harsh conditions, the torque will never reach this value, and the limit should be set to 1.26 Nm engine torque, which corresponds to 60 Nm gearbox output torque.

4.1.11 Motor controller

The robot will be controlled by the same network as the first robot, CANopen. The motor controller has to be applicable with this network, and the set up and programming of the motor controller will be done by Lars Grimstad.

Electro Drives suggested the Nix Digital Servo Drive, which is very compact, and still have high performance. It has one channel capable of a continuous current of 10 A, a maximum current of 20 A, and a maximum voltage of 48 V. It of course supports CANopen.

The Roboteq FBL2360 is a controller with two channels capable of a current of 60 A each, that can be combined to one channel of 120 A. It can handle a voltage of 60 V. This also supports CANopen, and is recommended for automatic guided vehicles. A big advantage is that this controller has two channels, and thereby can one controller be used for both propulsion and steering.



Figure 4-10: Roboteq FBL2360. Image: Roboteq

From the first robot, the experience with controllers from Roboteq was positive. The program made for the robot is well suited for this brand. Even though the NIX controller is very compact, we would have to use two controllers in each module, since it only has one channel. Seen in Figure 4-10 is Roboteq FBL2360, the choice of controller for Thorvald II.

4.1.12 Encoder

The incremental encoder is selected because it measures the motion of the shaft, and not the actual position like an absolute encoder. Even though the homing process can be eliminated with an absolute encoder, it can only rotate one round. In this case, the encoder will be positioned on the motor, which will make an absolute encoder go through to many revolutions.

Autonics E-40 is an incremental encoder with hollow shaft made for narrow space. It has a resolution of 1024 pulses per revolutions, and are made to fit directly on the modified motor shafts. This model will be used both for propulsion and steering. The encoder is shown in Figure 4-11.



Figure 4-11: Autonics E-40 hollow-shaft

4.1.13 Caster wheel

A trip to Røwdehjul was arranged to look at different wheel solutions. They had caster wheels that will fit well for the caster-module. Unfortunately, this cannot be delivered before the thesis is sent to printing, and no picture has been taken. The casters are very durable, and the men at Røwdehjul says it is more than tough enough for our robot [26]. No datasheet of the caster is available.

4.2 MATERIALS AND ASSEMBLY TECHNIQUE

4.2.1 Materials

One of the most important demands of this construction is low weight. The weight of aluminum is a third of the weight of steel. When assembled with the right methods, aluminum constructions can be much lighter than a steel construction of the same strength. However, the material itself is not as strong as steel, and should therefore not be used in the most critical parts.

The materials are provided by Stena Stål, Ås VGS, and the workshop at NMBU. For most of the components, aluminum of the 5000-series is used. The bearing house, the axle, and the parts used to combine the modules and the frame, need to be more durable than others. Steel of s355 2J will be used on these components.

The design must be done to protect the materials against corrosion. Limber holes will be integrated in the design, so water can seep out if condensate occur. Gatherings of water are one of the main reasons for corrosion. The components are going to be protected by applying a protective coat. For the steel components, Quick Bengalack will be used; a primer developed especially to protect metal against corrosion[46]. Powder-coating is highly resistant against

corrosion, and can be used on the aluminum components, the drawback is that damages are difficult to repair. Aluminum can also be anodized.

4.2.2 Assembly technique

On the prototype, the main assembly technique was glue. Because of availability, another adhesive than preferred was used, and it did not hold. The frame therefore had to be bolted together, even though it was not constructed for this method. With this incident in mind, gluing will not be used as main technique during the assembling of Thorvald II.

Most of the steel components will be welded. This is a fast and strong way to combine the components, but it is a permanent solution. It has to be possible to dismantle the module from the frame when it is combined, and these components will be bolted even though they are made of steel.

For the aluminum parts, most of them will be riveted. This provides a stable construction, that are more compact than a solution with bolts. Bolting would be more practical in terms of dismantling, but it also comes with a risk of the bolts to loosen. The rivets can easily be removed by drilling them, and this will not damage the construction material. The foot is supposed to be waterproof, and to prevent water from leaking in, glue or joint filler will be used between the riveted surfaces.

The riveting is done by Øystein Sund, who is an experienced flight mechanic. Since a compact size is such a high priority, the positions and numbers of the rivets will not be planned until the parts are made. Riveting requires some space, and it is therefore easier to place them when the whole construction can be felt physically.

5 CONTROL AND CONNECTIONS

For the robot to handle the necessary tasks, all of the components need to communicate with each other. Since it is supposed to be autonomous, it needs to be able to handle all by itself. It need to know the position and the orientation at all time. For this to happen, the motors have to be equipped with a couple of sensors, and a motor controller.

This thesis will examine the necessary connections for the system to control the robot, and implement them on a PCB. The components were ordered from Elfa Distrelec and RS, and are listed in Table 5-1.

Table 5-1: Components for the PCB

Component	Model	Quantity
Resistor	-	4
Transistor	NPN	4
Terminal	Phoenix MKKDS 1/5-3.81	1
Terminal	Phoenix MKKDS 1/6-3.81	1
Terminal	Phoenix MKKDS 1/8-3.81	1
Terminal	Phoenix MKDS 1/2-3.5	1
Fuse holder	Littleuse 178.6164.0001	1
Switch	Knitter-switch MMP 1010 D-1	1
DC/DC-converter	Recom R-78HB12 0.5	1
D-sub connector	Harting 25 way right angle	1
LED	3mm	1
Earth block	4-way RS pro	1
Molex connector	Microfit	1

The circuit diagram is shown in Figure 5-1. The Roboteq FBL2360 receives signals from a 25-pin D-sub connector. This is very practical in reality, but it makes the circuit diagram quite chaotic. The different pins are numbered in the figure, and to make it easier to see what their function is, and what they are connected to, this is listed in Table 5-2. The pins that don't are listed in the table are unused.

Most of the terminal blocks used, belongs to the MKKDS series, these have two floors and thereby uses less space. Most of the terminals leads to the D-sub.

Table 5-2: The function of the different pins on the D-sub

D-sub pin	Application	Output
1	D-sub GND	A10, B2, B4, B8
2	RS232Tx	A11
3	RS232Rx	A5
8	CanLo	B3, B5
12	Encoder 1B	A7
15	Digital in	A6
18	Digital out	A12
20	CanHi	B11, B13
21	Encoder 2A	A3
22	Encoder 2B	A9
24	Encoder 1A	A1
25	5V out	A2, A4

In addition to this, the MKKDS terminal with 2x5 terminals and the Molex contact are placed on the board. These are connected to each other, but not to the rest of the circuit. The motor controller needs information from the hall sensors, and a “passage” is made on the PCB to make it more organized. This passage is also used to deliver a voltage of 5 V to the encoders. The earth block is providing a voltage of 48 V to the motors, and is placed outside of the PCB due to the high currents required.

For the capacitor (B10 & B12) to charge, the logic in the motor controller have to be turned off, and no current can flow through the DC/DC-converter. This is done with the Power CTRL Out terminal in combination with the transistors.

The LED light is just used for practical reasons, and will light up when the 12 V trace is active. The 12 V terminals are connected to the inductive sensor. The 5 V terminals are leads to the encoders.

Pin 2 and 3 will not be used during normal conditions. The motor controller has a USB port that can be used for almost the same applications. If the USB-port is defect or doesn't support the current request, the RS232Tx and the RS232Rx are needed.

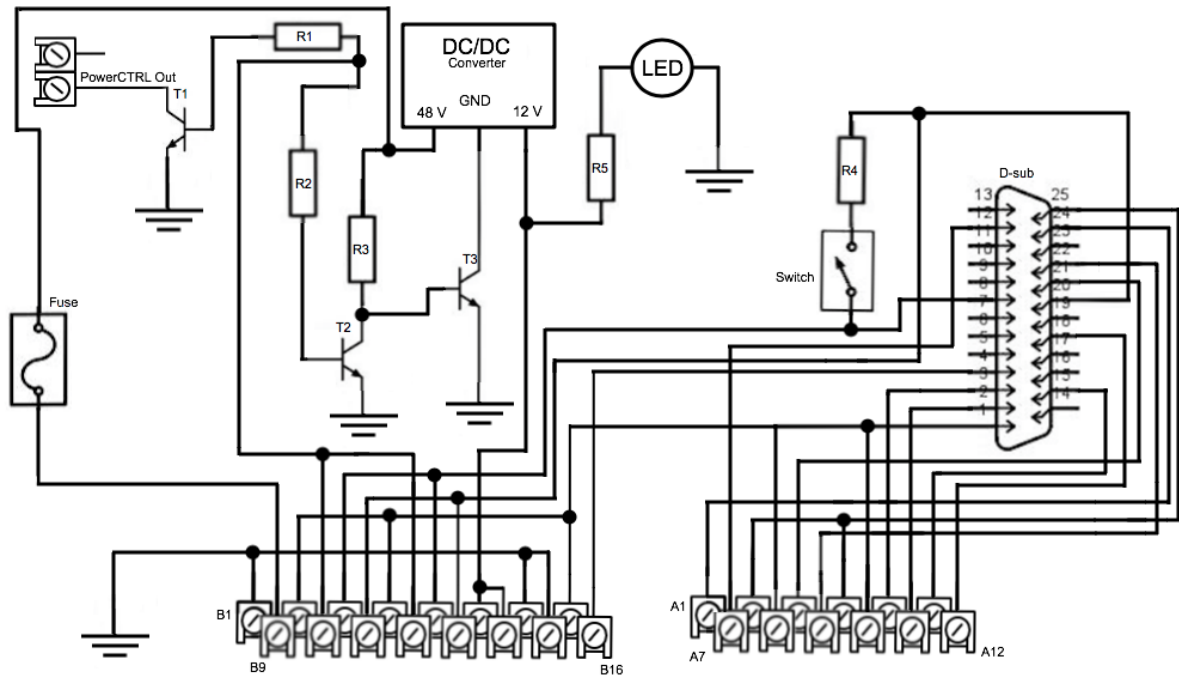


Figure 5-1: Circuit diagram of the PCB

The PCB is designed with Autodesk 123D circuit. All the footprints are drawn in and placed at the board with this program. The result is illustrated in Figure 5-2.

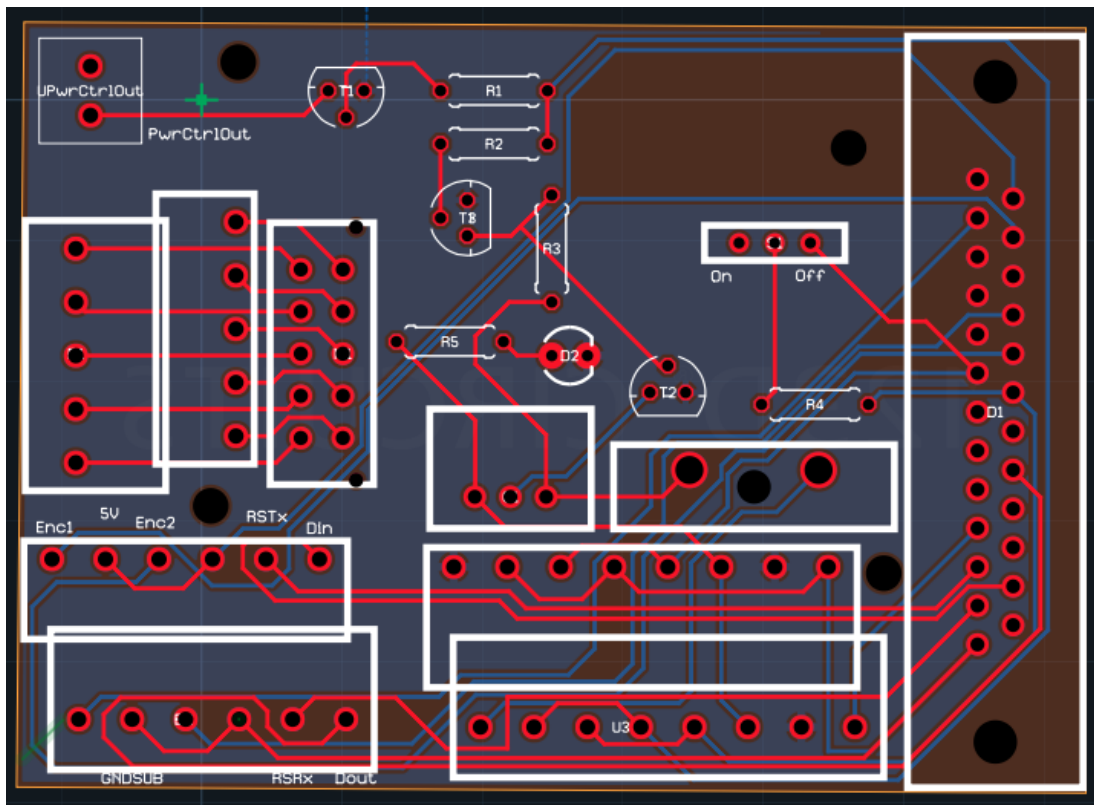


Figure 5-2: Picture of the PCB

6 DESIGN OF THE MODULES

6.1 PROPULSION FOOT

The propulsion foot will be used for both the main module, and the module with only propulsion. The foot's objective is to give power to the wheel, and make the robot move. During the designing process, weight and narrowness had highest priority.

The construction is quite complex, but also very stable. Since aluminum is the material used in all the parts, the changes are radical when compared to the prototype, where everything was welded steel. U-beams are used as a mid-layer to add great stability when the plates are riveted together with it. The width of the U-beams is chosen to 40mm so timing belt and timing pulleys can be installed inside of the module. This will provide great protection of the timing belt and pulleys. The gearbox doesn't fit directly on the module, and a spacer is installed to adjust the positioning.

Two brackets are combining the support beam with the foot. The bent bracket is used as one of the walls for the box protecting the motor. Not shown in the exploded view are lids fitted on the end of the motor box and the support beam, which protects the motor from water.

An exploded view of the propulsion foot is shown in Figure 6-1

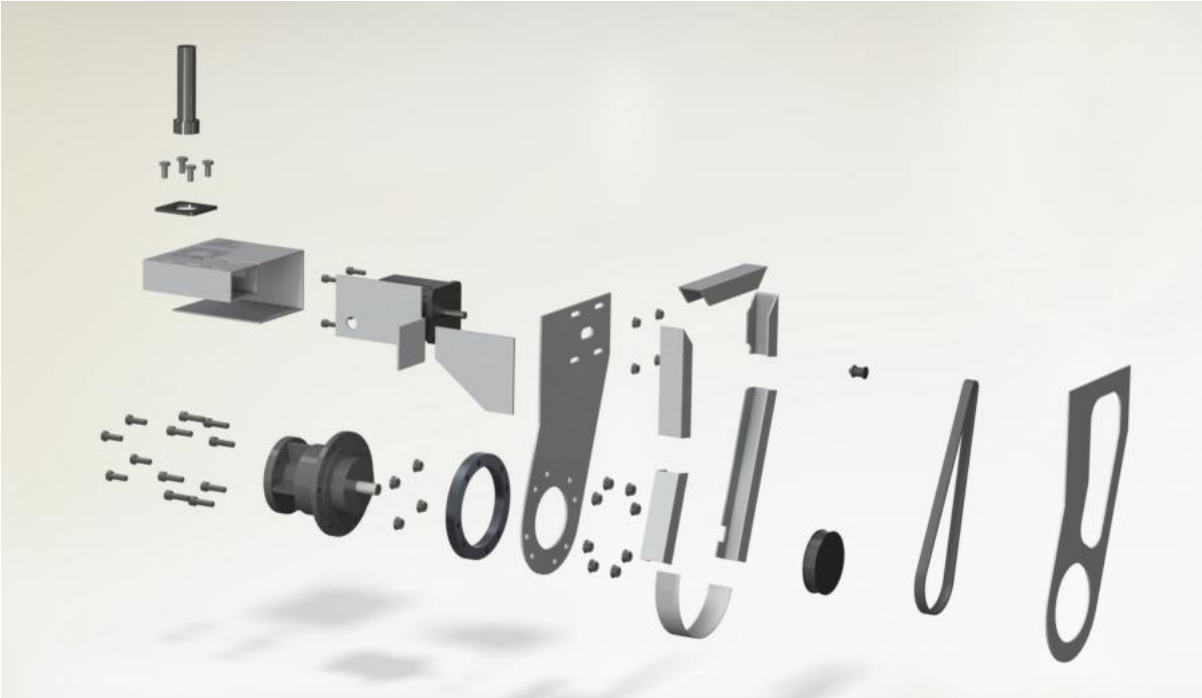
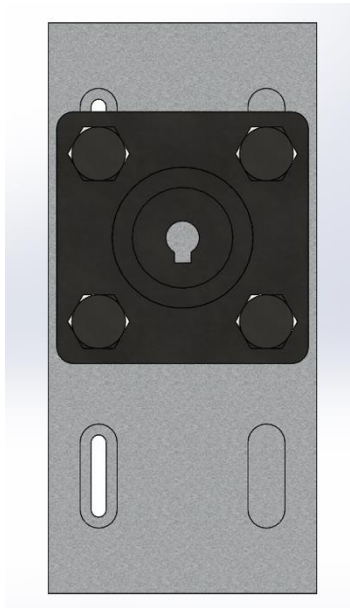
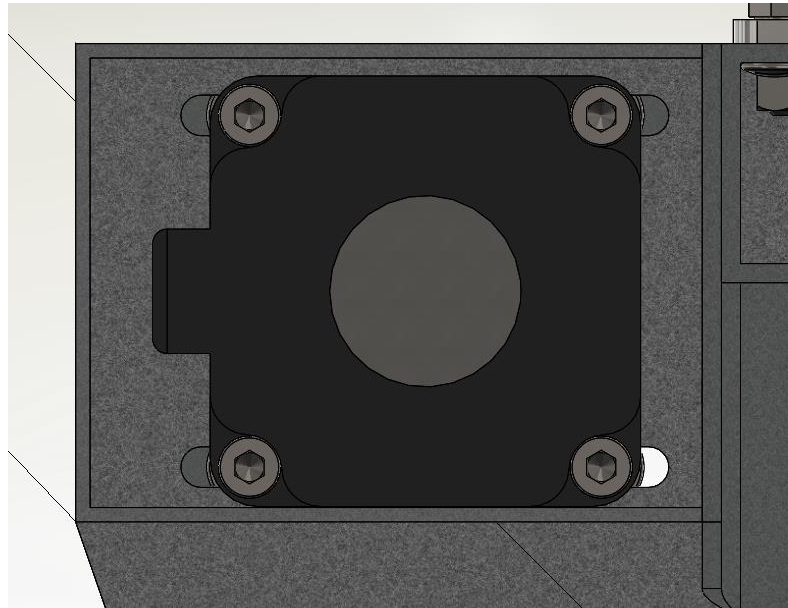


Figure 6-1: Exploded view of the propulsion foot



(a) *Steering shaft*



(b) *Motor*

Figure 6-2: Adjustments of shaft and motor

Seen in Figure 6-2 is the adjustment possibilities of the foot. One of the main goals of this thesis is to make the new modules very modular. If someone wants to use another wheel than the one currently mounted, the position of the steering shaft can be adjusted in or out. The modules are dimensioned with no kingpin-offset, and this offset can be kept even if someone changes the wheel. If the kingpin off-set is changed, it will be harder for the modules to turn around their own axis.



Figure 6-3: The propulsion module

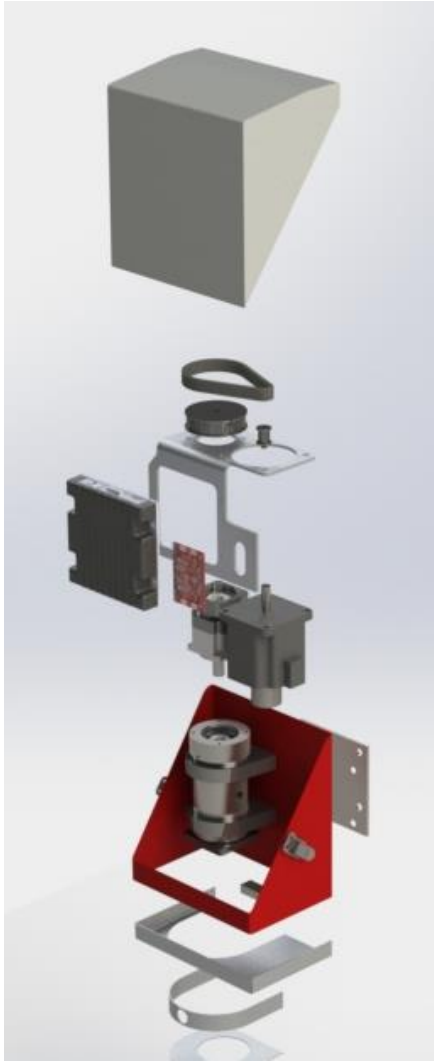
The finished design of the propulsion foot is shown in Figure 6-3.

6.2 TOWER

The tower construction is all about utilization of space. There are many components in this assembly, and they have to be position smart to make room for all of them. Exploded views of the whole tower and the bearing house are illustrated in Figure 6-4.

To motor in the tower is flipped over, and a belt transmission is inserted between the motor and the gearbox. This is to make the construction as compact as possible. A bent brack of aluminum is fastened to the gears, and bears the loads of the motor, the motor controller, and the PCB. This makes all the loads distributed to the welded rings on the bearing house. The floor and cabinet only needs to function as protection. A rubber packing is fitted between the cabinet and the top-cover, to keep water from leaching in.

The welded rings are made of steel, along with the bearing house, bearing house lid, and the axle. These parts are holding the whole load of the robot, and have to be very durable.



(a) The whole tower



(b) The bearing house

Figure 6-4: Exploded views

In figure Figure 5, a cross-section of the bearing house can be seen. The roller bearings are subjected to preloads by the axle, and a nut screwed on the axle. To protect the bearing from water and dirt, a seal is inserted at the bottom. This is provided by TTP seals.

Both the bearings and the seal are produced to be installed in H8 fittings.

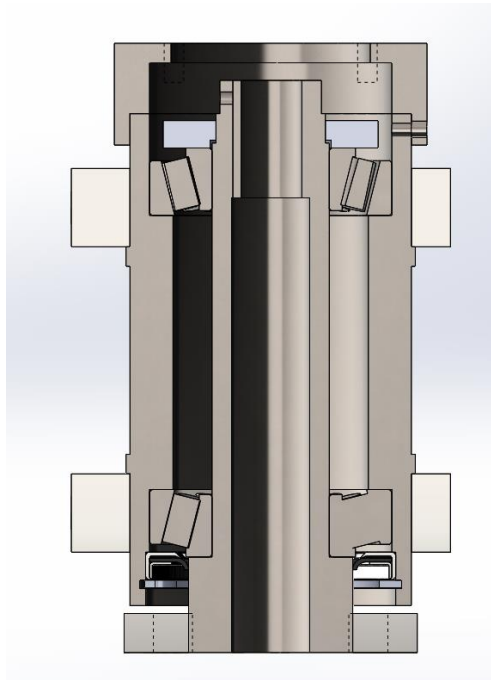
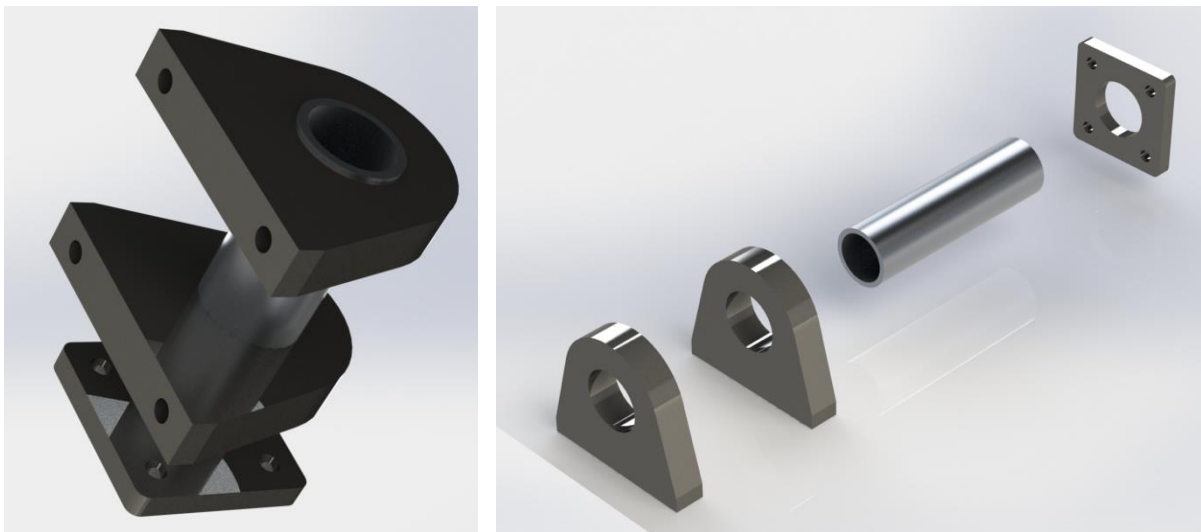


Figure 5: Cross-section of the bearing house

6.3 PROPULSION MODULE

For the module that only provides propulsion, only small modifications are done. The propulsion foot will be identical to the one used for the main module, but the tower will be modified. In Figure 6-6 the modifications can be seen.

Almost every component of the tower is removed, but the cabinet and the motor controller will be kept. The flange that combines the steering tower and the propulsion module is modified to fit a 40 mm tube instead of the steering shaft. The welded rings have the same modification; the hole-diameter is reduced from 72 mm, to 40 mm. The length of the tube is set to 146 mm to ensure that the total height of this module is the same as the height of the main module.



(a) *Assembly*

(b) *Exploded view*

Figure 6-6: Modifications done for the propulsion module

6.4 CASTER MODULE

The caster module will have its origin in the caster provided by Røwdehjul. However, this has not been delivered yet, and no measurements is available. The current design plan is to have similar rings as for the propulsion module, and a longer tube with a flange that is formed for the caster wheel. This will be a fast, simple and lightweight solution. The design plan is shown in Figure 6-7.



Figure 6-7: Design plan of the caster module

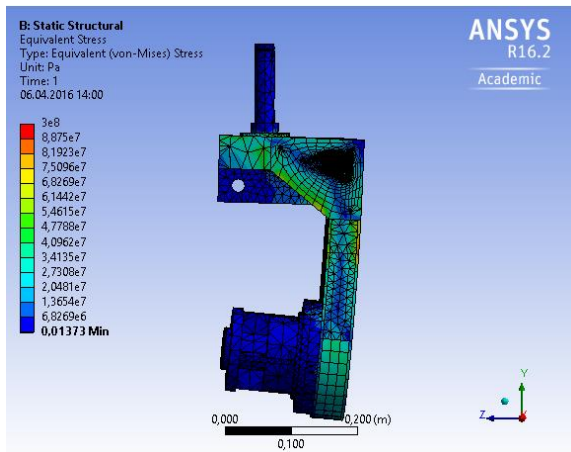
6.5 VERIFICATION OF LOADS

6.5.1 ANSYS

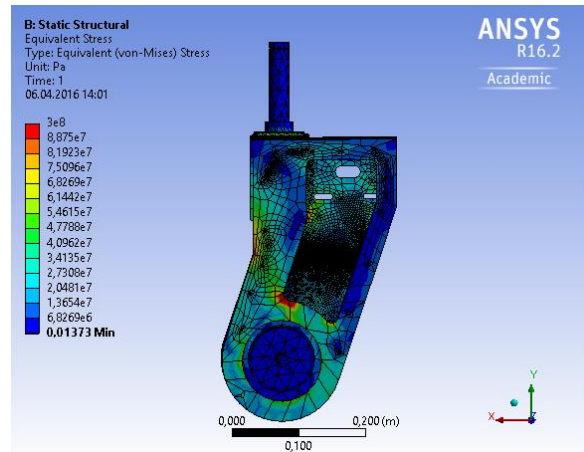
To confirm that the design is strong enough, ANSYS Workbench 16.2 is used for the analyzation. In the foot assembly, all the parts that's not applied by loads are suppressed. This is done to avoid error sources.

Three different situations are evaluated. They are all very similar, the only difference is the thickness of the foot covers. In situation 1, both of the foot covers have a thickness of 3 mm, and a smaller radius of the fillets. Of the two covers, the back cover will take the bigger part of the load. Therefore, situation 2 will have a back cover made of 4 mm plate, while the front cover is kept at 3 mm. In situation 3, both of the foot covers will be made of 4 mm plate.

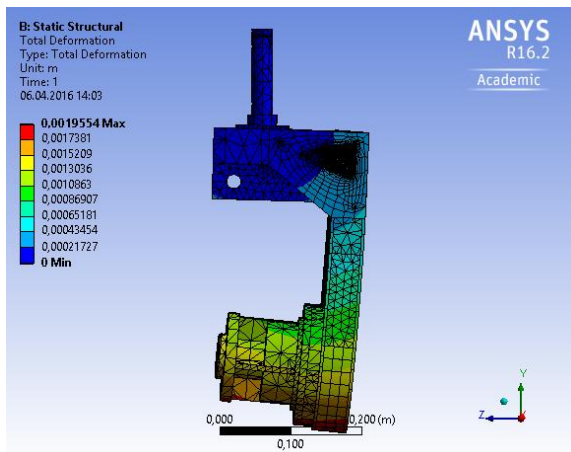
For the result to be as realistic as possible, a load of 2000 N is positioned at gearbox, directly under the steering axle. The axle is fixed. The robot is rated with a maximum weight of 400 kg, which would yield 100kg on each wheel. Most of the time, 50 kg will be the load of each module. The applied load is twice the size of the worst case scenario. The following figures shows the equivalent stress and the total deformation of the different situations.



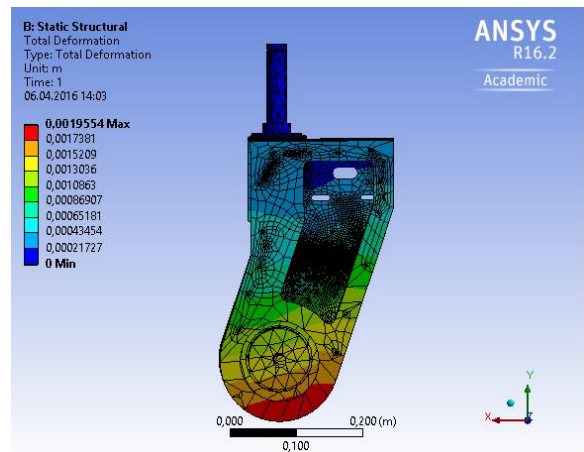
(a) Equivalent stress - Side



(b) Equivalent stress - Front



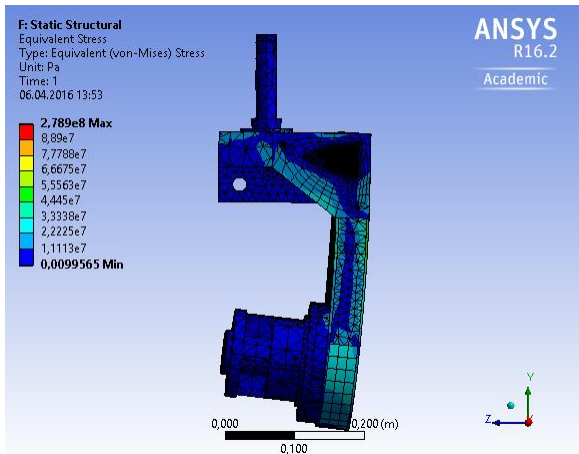
(c) Total deformation - Side



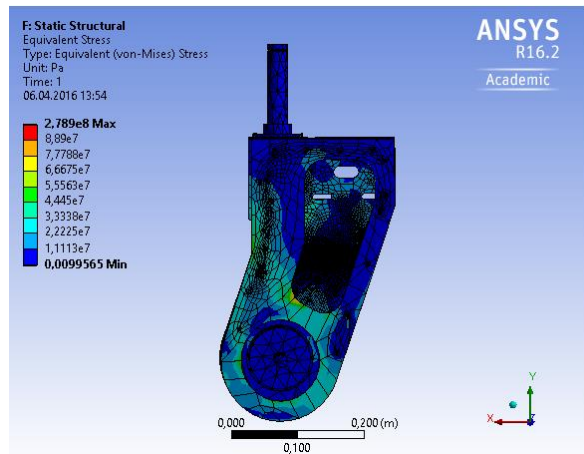
(d) Total deformation - Front

Figure 6-8: ANSYS analysis for situation 1

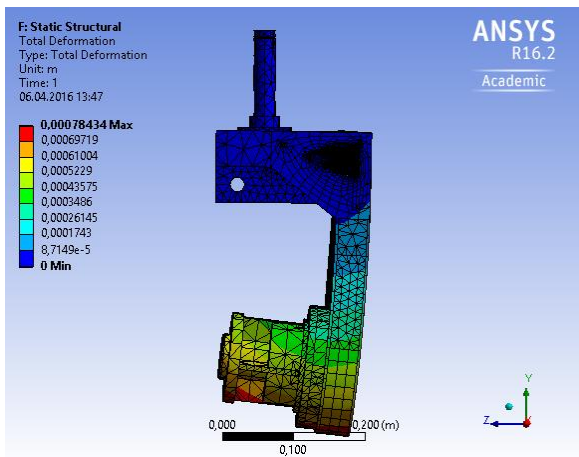
Figure 6-8 shows the results for situation 1. The scale shows that the highest value of stress is 300 MPa, which occurs in the areas marked with red. In this situation, this is on the crooked section straight under the axle. This is as expected, since this is the main direction of the applied load. These small areas have significantly larger values than the rest of the construction, where the values seldom exceeds 88.75 MPa. The total deformation is naturally maximal at the bottom of the foot, with 2 mm deviation.



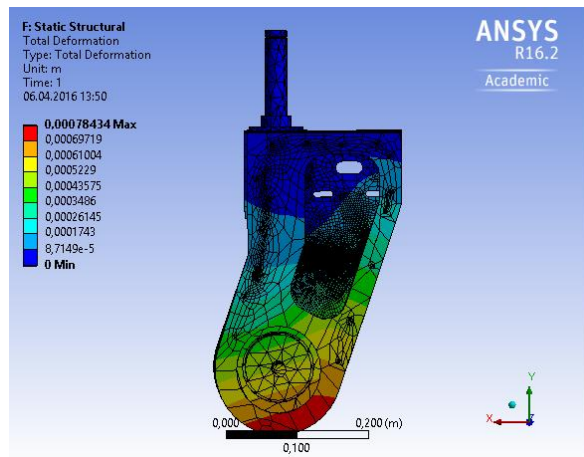
(a) Equivalent stress - Side



(b) Equivalent stress - Front



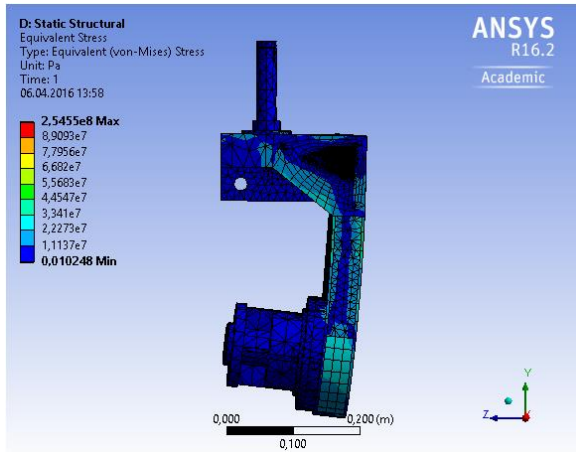
(c) Total deformation - Side



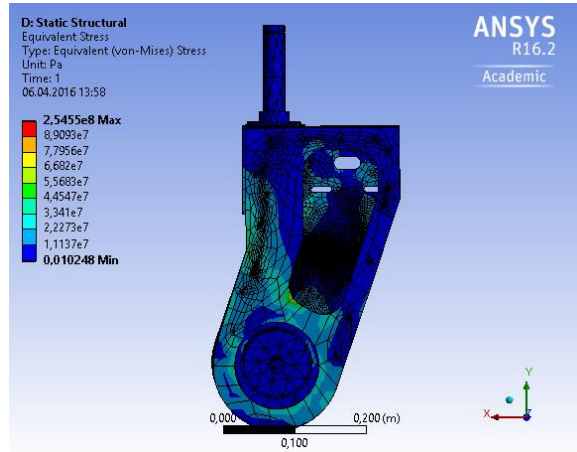
(d) Total deformation - Front

Figure 6-9: ANSYS analysis for situation 2

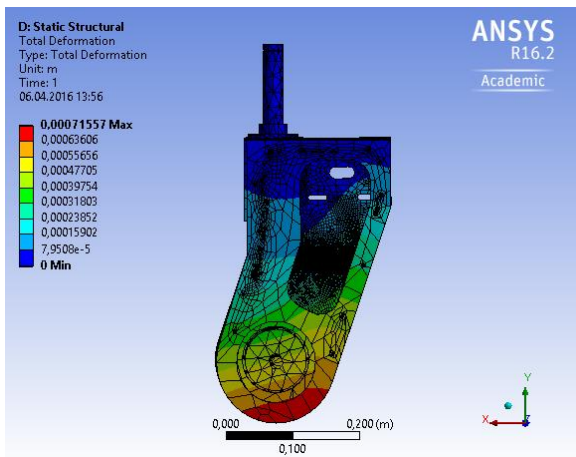
Figure 6-9 shows the results for situation 2. The highest value is 279 MPa, but only appears in small concentration points. Apart from this, the stress doesn't exceed 88.9 MPa, and rarely exceeds 50 MPa. The total deformation is reduced to 0.8 mm. As expected, the values are highly reduced when the back cover is thicker.



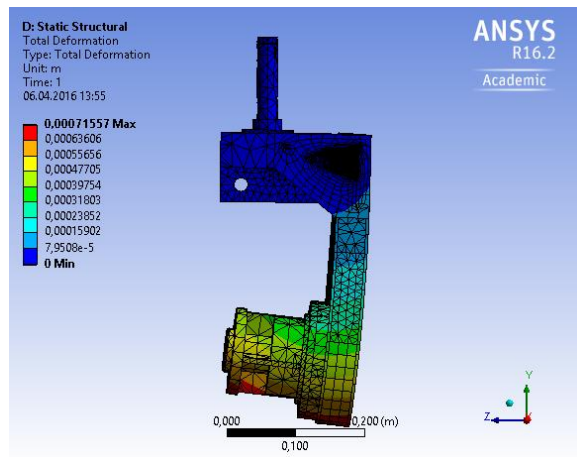
(a) Equivalent stress - Side



(b) Equivalent stress - Side



(c) Total deformation - Side



(d) Total deformation - Side

Figure 6-10: ANSYS analysis for situation 3

Figure 6-10 shows the results for situation 3. The equivalent stress is now much lower, and rarely exceeds 40 MPa. The maximum stress is still very high, 255 MPa, but is nowhere to be seen on the construction. This could probably be avoided with different meshing. The deformation is 0.7 mm.

From Table 2-1, the yield strength of 5000-series aluminum is 195 MPa. The stresses in the construction gives a safety factor of:

$$n = \frac{195 \text{ Mpa}}{40 \text{ MPa}} = 4.875$$

Logically, this should not give any deformation. Even though ANSYS gives a deformation of 0.7 mm, this is probably due to other values of yield strengths. Because of the risk of concentration points, situation 3 is used in the design.

6.5.2 Roller Bearings

SKF was contacted for calculations of roller bearing loads. Rather than providing formulas, they provided finished calculations [47]. They had the dimensions of the module, and these assumptions were made:

- All the weight distributed to one module, $F_r = 4\text{kN}$
- Speed = 100 rpm
- Temperature = 50°C

From the listed assumptions, it is clear that the calculations are very conservative. The recommended bearing is SKF 30206 J, which is the same bearing used in Thorvald I. From the calculations, this bearing should withstand a continuous drive of 3 years.

7 PRODUCTION OF THE ROBOT

Thorvald II is produced with Ås VGS and the workshop at NMBU. Bjørn, the new apprentice at NMBU, has just graduated from Ås VGS, and has full admission to the workshop there. The reason for the collaboration with Ås VGS, is that they have much better tools available than the workshop at the university. With the recently purchased plasma-cutter the production speed of parts is excellent. The design is adapted to take use of the plasma-cutter and the bending machine. With these production methods, files of the components are loaded into the machines, and they produce the components automatically. This eliminates the human error in most cases, and the precision is very high. The construction drawings are therefore easier to understand, since the only necessary measurements are for the bends and thickness.

When this thesis is printed, the production has started, but isn't finished yet. Therefore, the following pictures from the production are only of the propulsion foot.

In Figure 7-1 the bending machine is shown. This is primarily used for the tower, but one of the bracks on the foot is bent. The plasma cutter is shown in Figure 7-2. This is used for the cover plates on the foot, and every part made for the bending machine. The components for the foot made with the bending machine and the plasma-cutter are shown in Figure 7-3.

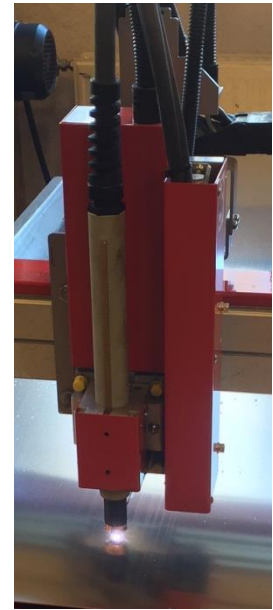
The U-beams seen in Figure 7-4 are cut, and the holes are processed in a CNC-machine. The support beam in Figure 7-5 is produced with the same method.



Figure 7-1: Bending machine



(a) The whole plasma-cutter



(b) In action

Figure 7-2: Plasma-cutter

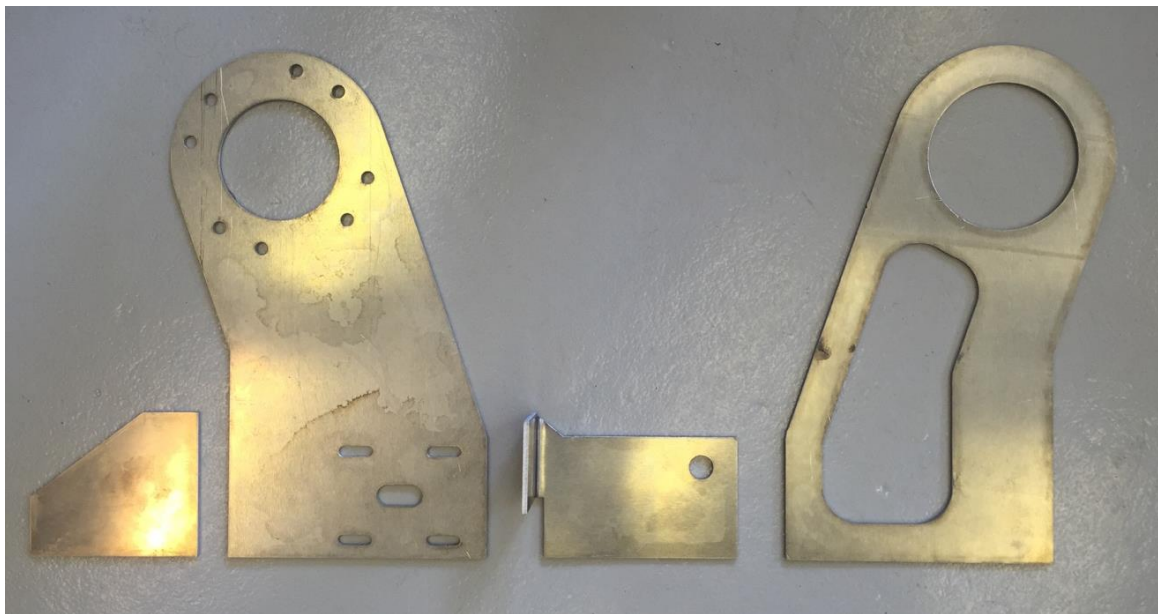


Figure 7-3: Side brack, foot covers and the bent brack



(a) Positioned



(b) All the U-beams

Figure 7-4: U-beams

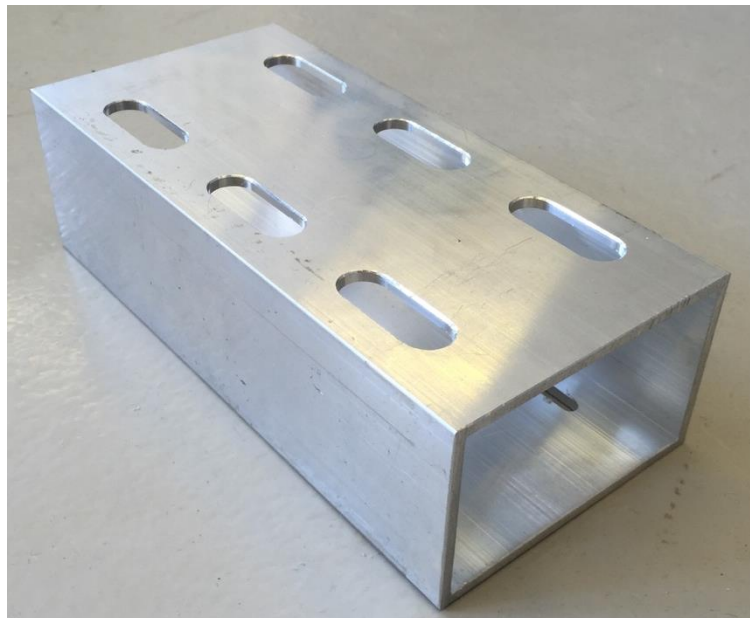


Figure 7-5: Support beam

The components are sent to the university as they are produced. A quick composition of the components was made to make sure that the dimensions are correct, this is visualized in Figure 7-6. As seen, the components fit just as they are supposed to.



(a) plain composition



(b) Composition with gear and motor

Figure 7-6: Compositions to verify the dimensions

8 DISCUSSION

The goals set for this thesis are quite ambitious; to design a product to the grade of 9 on the TRL-scale in only four months. The prototype provided a platform to develop further, so the main focus was to improve those parts that weren't good enough, and implement modularity in the modules.

Contact was quickly established with some of the companies the parts for the first robot was bought from, so the component selection for the new robot could start at an early stage. Other firms were also contacted, and even though they had similar solutions, the dialog was better with the firms already known. Since they already knew the project, and which parts were used on the last model, they could easier relate to the problems, and what kind of solutions best suited for the project.

The new robot frame will be stronger and a bit heavier than the prototype, and with bigger wheels the power from the motor is bigger. Still, the propulsion motor is 500 W, which is 100 W less than before. The calculations prove that the motors are strong enough for an incline of 20%, and contrary wind off 15 m/s. These conditions are really tough, the robot will not meet tougher conditions than this, and bigger motors are not necessary. On the other hand, the robot with skid-steering only has two motors, and half the power of the 4WD version. This robot should not be used in uneven terrain. Of the calculated resistances, the gradient resistance was the biggest. The point of having a 2WD version is to offer a robot that is cheaper and less heavy. This can of course not be expected to handle the same terrain as the 4WD robot.

The gears supplied by Allweier for propulsion is very tough and heavy, much tougher than needed, but Allweier is specialized on these products. They have IP67 certification, which make them completely protected against dust, and water-proof down to 1 m of immersed water. The IP-certification had a high priority. The intention was to have a two-stage gear, but by adding a ratio in the belt drive a single-stage gear could be used. This made the module significantly narrower. The weight of the gearbox is over 7 kg, which is nearly twice the weight of the old gearbox. A gearbox with less weight would only have IP65 certification. The gears will be the lowest component together with the wheels, and will be vulnerable in wet conditions. IP67 is a much more secure alternative, and outweighs the difference in weight.

For the steering a much more powerful motor than before is used; 350 W in Thorvald II, but only 134 W in Thorvald I. The main reason for this adjustment is that the wheels are bigger, which requires significantly more torque to rotate. The old solution was more expensive than the new one, since it came with integrated motor controller that already was set up. The new solution requires a bit more work before it is ready to function, but in total, it is more powerful, less expensive and very compact. The steering gears are the same model as previously used, but with one stage instead of two.

Both the encoder for propulsion and steering are incremental, but an absolute encoder could be practical for the steering. The problem is that it had to be placed after the transmission, which would be very impractical for the design. Electro Drives could deliver a multi-turn absolute encoder, but it wasn't applicable with the chosen motor controller.

A lot of time was used on the design of the main module, and many different versions was drawn. Because of the collaboration with Ås VGS, the design had to be done in a way for them to be able to produce the components. At first, the plan was to bend the the material to form the module. This would be a more stable construction if steel was the material of choice, but it is very heavy when compared to aluminum. Aluminum will be the main material of the robot, and it is not advised to weld without proper education; it easily cracks up, and are not very good with dynamic loads. By using rivets as method of assembly, it is designed to make a stable aluminum-construction. The solution is really flexible, and most of the parts are identical on the regular version and the mirrored version. This is a huge advantage during production, which will be faster, more organized and less expensive.

The communication with Ås VGS should have been better at an earlier stage to avoid unnecessary changes of the design. Even though they couldn't start the production until April, all of the decisions regarding the design should have been made beforehand. They were helpful, and had plenty of experience to contribute with, unfortunately, they were also slow starters.

The focus of the thesis has been on the main module, even if there in total has been designed three different modules. The module with both steering and propulsion is by far the most complex of the modules, and the other modules can be considered as simpler versions of this. The modules are based on the same platform, but for different applications, the module with only propulsion is a modification of the main module, and the caster module is totally ripped with the same fastening device. Unfortunately, the casters haven't been delivered when this thesis is printed, and the complete design of this module isn't finished yet.

The final module has to be water-proof for all the components to fully function during all kinds of conditions. Other than the waterproof gears, the components that are going to be riveted will be concealed with glue to keep water from leaking to the inside.

9 CONCLUSION

9.1 FURTHER WORK

There is still a lot of work left. The production has just started, and the first robot is planned to be finished June 1th. When this thesis is sent to printing, the parts for the foot is produced, but the tower has not been started on.

For the foot to become waterproof, a lid has to be made. This has to be removable to access the timing belt and pulleys. Some sort of packing can be cut to fit around the hole, and a solution to fasten the lid must be designed.

Number and positioning of the rivets has to be decided. Øystein is a rivet expert, and will contribute in this area.

9.2 GOAL EVALUATION

The goals of this thesis was very ambitious, and the time resources was the biggest obstacle. The development hasn't gone as fast as planned, and therefore, some work remains for the modules to reach the grade of 9 on the TRL-scale.

Before a grade of the robot can be concluded, it has to go through proper testing, and as of now, only speculations can be made.

Thorvald I is graded at TRL4. As soon as Thorvald II is produced and tested, it certainly will score a lot higher than the prototype. The design looks really promising; it is light weight, much narrower than the prototype, and more practical. If the results of the testing are as promising as the design, these modules are ready for the market.

10 REFERENCES

1. Landbrugsavisen.dk. *Selvkørende robotter gødsker og sprøjter*. Landbrugsavisen 2009 25.11.09 [cited 2016 07.04.2016]; Available from: http://landbrugsavisen.dk/Landbrugsavisen/2009/9/25/Selvkoerenderobottergoedskero_gsproejter.htm.
2. *Comparison results*. 2016 [cited 2016 21.03]; Available from: <http://agriculture1.newholland.com/nar/en-us/about-us/buying-services/pre-sale/compareresults?family=TractorsArchive&seriesId=2255>.
3. Grimstad, L., *Powertrain, steering and control components for the NMBU Agricultural Mobile Robotic Platform*. 2014.
4. Blomberg, F., *Rammekonstruksjon for autonom landbruksmaskin*. 2014.
5. Amazonen-Werke, *BoniRob field robot establishes the basis for the future agricultural technology*. 2014.
6. Merchant, B. *Solar-Powered Robot Farmers Are Almost Ready to Start Working the Land*. 2014 [cited 2016 25.03]; Available from: <http://motherboard.vice.com/read/solar-powered-robot-farmhand-automatically-detects-pests-and-picks-weeds>.
7. *The TRL Scale as a Research & Innovation Policy Tool, EARTO Recommendations*. 2014: EARTO. p. 16.
8. Commission, E., *Horizon 2020 - Work Programme 2014-2015*. 2014. p. 36.
9. Wong, J.Y., *Theory of Ground Vehicles*. Four ed. 2008.
10. Buchanan, R.A. *History of Technology*. Encyclopædia Britannica 2014 06.02.2014 [cited 2016 12.04]; Available from: <http://global.britannica.com/technology/history-of-technology/The-20th-century>.
11. Baglione, M.L., *Development of system analysis methodologies and tools for modeling and optimizing vehicle system efficiency*. 2007, University of Michigan.
12. Knothe, G., J. Krahl, and J. Van Gerpen, *The biodiesel handbook*. 2015: Elsevier.
13. Motor, M. *Maxon Motor online product catalog*. 2016 [cited 2016 21.04]; Available from: <http://www.maxonmotor.com/maxon/view/catalog/>.
14. Siemens. 2016 [cited 2016 21.04]; Available from: <http://www.industry.siemens.com/drives/global/en/motor/high-voltage-motors/Pages/high-voltage-motors.aspx>.
15. *DC motor operation*. 2016 [cited 2016 21.04]; Available from: <http://hyperphysics.phy-astr.gsu.edu/hbase/magnetic/motdc.html>.
16. Wandel, M., *How DC motors and universal motors work*. 2014, youtube.
17. Lazaridis, G., *How DC motors are made and how they work*. PCB heaven, 2010.
18. Semiconductor, O., *DC Motor Driver Fundamentals*. 2014. p. 9.
19. Yedamale, P., *Brushless DC (BLDC) motor fundamentals*. Microchip Technology Inc, 2003. **20**: p. 3-15.

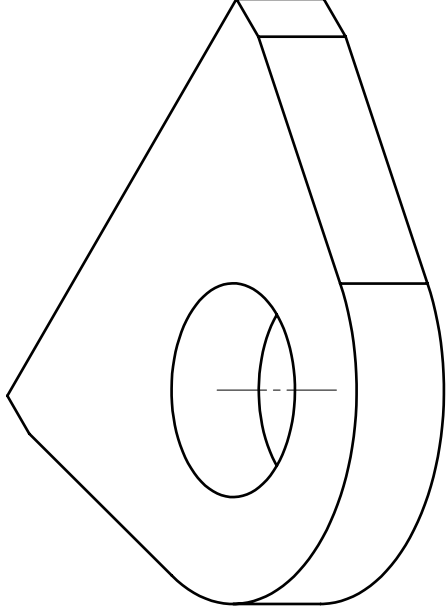
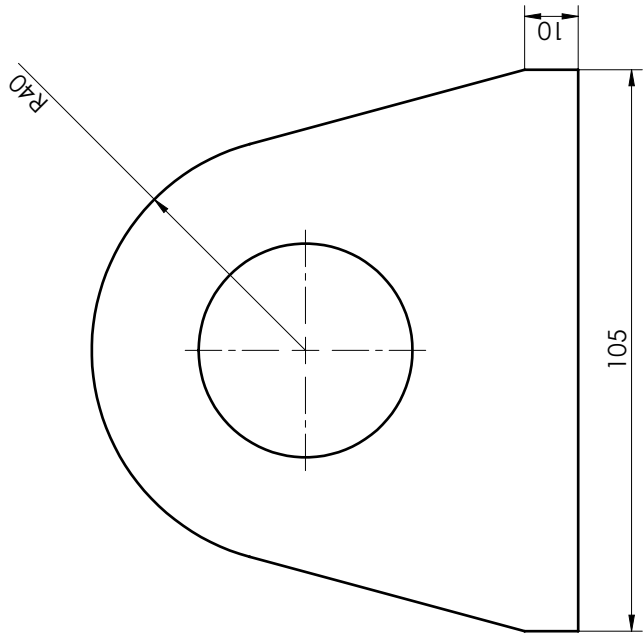
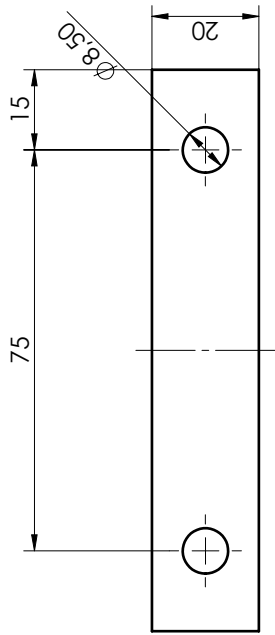
20. Brittanica, T.E.o.E. *Transmission*. 2016 12.02.2014 [cited 2016 24.04]; Available from: <http://global.britannica.com/technology/transmission-engineering>.
21. M.M.Mayuram, P.K.G.P. [PDF lecture] 2016 [cited 2016 24.04]; Available from: [https://www.google.no/?client=safari - q=nptel.ac.in/courses/IIT-MADRAS/+Machine Design II/pdf/2 1.pdf.&gfe rd=cr](https://www.google.no/?client=safari - q=nptel.ac.in/courses/IIT-MADRAS/+Machine+Design+II/pdf/2+1.pdf.&gfe_rd=cr).
22. Walton, D., *GEAR MANUAL*. 2013, Martin Sprocket & Gear, Inc. p. 58.
23. *Gibbs Gears*. [Company web page] 2016 [cited 2016 24.04]; Gear types]. Available from: <http://www.gibbsgears.com/index.php>.
24. *Gear manufacturing*. 2016 [cited 2016 24.04]; Company web page]. Available from: <http://www.hewitt-topham.co.uk/manufacturing.html>.
25. Rohloff. *PLANETARY GEAR SYSTEM*. 2016 [cited 2016 24.04]; Company web page]. Available from: http://www.rohloff.de/en/technology/speedhub/planetary_gear_system/.
26. Gupta, R.S.K.J.K., *A Textbook of Machine Design*. 14 ed. 2005: Eurasia Publishing House (PVT.)LTD.
27. Instruments, S.D.P.-S., *Handbook of Timing Belts, Pulleys, Chains and Sprockets*.
28. Rethwisch, W.D.C.D.G., *Materials science and engineering*. Vol. 8. 2010: Wiley. 885.
29. Terjesen, G., *Spenningsanalyse og trykkbeholdere*, in *TMP301*. 2015: NMBU. p. 44.
30. Standardization, t.I.O.f., *general purpose screw threads*. 1998: ISO online browsing platform.
31. *STANDARD AVIATION MAINTENANCE HANDBOOK*. 1985: JEPPESEN Sanderson Training Products.
32. Terjesen, G., *Skrueforbindelser*, in *TMP301*. 2015: NMBU. p. 32.
33. Terjesen, G., *Press og krympepasninger*, in *TMP301*. 2015, IMT. p. 18.
34. Gravdahl, P.J.F.T., *Innføring i Dynamikk of Reguleringsteknikk*, in *TEL240*. 2013, IMT: NMBU.
35. Sandin, P.E., *Robot mechanisms and mechanical devices illustrated*. 2003: McGraw-Hill New York, NY.
36. SFUPTOWNMAKER. *PCB basics*. [cited 2016 7.05]; PCB tutorial written by an electrical engineer]. Available from: <https://learn.sparkfun.com/tutorials/pcb-basics>.
37. Dahl, Ø.N. *Basic Electronic Components Used in Circuits*. 2013 [cited 2016 07.05]; Available from: <http://www.build-electronic-circuits.com/basic-electronic-components/>.
38. Jimbo. *Transistors*. [cited 2016 07.05]; Written by computer/elictrical engineer]. Available from: <https://learn.sparkfun.com/tutorials/transistors>.
39. *The friction and rolling resistance coefficients*. [Calculator] [cited 2016 24.02]; Available from: <http://hpwizard.com/tire-friction-coefficient.html>.
40. Terjesen, G., *Grunnlag drivkraftteori*, in *TMP 270*. 2015, IMT: NMBU.
41. John B. Liljedahl, P.K.T., David W. Smth & Makoto Hoki, *Tractors and their Power Units*. 1989: Van Nostrand Reinhold, New York. 442.

42. Wittren, R.A. and A.S.o.A.E.W. Meeting, *Power Steering for Agricultural Tractors*. 1975: American Society of Agricultural Engineers.
43. Bøe, J.K., *Ideutvikling og tidligseleksjon, Pughs metodikk, Eksempler på prosjektprosesser*, in *Konsept- og produktrealisering*. 2015, IMT: NMBU. p. 34.
44. Egeberg, O., *Specifications of components*. 2016: Mail.
45. Røwdehjul, *Røwdehjul - prisliste*. p. 42.
46. bengalack, Q., *Corrosion protetion*. 2016.
47. Trygve Pedersen - Application engineer, S., *Roller bearing calculations*. 2016: E-mail.

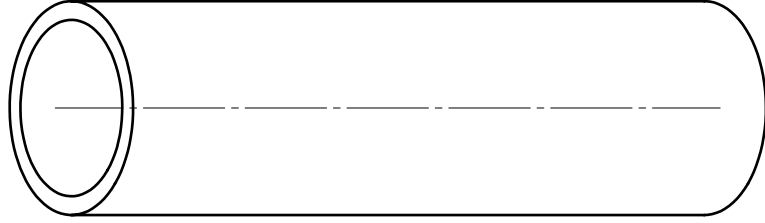
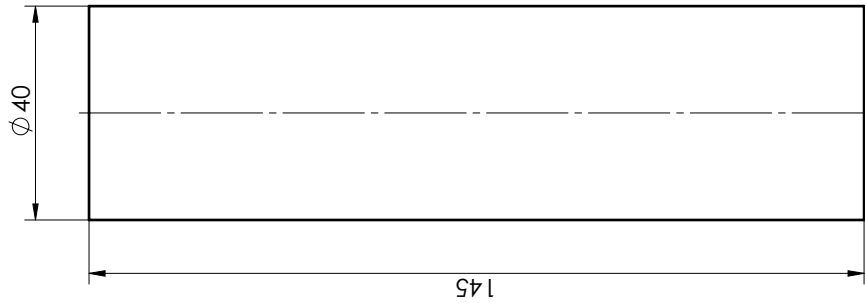
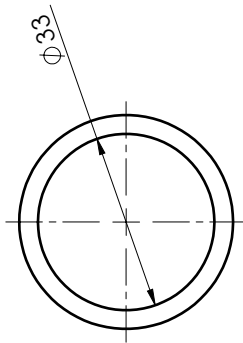
This page is intentionally left blank


11 VEDLEGG

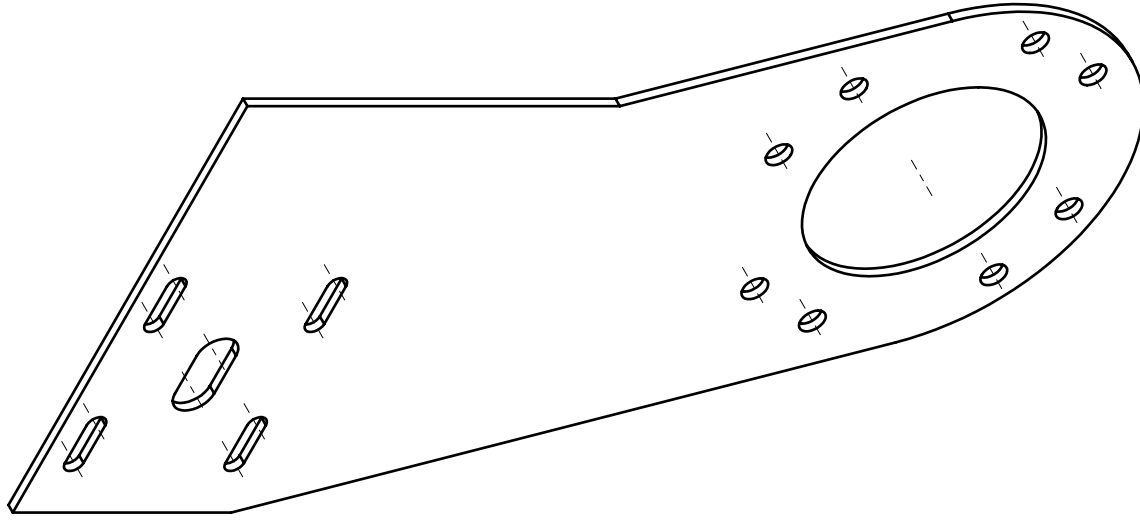
- Construction drawings. 36 pcs.
 - The drawing are made with extra files for the plasma-cutter and the bending machine. All the measurements are not present.



Dato: 12.05.16	Konstr./Tegnet: M.A.	Projeksjon:	Målestokk: 1:1	NMBU	
Thorvald II			Erstatning for: Erstatlet av:		
Ring propulsion			A1		
Materiale:			Toleranse:		



Dato: 12.05.16	Konstr./Tegnet: M.A.	Projeksjon: 	Målestokk: 1:1	NMBU	
Thorvald II					
Tube propulsion				A1	
Materiale: Aluminium			Toleranse: ISO 2768-1 - medium		



NMBU

Erststøtlet av:

A1

Målestokk:
1:2

Projeksjon:
M.A.

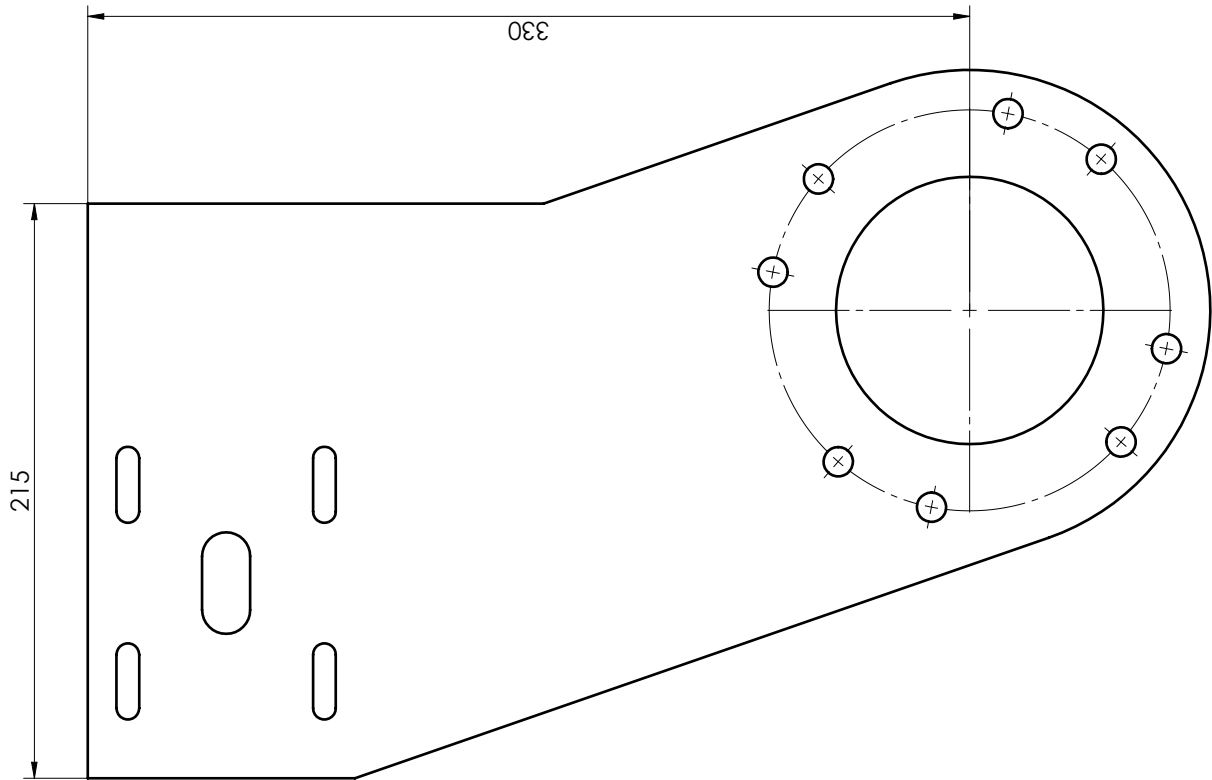
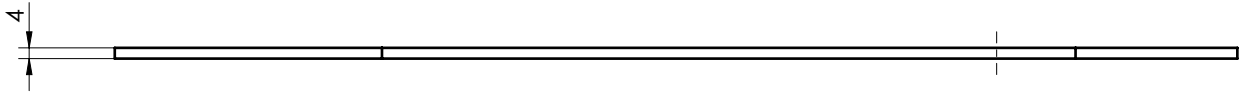
Konstr./Tegnet:
M.A.

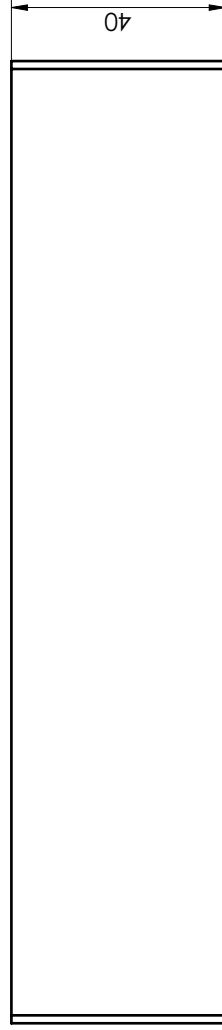
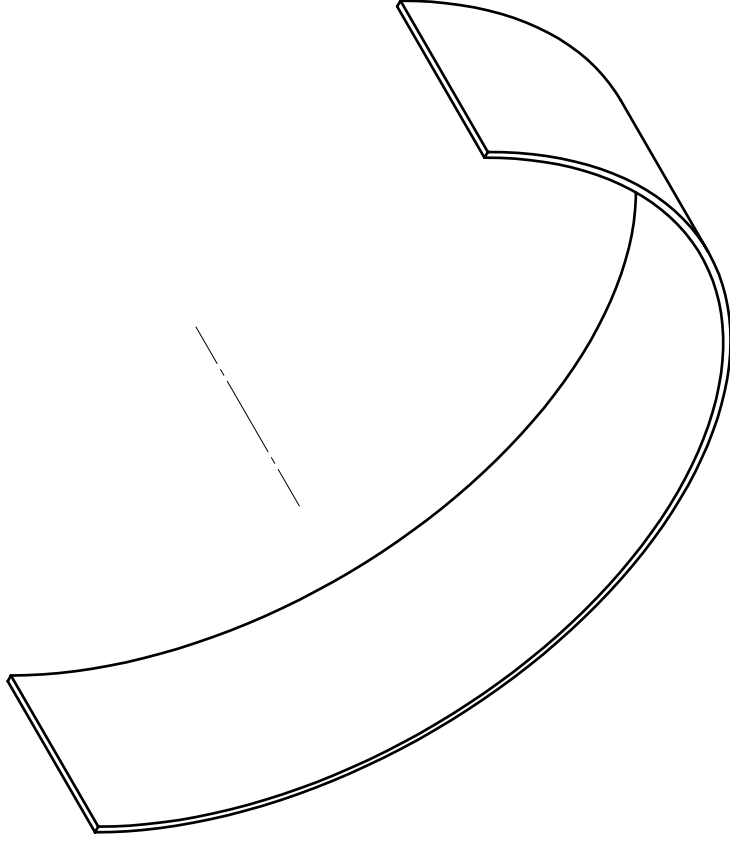
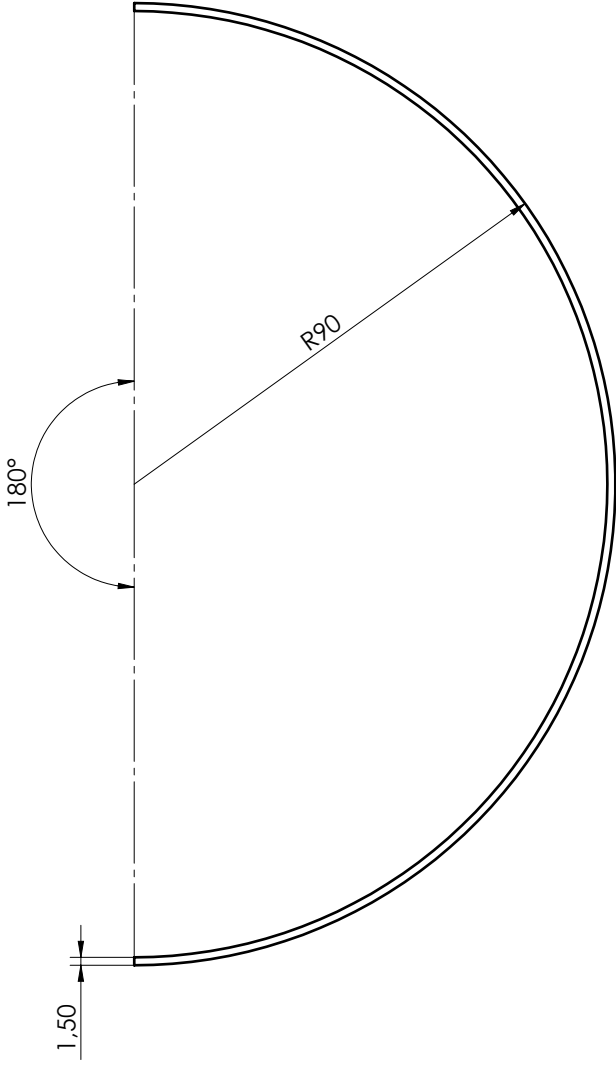
Dato:
12.05.16

Thorvald II
Back Cover

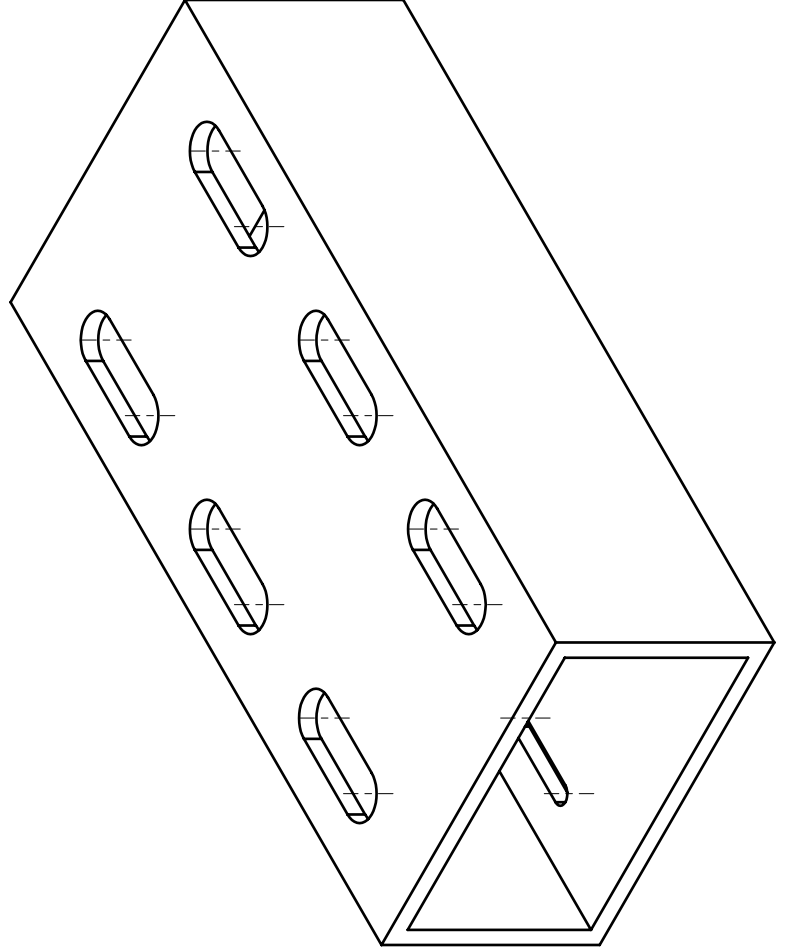
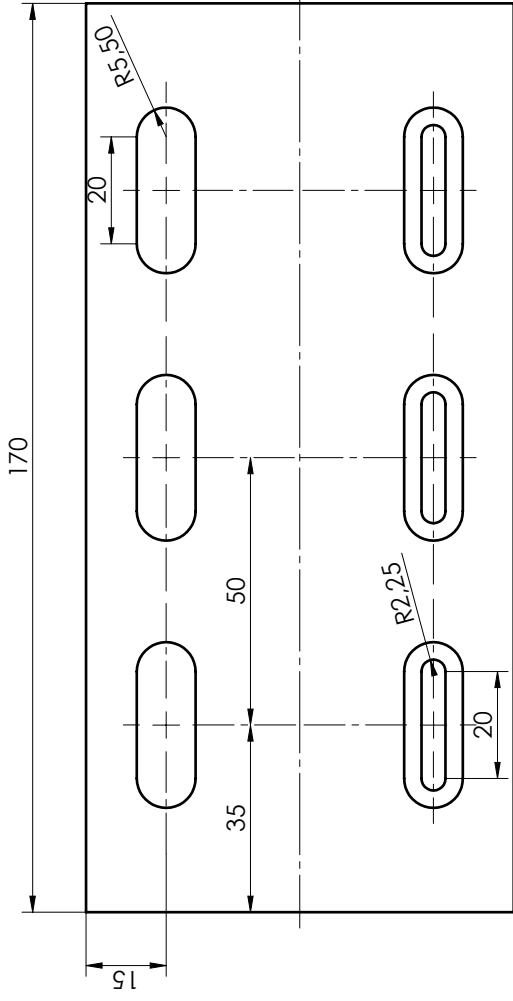
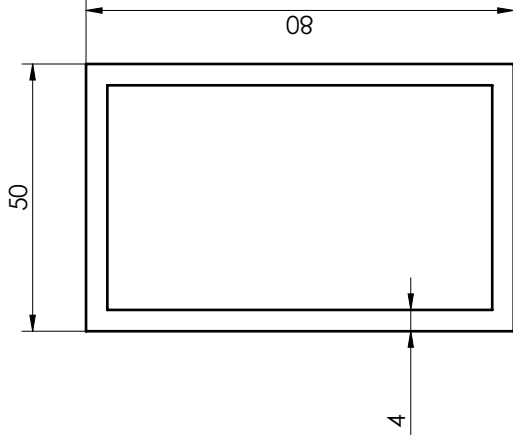
Materiale:
Aluminium

Toleranse:
ISO 2768-1 - medium

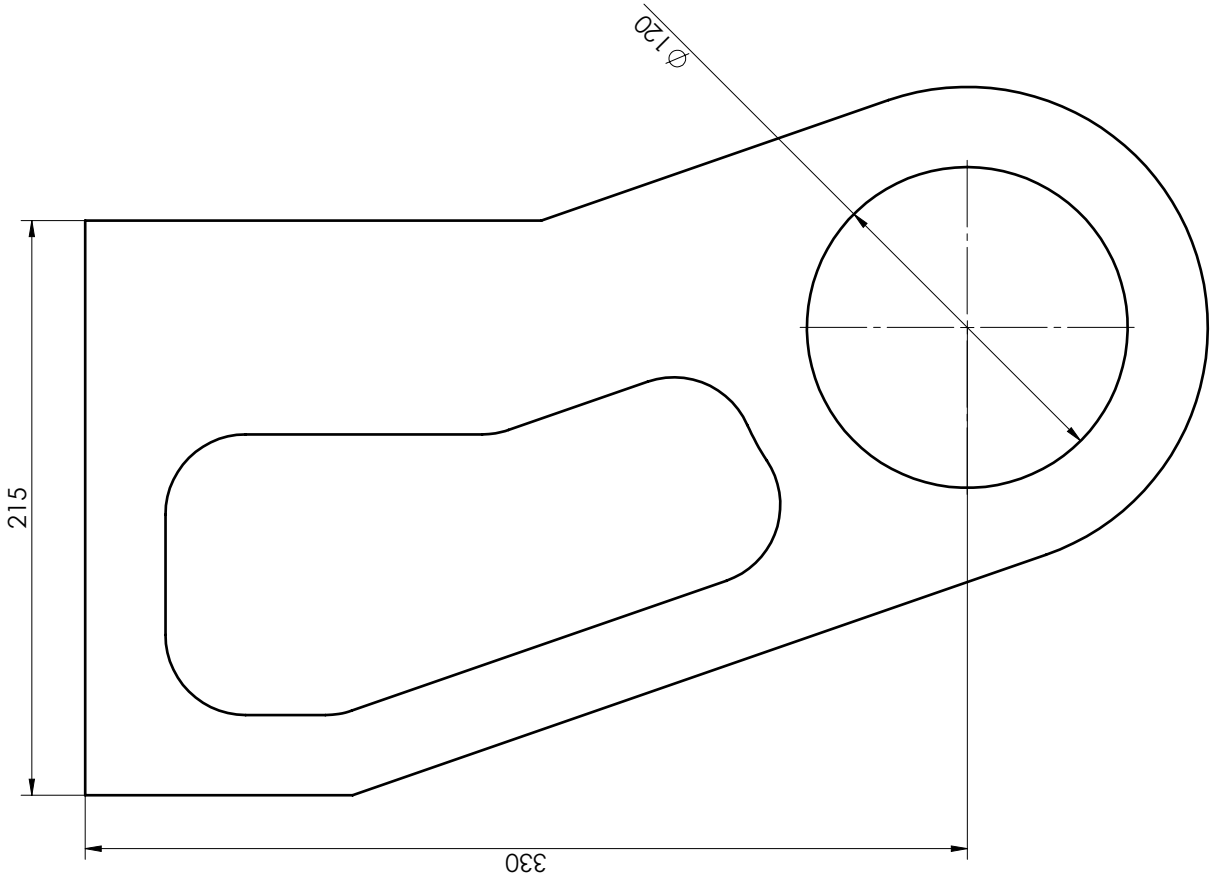
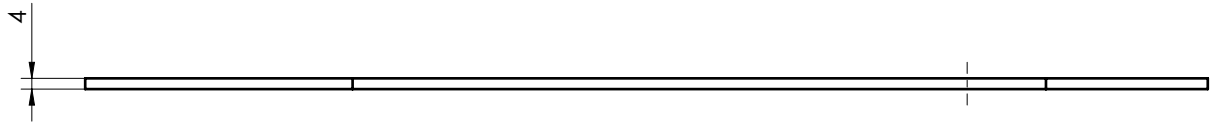
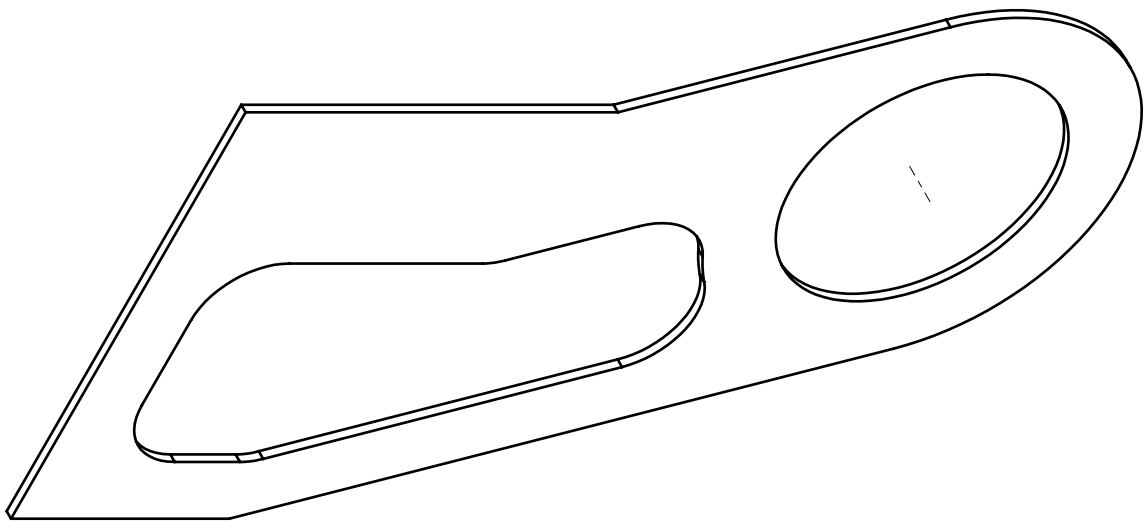




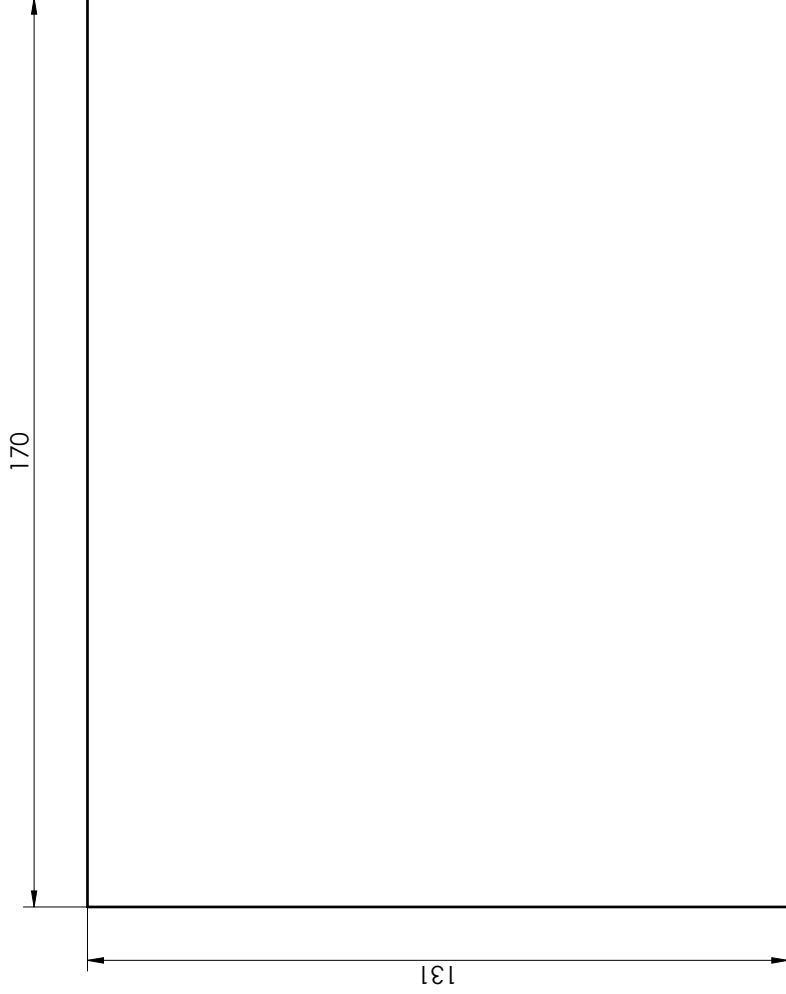
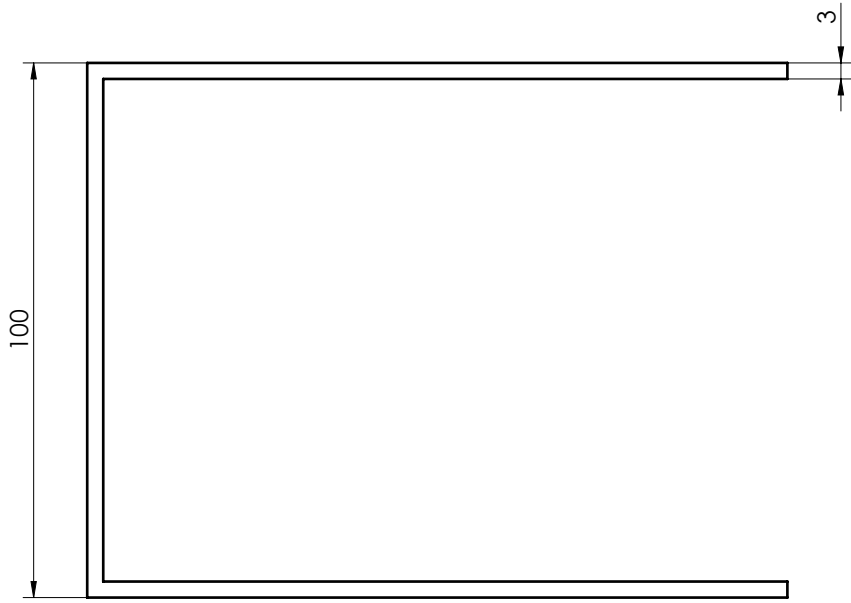
Dato: 02.05.16	Konstr./Tegnet: M.A.	Projeksjon:	Målestokk: 1:1	NMBU	
Thorvald II			Erstatning for: Erstatlet av:		
Øvingsoppgave			A1		
Material: Aluminium			Toleranse: ISO 2768-1 - medium		




Dato: 05.04.16	Konstr./Tegnet: M.A.	Projeksjon:	Målestokk: 1:1	NMBU	
			Erstatning for: Erstatet av:		
Thorvald II			A1		
Firkantrør					
Material: Aluminium			Toleranse: ISO 2768-1 - medium		

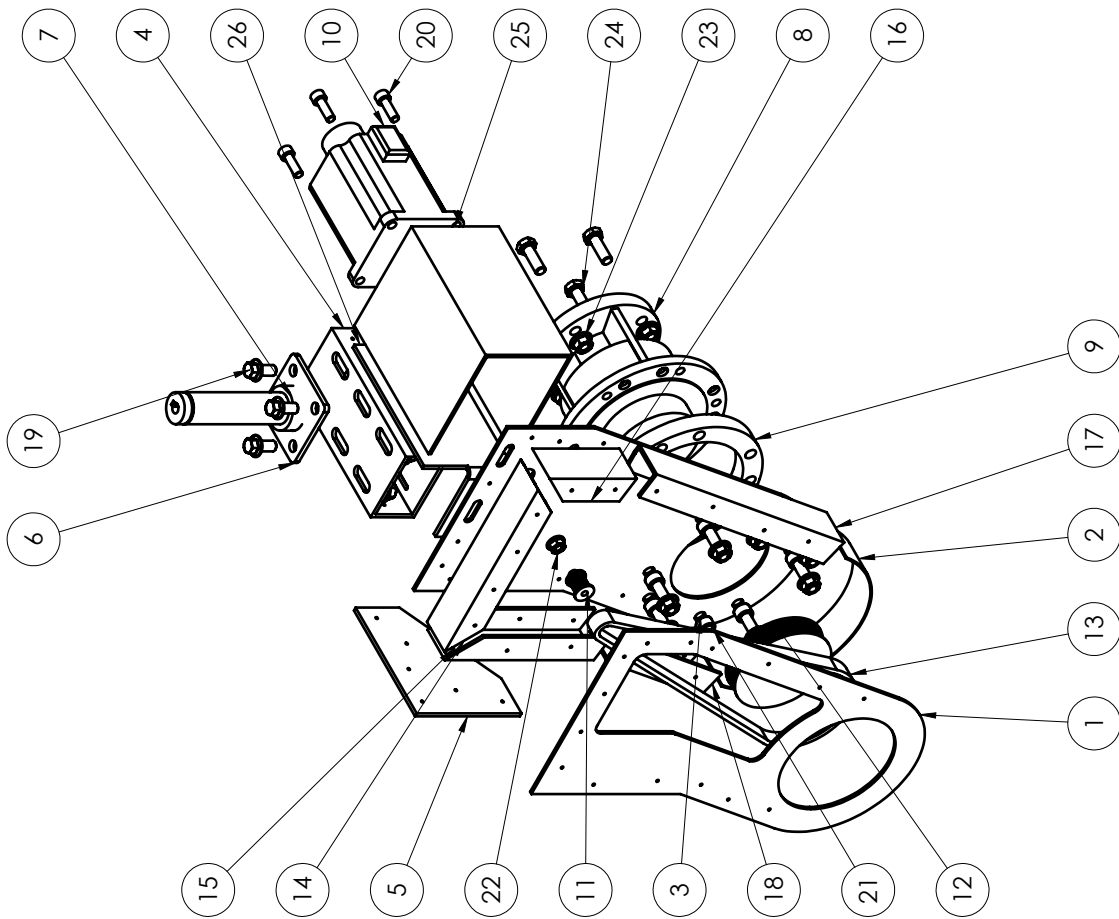


Dato: 12.05.16	Konstr./Tegnet: M.A.	Projeksjon:	Målestokk: 1:2	NMIBU
Thorvald II frontCover				Erstatning for: Erstatet av:
Material: Aluminium				A1
Toleranse: ISO 2768-1 - medium				

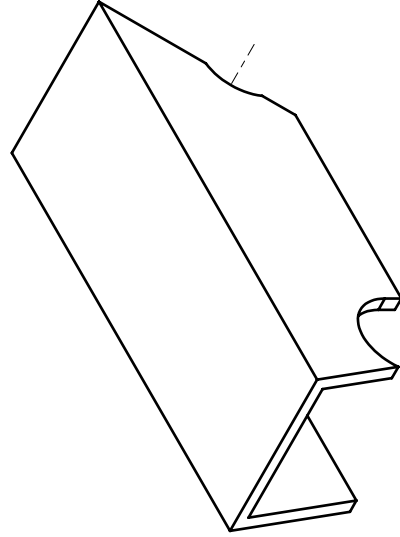
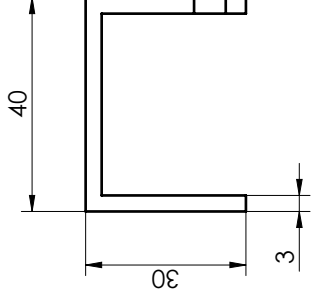
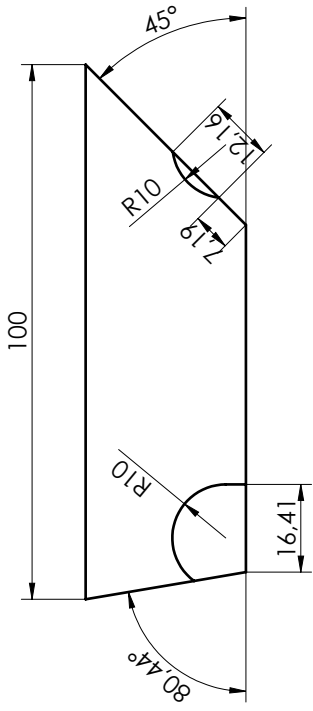


Dato: 05.04.16	Konstr./Tegnet: M.A	Projeksjon: 	Målestokk: 1:1	NMBU	
Thorvald II			Erstatning for: Erstatlet av:		
Motor Box			A1		
Material: Aluminium			Toleranser: ISO 2768-1 - medium		

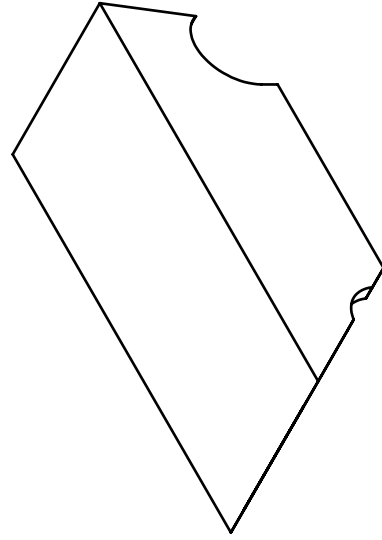
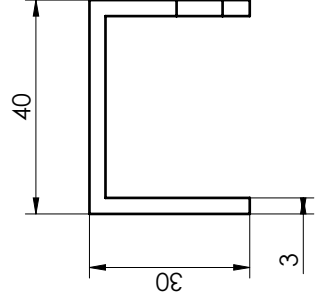
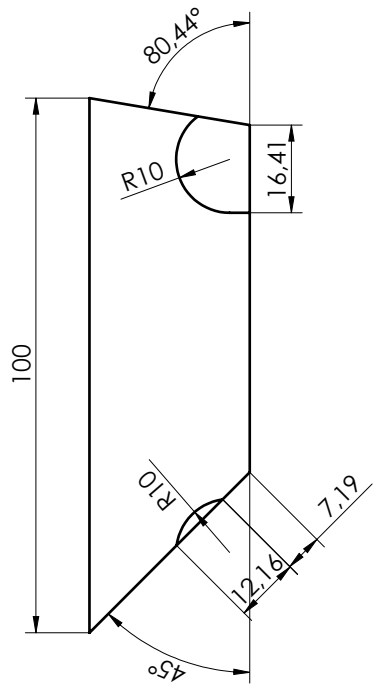
26	1	wallBrack			
25	1	MotorBox			
24	4	hex screw gradeab_iso			
23	16	hex flange nut gradea_iso			
22	4	hex flange nut gradea_iso			
21	8	socket head cap screw_iso			
20	4	socket head cap screw_iso			
19	4	hex flange bolt small_iso			
18	1	20160321u-profil			
17	1	20160321u-profil			
16	1	20160321u-profil			
15	1	20160321u-profil			
14	1	20160321u-profil			
13	1	Belte			
12	1	Reimhjul 94.64			
11	1	Reimhjul 15.05			
10	1	BL821motor	AISI 1045 Steel, cold drawn	6868	
9	1	wheelspacer			
8	1	Tyske gir			
7	1	Styringsaksel			
6	1	Styringsaksel flens			
5	1	sideBrack			
4	1	firkantrør			
3	1	aluBack			
2	1	Deksel gir			
1	1	aluFront			
Pos.	withMotor/QTY.	Tittel/benevning/dim.	Materiale	Vekt	Art. nr./ref.



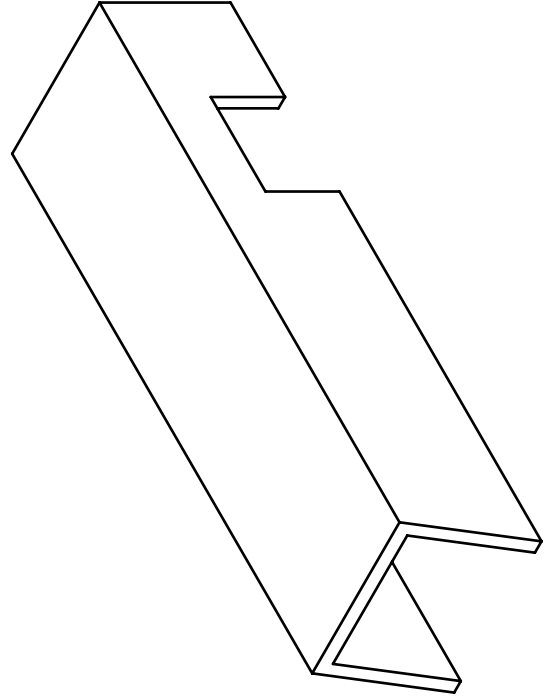
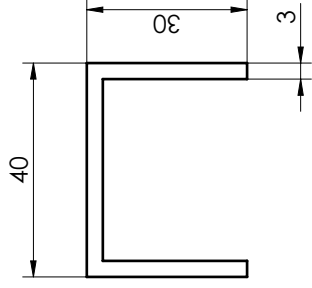
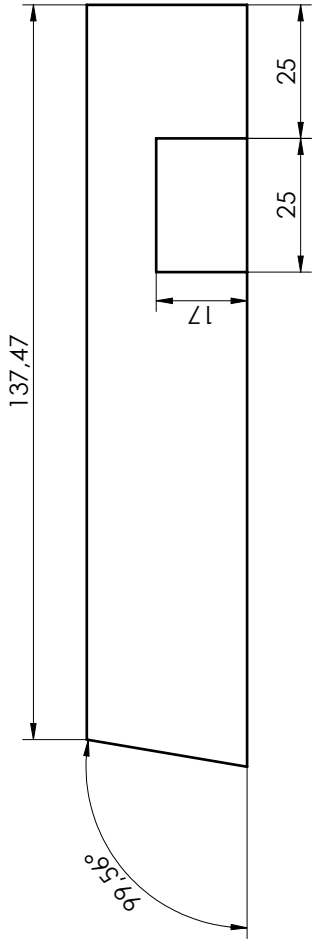
Dato:	06.04.16	Konstr./Tegnet:	M.A.	Projeksjon:		Målestokk:	1:5	<h1 style="text-align: center;">NMBU</h1>	
<h2 style="text-align: center;">Thorvald II</h2> <h3 style="text-align: center;">Sammenstilling av hjulmodul</h3>							Erstatter for:		Erstatter av:
Henvising:							Ås VGS		
Beregning:									



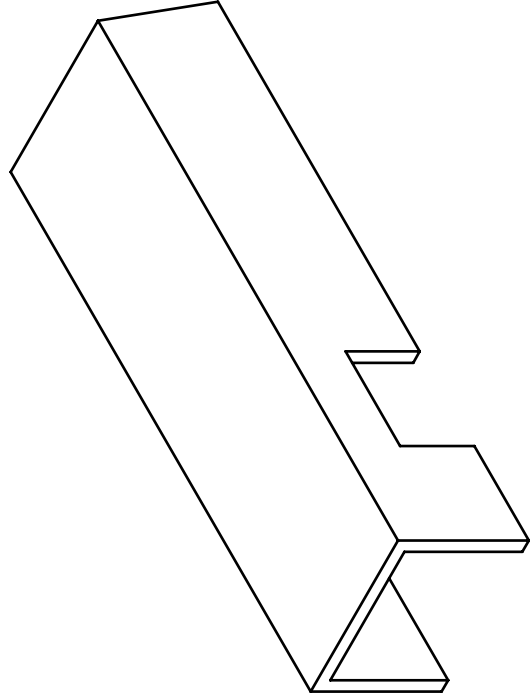
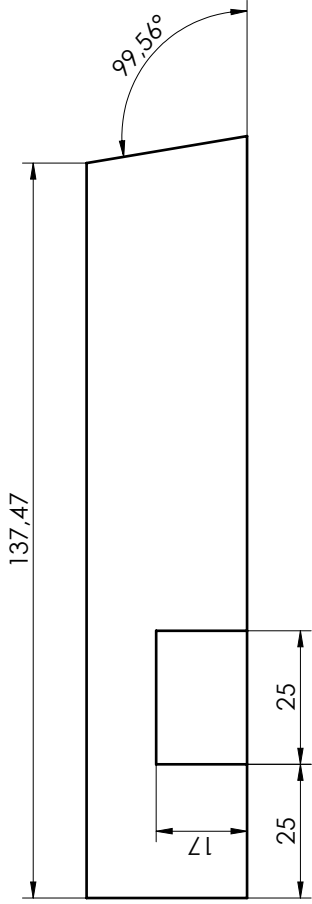
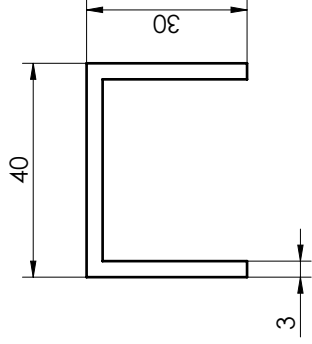
Dato: 05.04.16	Konstr./Tegnet: M.A.	Projeksjon:	Målestokk: 1:1	NMBU	
Thorvald II			Erstatning for: Erstatlet av:		
U-profil 100			A1		
Materiale: Aluminium			Toleranse: ISO 2768-1 - medium		




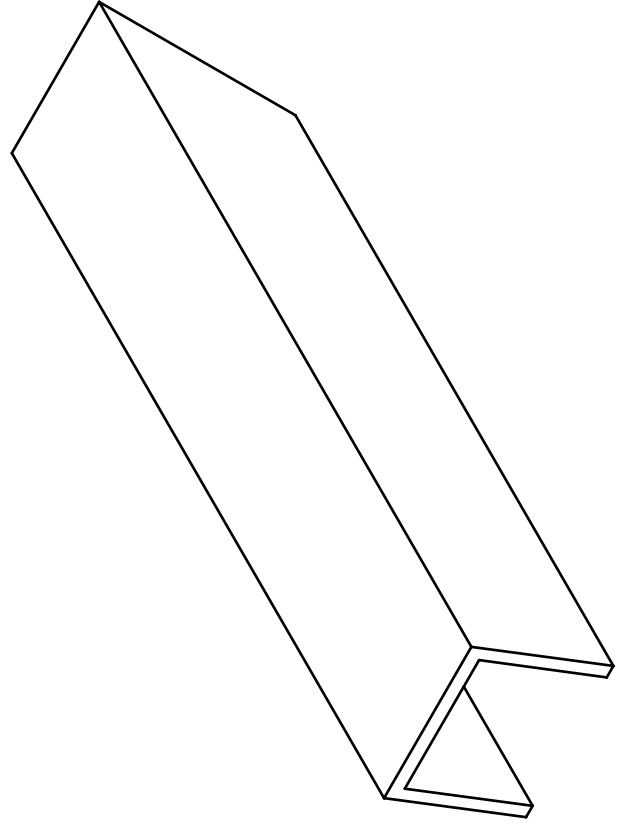
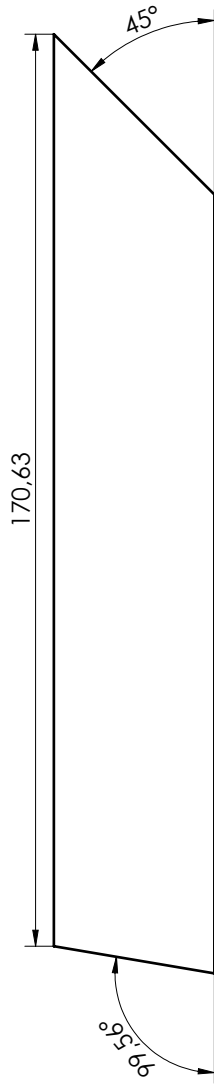
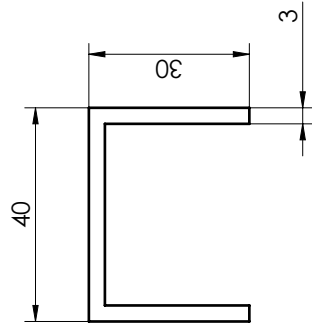
Dato: 07.04.16	Konstr./Tegnet: M.A.	Projeksjon:	Målestokk: 1:1	NMBU	
Thorvald II			Erstatning for: Erstatlet av:		
U-profil 100 mirror			A1		
Material: Aluminium			Toleranse: ISO 2768-1 - medium		



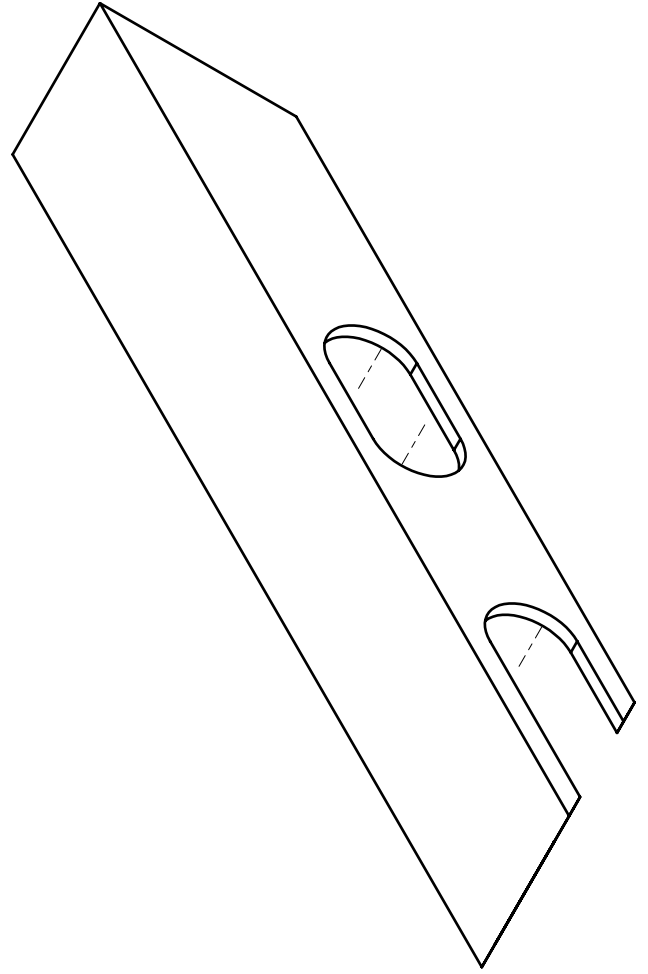
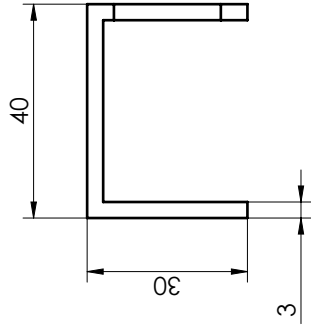
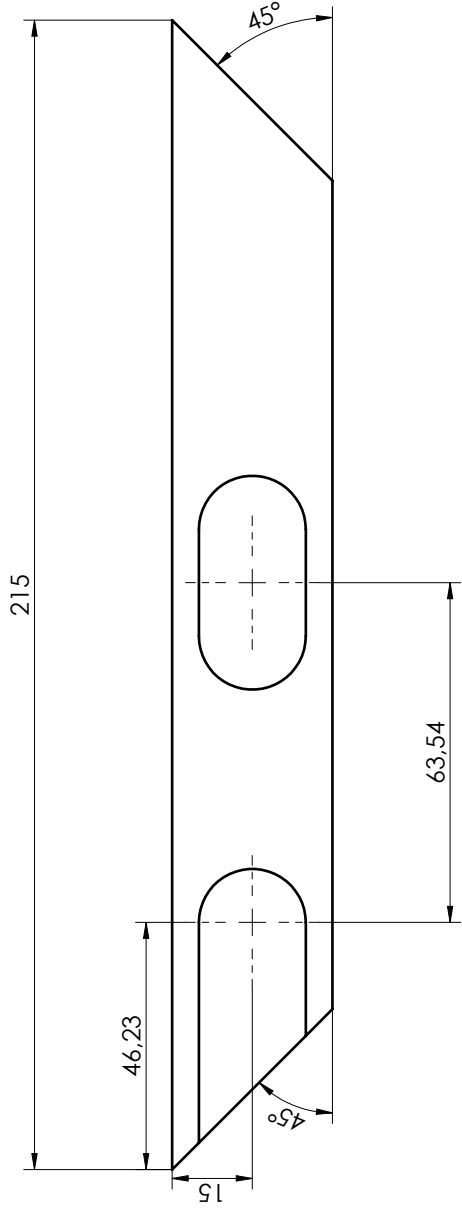
Dato: 05.04.16	Konstr./Tegnet: M.A.	Projeksjon:	Målestokk: 1:1	NMBU	
Thorvald II			Erstatning for: Erstatlet av:		
U-profil 137.47			A1		
Material: Aluminium			Toleranse: ISO 2768-1 - medium		




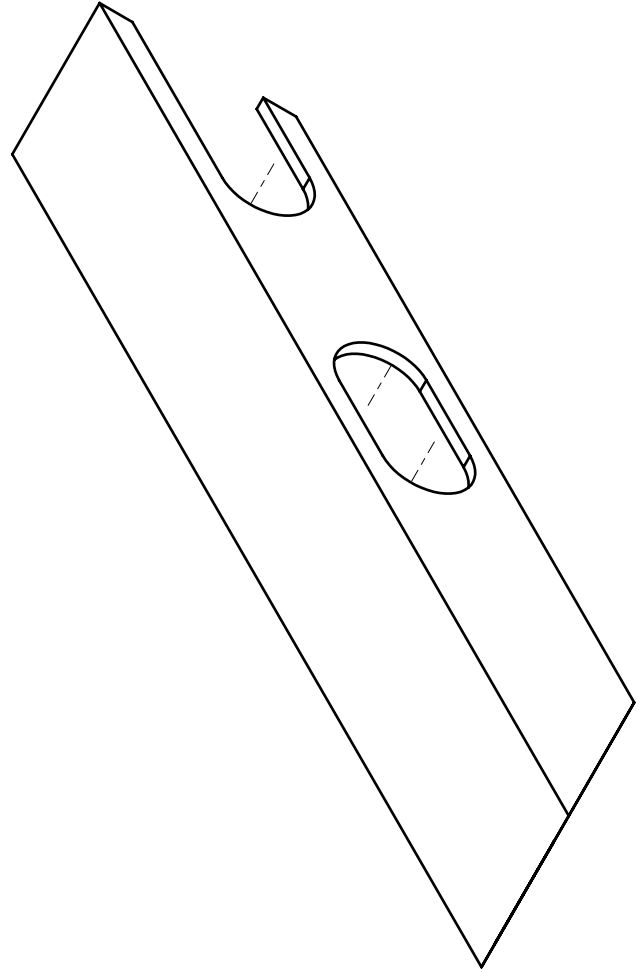
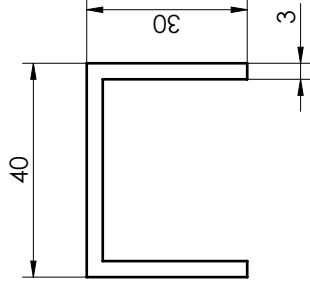
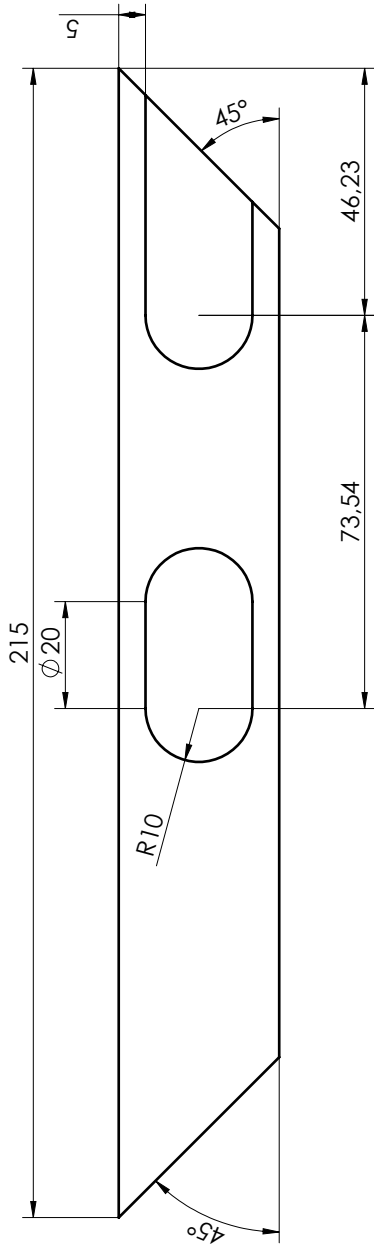
Dato: 07.04.16	Konstr./Tegnet: M.A.	Projeksjon: 	Målestokk: 1:1	NMBU	
Thorvald II			Erstatning for: Erstatlet av:		
U-profil 137,47 mirror			A1		
Henvising: Aluminium			Beregning: ISO 2768-1 - medium		



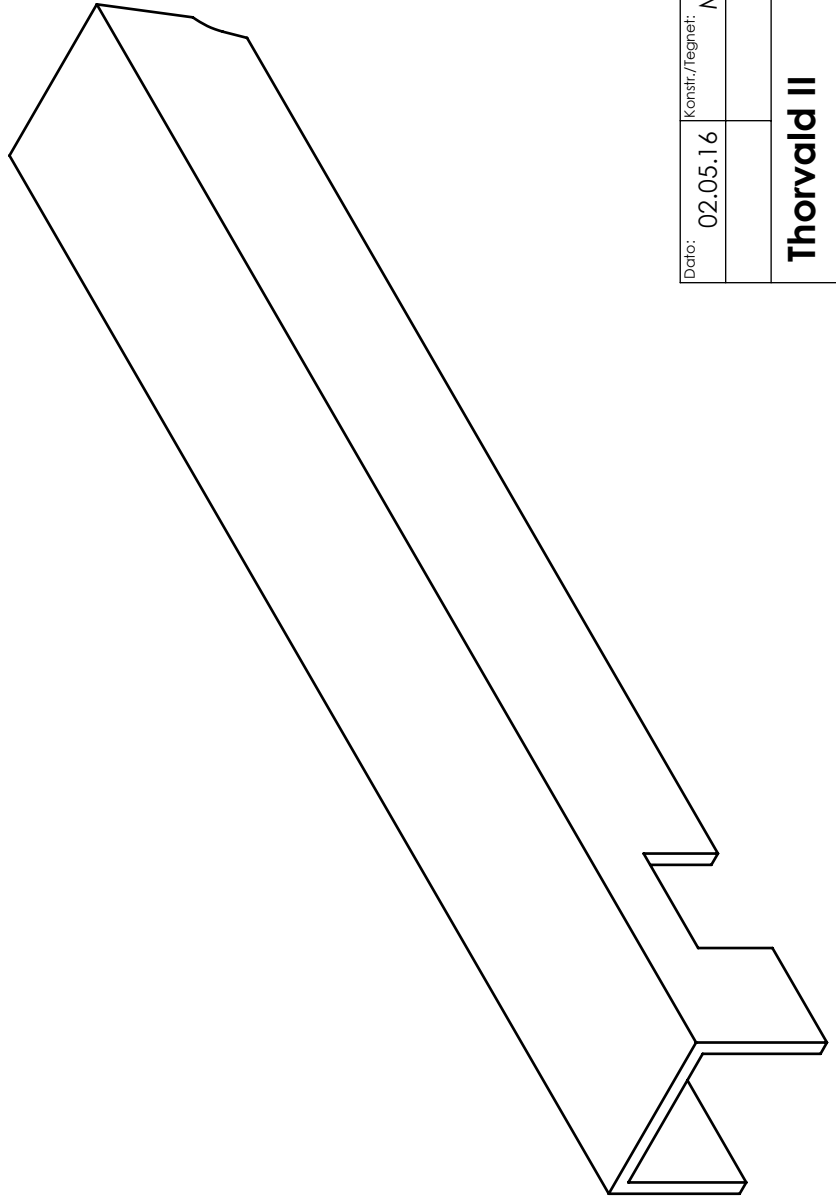
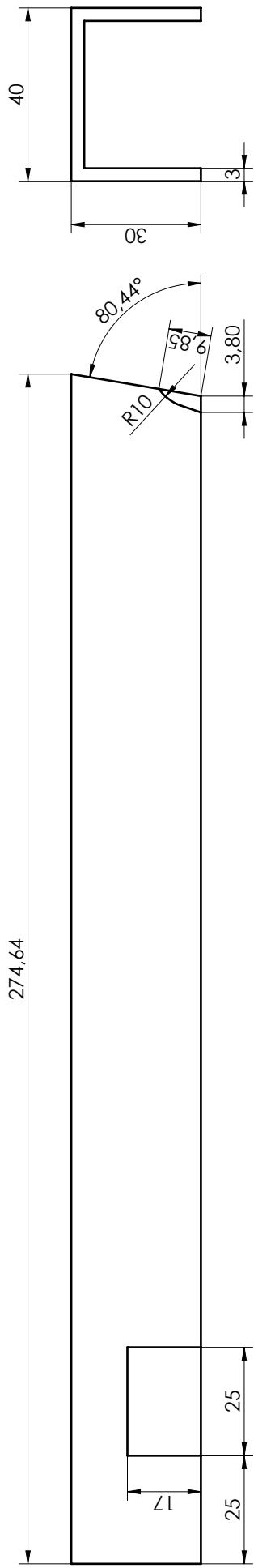
Dato: 05.04.16	Konstr./Tegnet: M.A.	Projeksjon:	Målestokk: 1:1	NMBU	
Thorvald II			Erstatning for: Erstatlet av:		
U-profil 170.63			A1		
Material: Aluminium			Toleranse: ISO 2768-1 - medium		



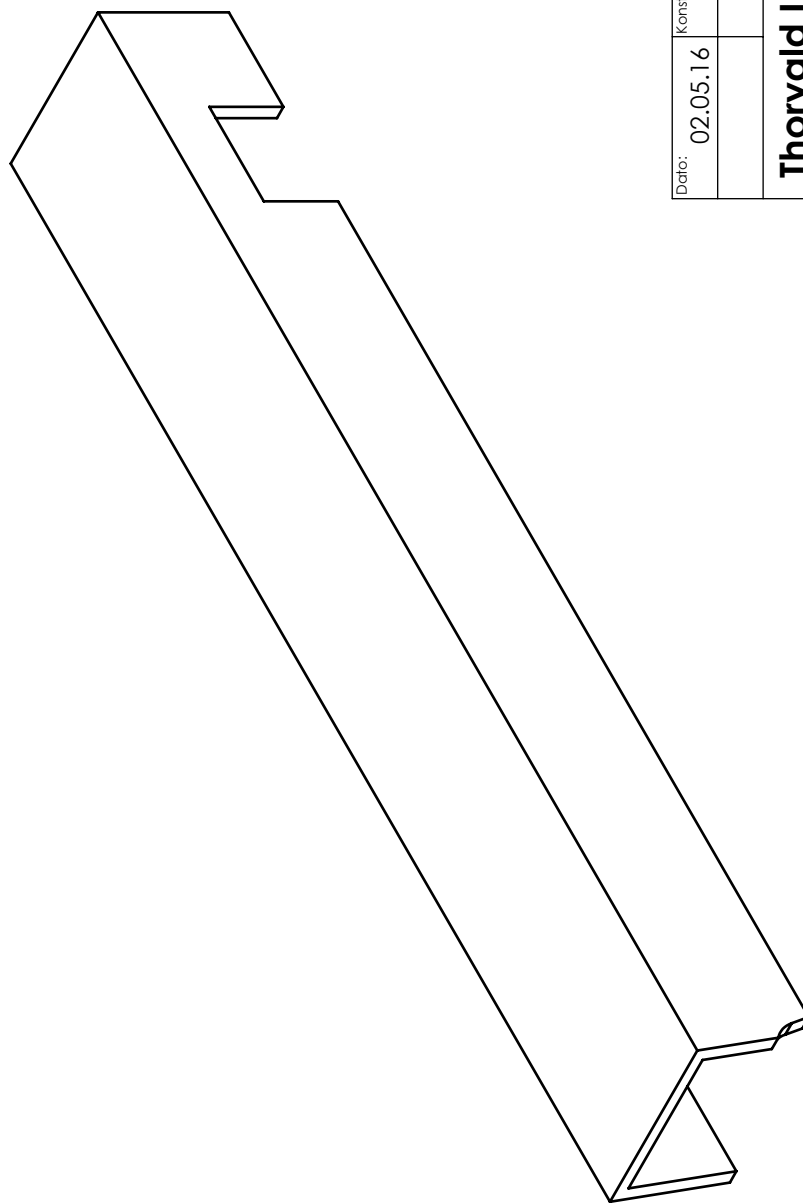
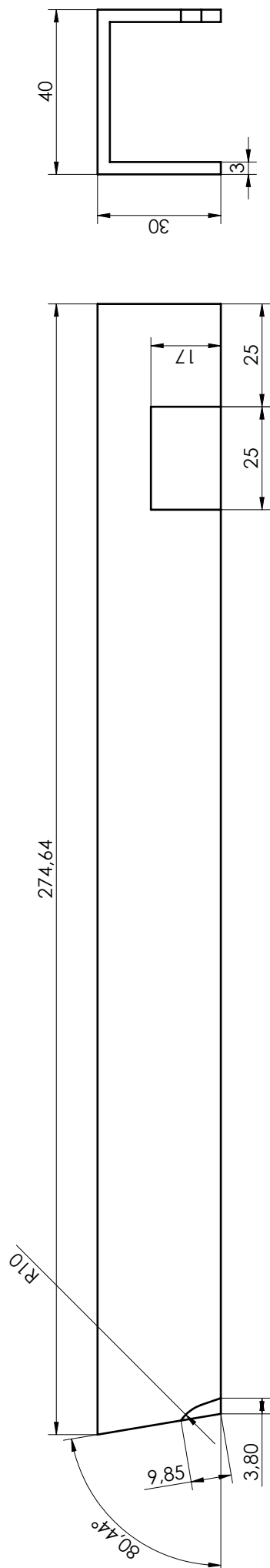
Datum: 05.04.16		Konstr./Tegnet: M.A.	Projeksjon: 	Målestokk: 1:1	NMIBU	
Thorvald II				Erstatning for: Erstatlet av:		
U-profil 215				A1		
Materiale: Aluminium		Toleranse: ISO 2768-1 - medium				



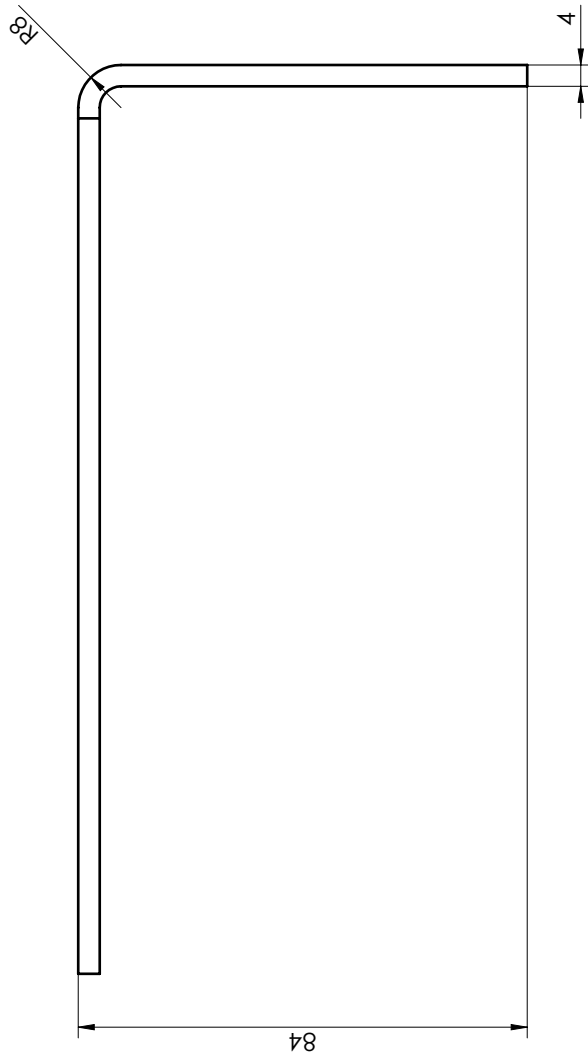
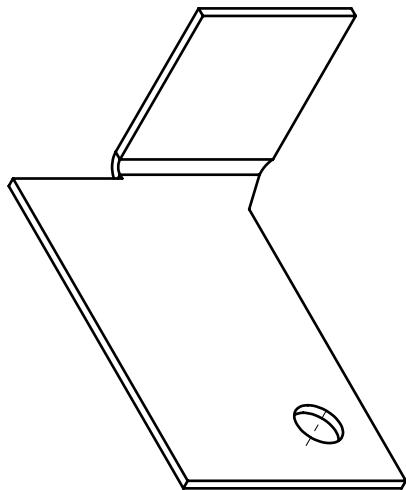
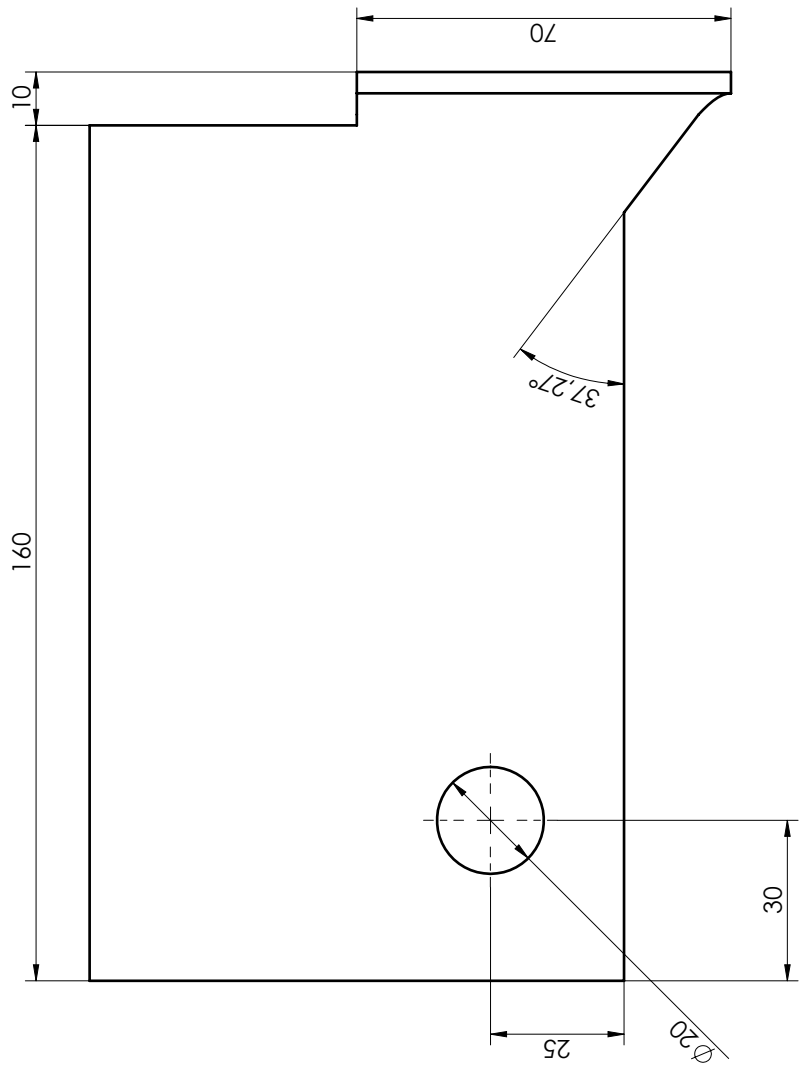
Dato: 07.04.16	Konstr./Tegnet: M.A.	Projeksjon:	Målestokk: 1:1	NMBU
Thorvald II				Erstatning for: Erstatlet av:
U-profil 215 mirror				A1
Material: Aluminium				Toleranse: ISO 2768-1 - medium



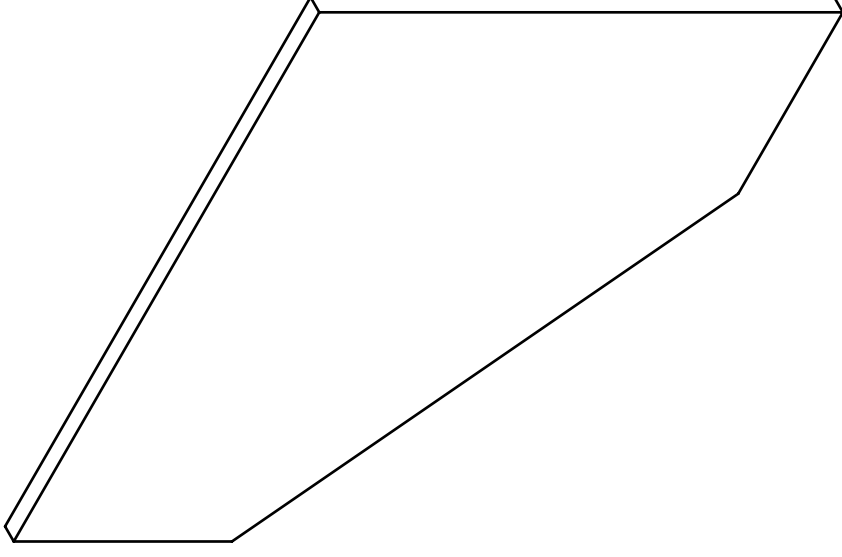
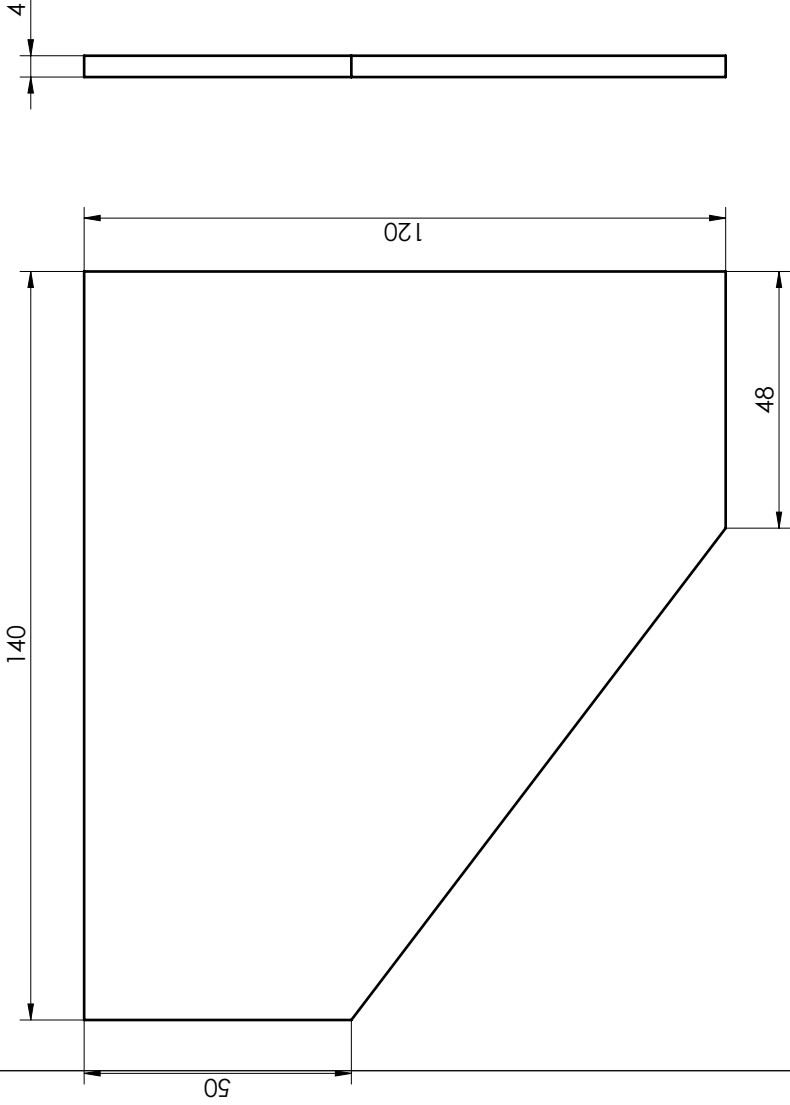
Dato: 02.05.16	Konstr./Tegnet: M.A.	Projeksjon:	Målestokk: 1:1	NMBU	
			Erstatning for: Erstatlet av:		
Thorvald II			A1		
U-profil 274.64					
Material: Aluminium			Toleranse: ISO 2768-1 - medium		




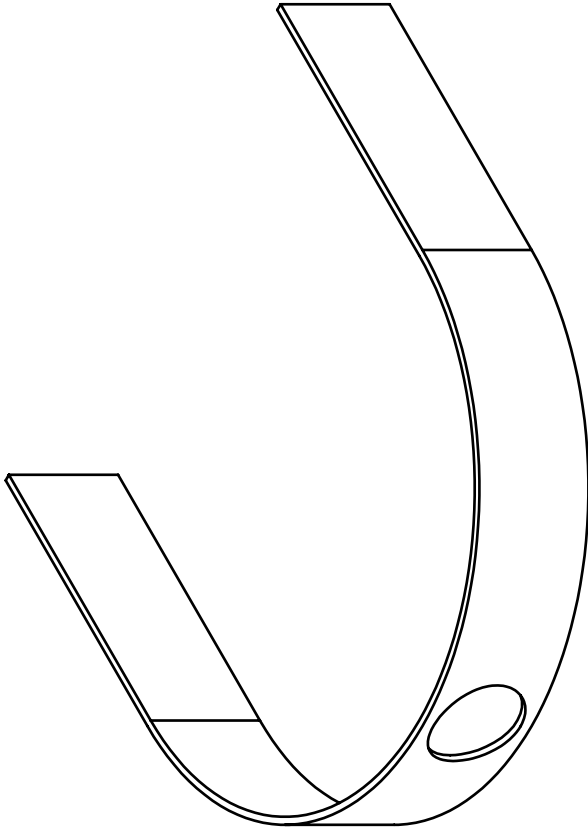
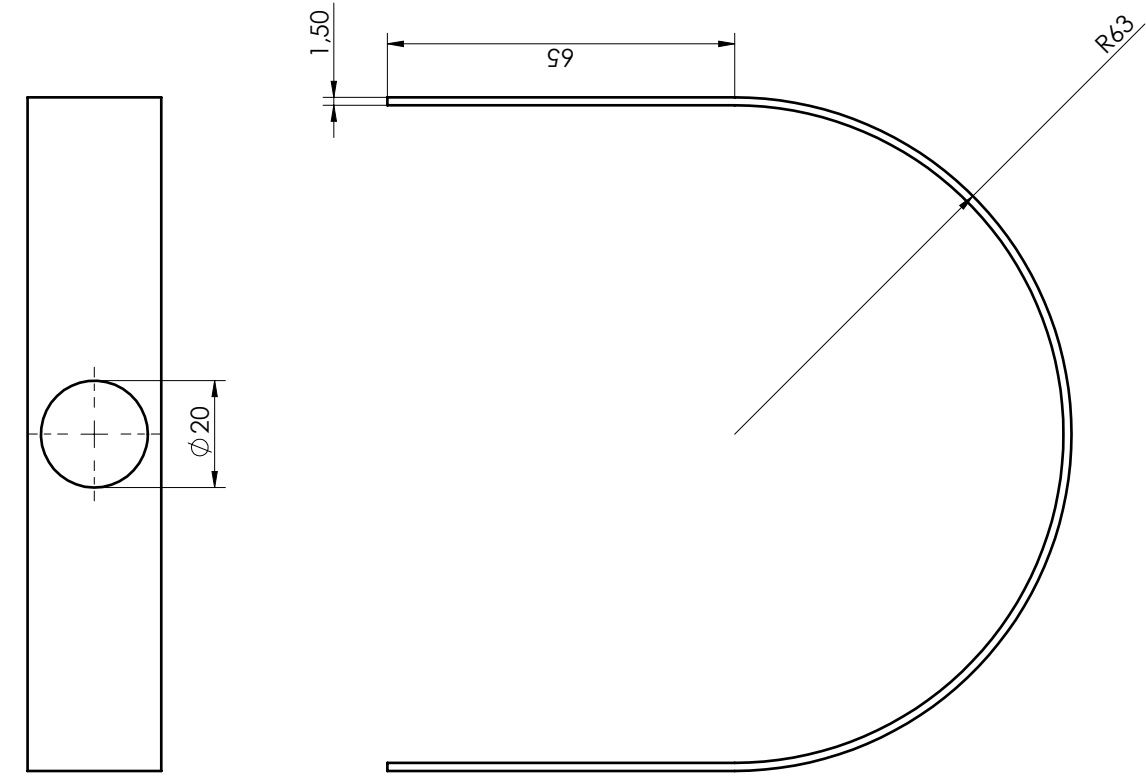
Dato: 02.05.16	Konstr./Tegnet: M.A.	Projeksjon:	Målestokk: 1:1	NMBU	
Thorvald II			Erstatning for: Erstatlet av:		
U-profil 274.64 mirror			A1		
Material: Aluminium			Toleranse: ISO 2768-1 - medium		




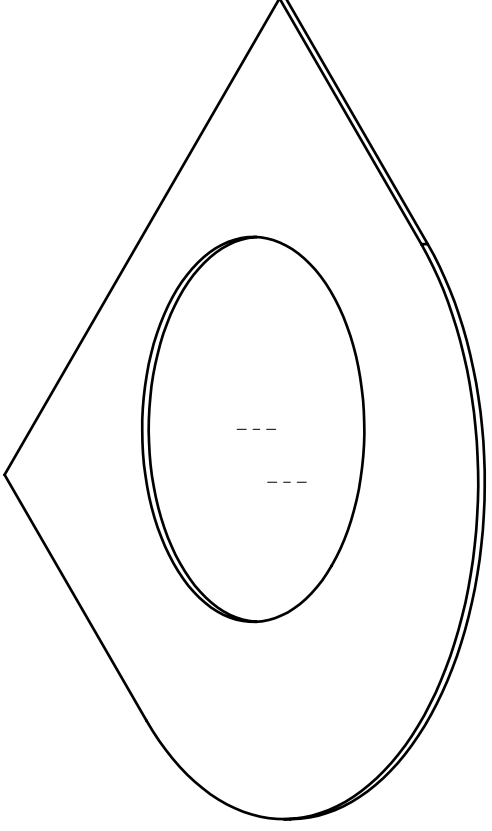
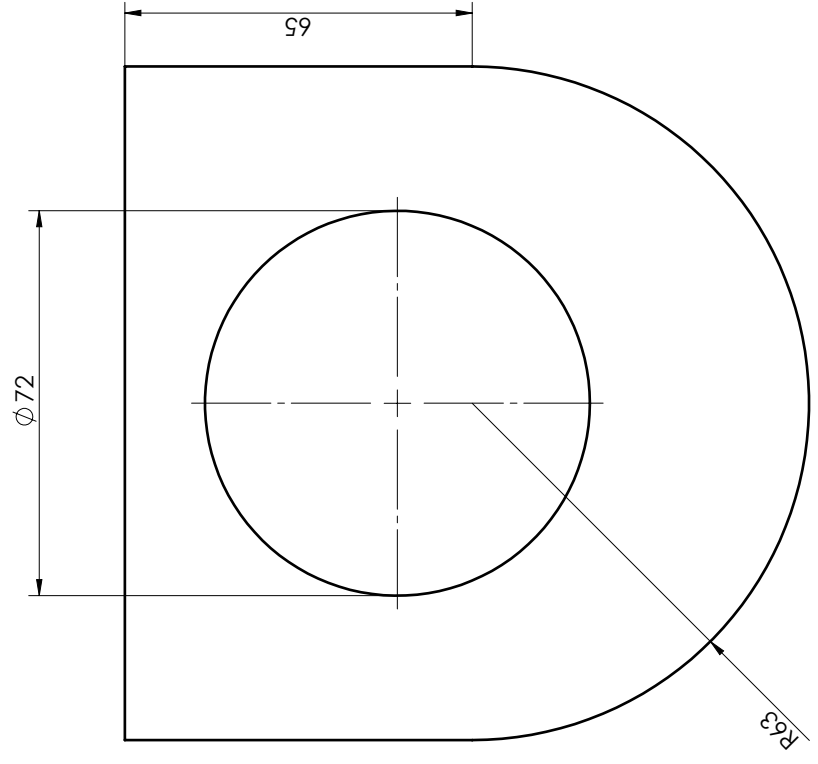
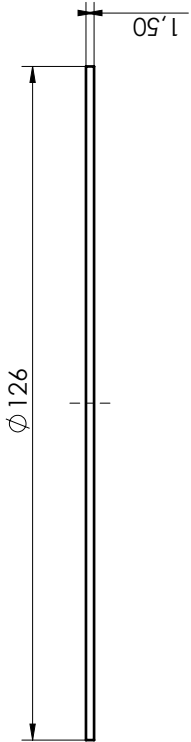
Dato: 05.04.16	Konstr./Tegnet: M.A.	Projeksjon:	Målestokk: 1:1	NMBU	
Thorvald II			Erstatning for: Erstatlet av:		
Wallbrack			Ås VGS		
Henvisning: Skal også lages med speilvendt knekk			Beregning:		



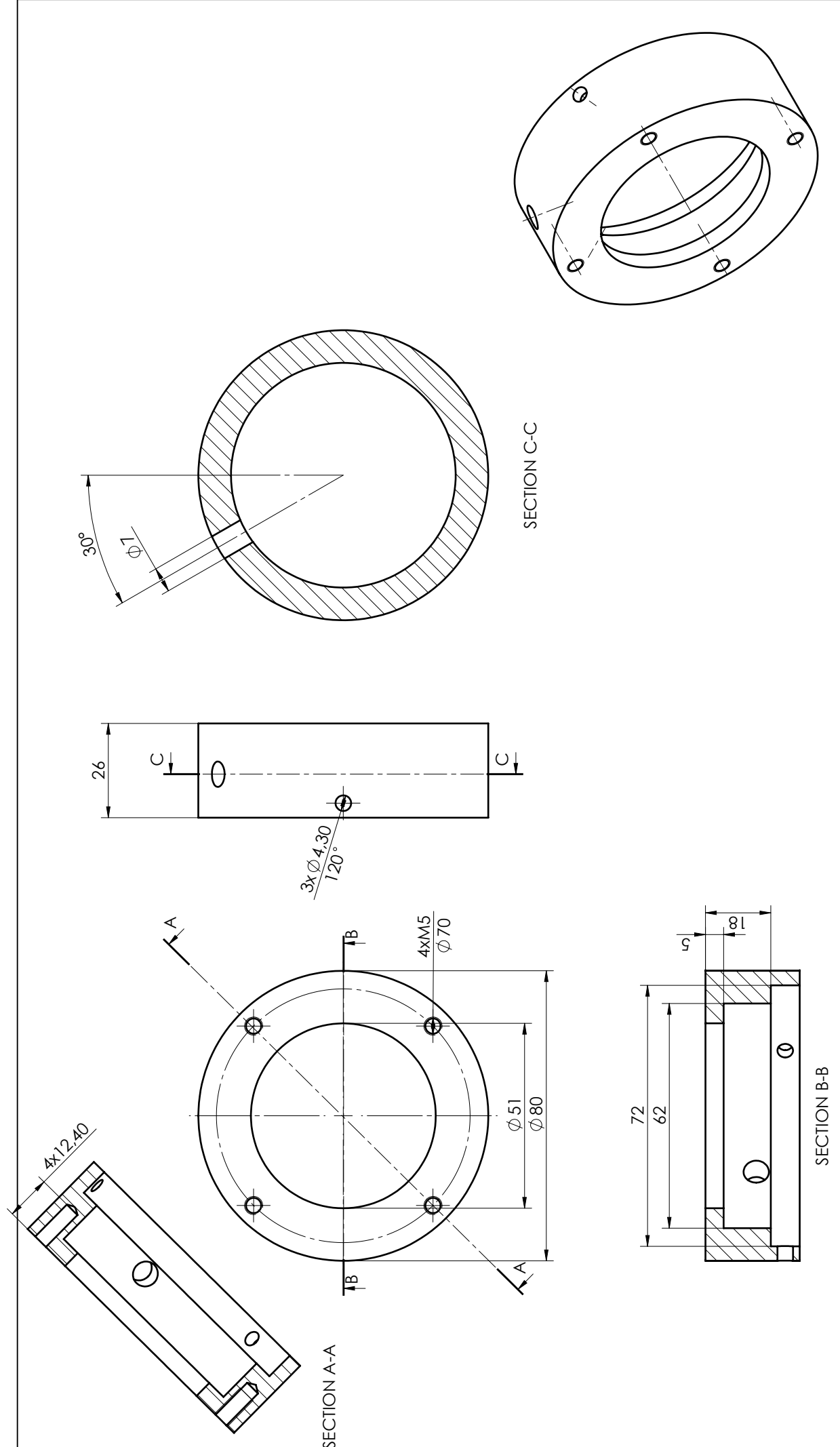
Dato: 12.05.16	Konstr./Tegnet: M.A.	Projeksjon: 	Målestokk: 1:1	NMBU	
Henvising:			Erstatlet av:		
Thovald II			A1		
Brack			Beregning:		



Dato: 20.04.16	Konstr./Tegnet: M.A.	Projeksjon: 	Målestokk: 1:1	NMBU	
Toleranse: ISO 2768-1 - medium				Erstatning for: Erstattelet av:	
Thorvald II		bottomCyl		A1	
Henviising:		Beregning:			

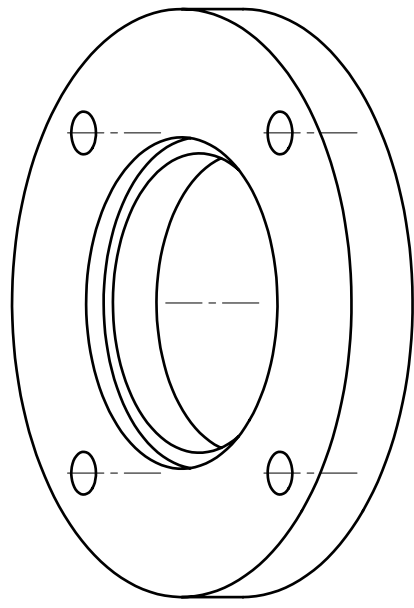
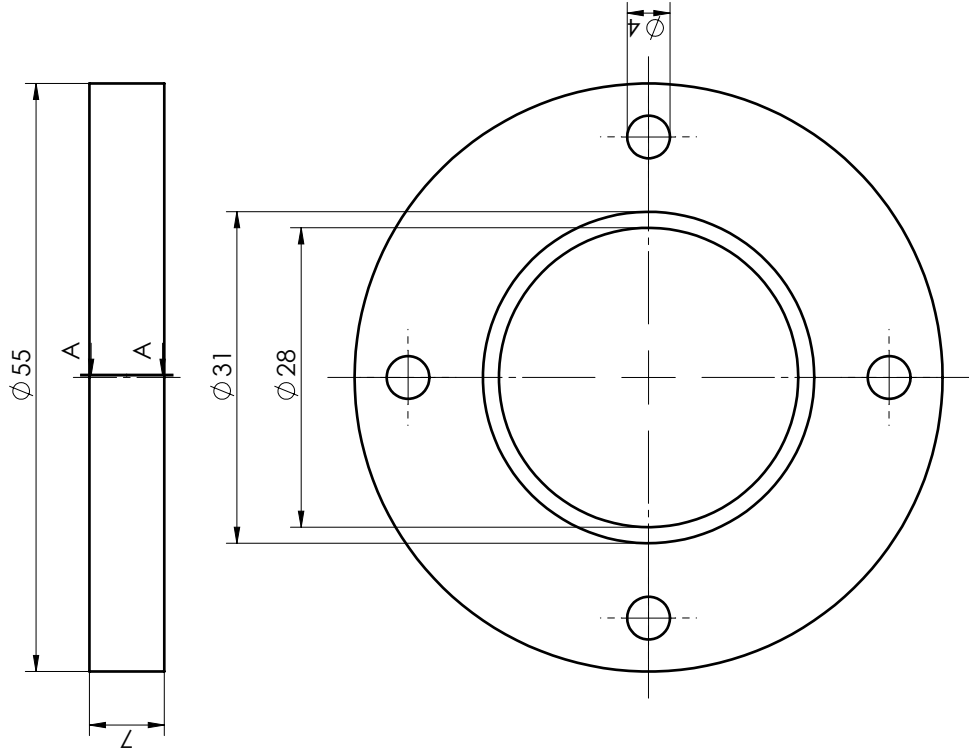
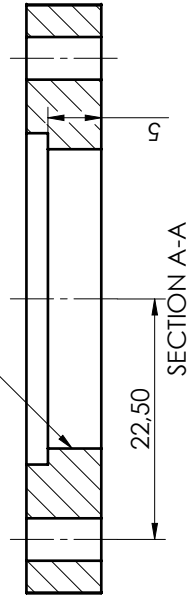


Dato: 20.04.16	Konstr./Tegnet: M.A.	Projeksjon:	Målestokk: 1:1	NMBU	
Toleranse: ISO 2768-1 - medium				Erstatning for: Erstatlet av:	
Thorvald II			A1		
bottomPlate					
Henvisning:			Beregning:		

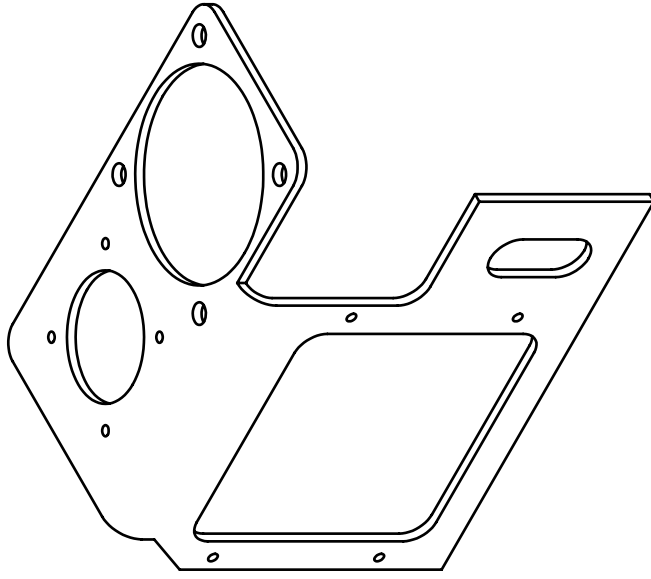
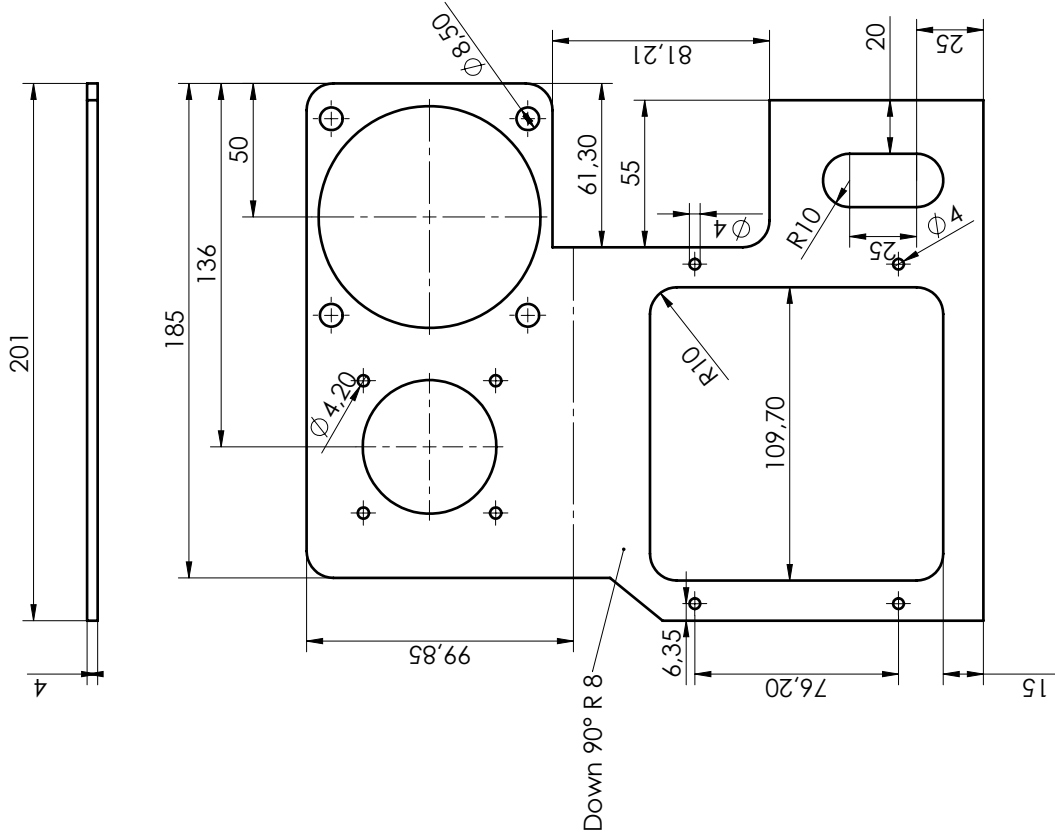


Dato: 01.05.16	Konstr./Tegnet: M.A.	Projeksjon:	Målestokk: 1:1	NMBU
Toleranse: ISO 2768-1 - m medium			Erstatning for: Erstatlet av:	
Thorvald II KulelagerTopp				B1
				Henviing:

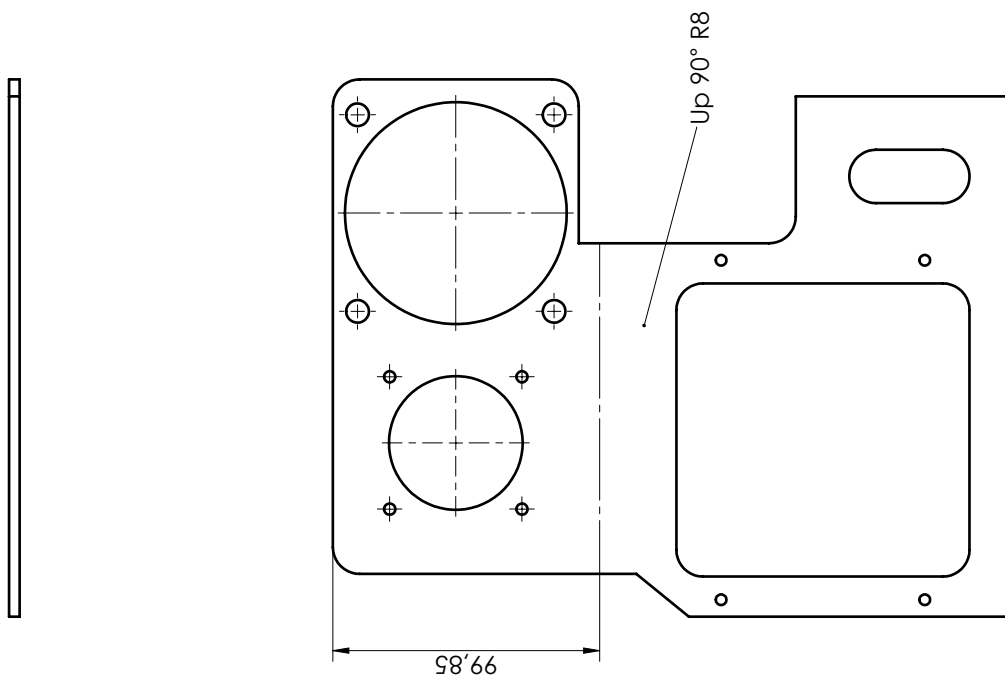
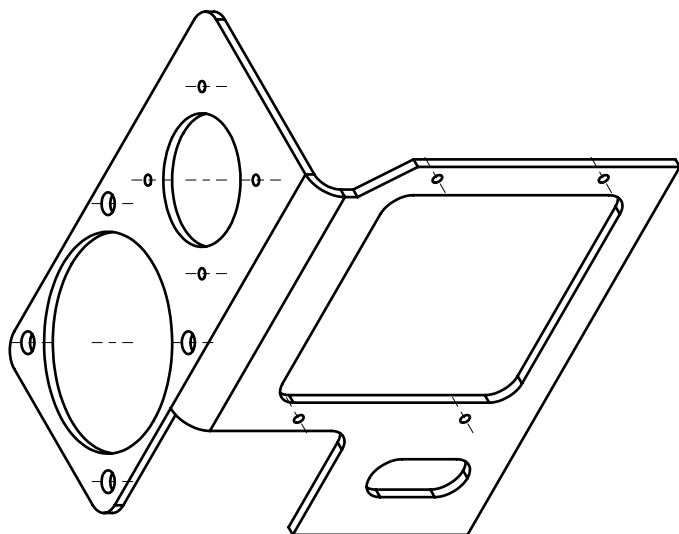
Gjenges til å passe styringsaksel




Dato: 27.04.16	Konstr./Tegnet: M.A.	Projeksjon:	Målestokk: 2:1	NMBU	
Toleranse: ISO 2768-1 - mellom				Erstatning for: Erstatlet av:	
Thorvald II				A1	
Lagermutter					
Henvising:			Beregning:		

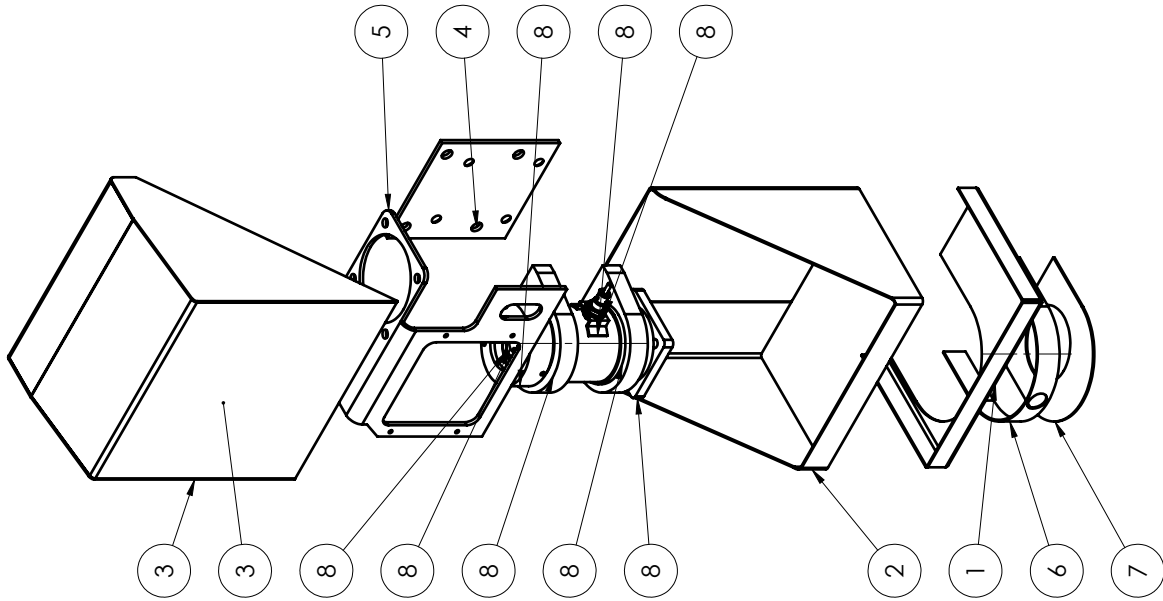


Dato: 27.04.16	Konstr./Tegnet: M.A.	Projeksjon:	Målestokk: 1:2	NMBU
Toleranse: ISO 2768-1 - medium		Erstatning for: Erstatlet av:		
Thorvald II		A1		
motorBrack		Beregning:		
Henvising:				



Identisk til MotorBrackA1, med knekk motsatt vei.

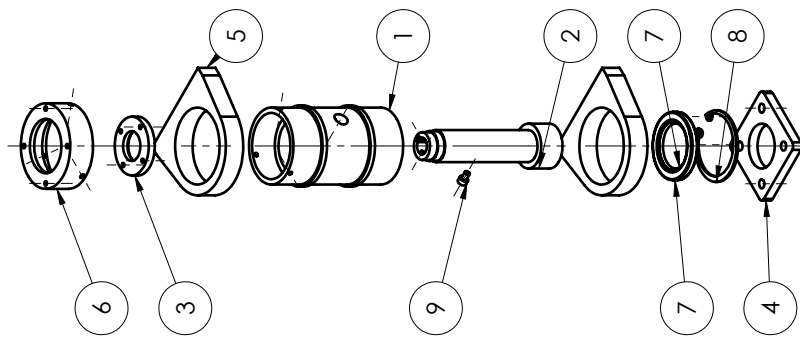
Dato: 01.05.16	Konstr./Tegnet: M.A.	Projeksjon: 	Målestokk: 1:1	NMBU
Toleranse: ISO 2768-1 - medium		Erstatning for: Erstatlet av:		
Thorvald II		A1		
motorBrackMirror				
Henviising:		Beregning:		



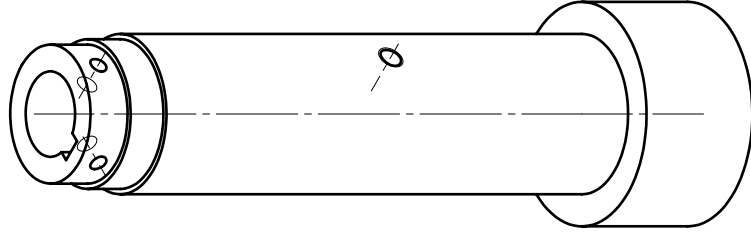
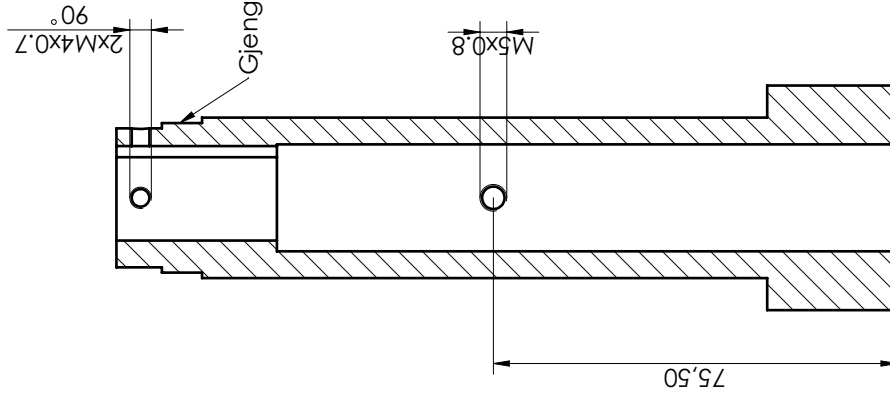
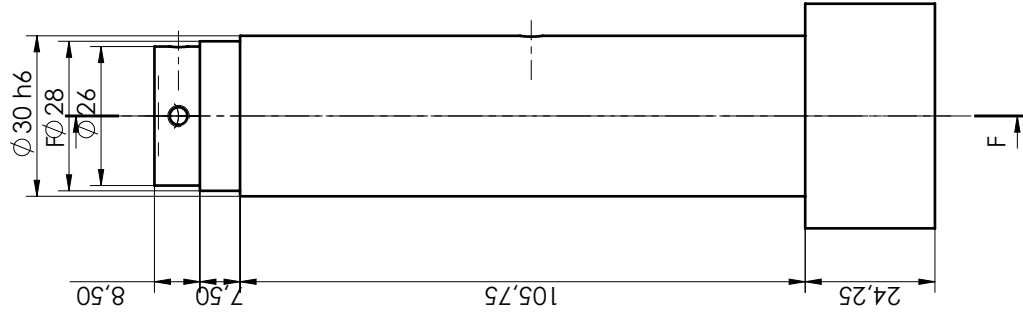
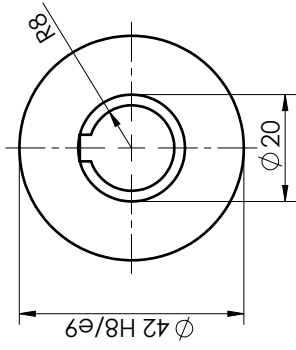
8	1	kulelagerhusAssembly			
7	1	BottomPLate			
6	1	bottomCyl			
5	1	motorBrack			
4	1	towerWall			
3	1	towerCoverBend and Side			
2	1	towerCoverLower			
1	1	towerCoverBottom			
Pos.	Clean/QTY.	Tittel/benevning/dim.	Materiale	Vekt	Art. nr./ref.

Dato:	01.05.16	Konstr./Tegnet:	M.A.	Projeksjon:	
Målestokk:	1:5				

Thorvald II		Erstatning for:	NMBU
Sammenstilling Tower		Erstatlet av:	A1
Henvising:		Beregning:	

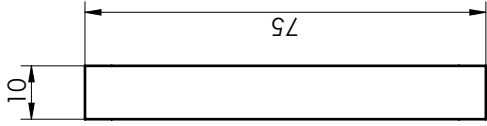
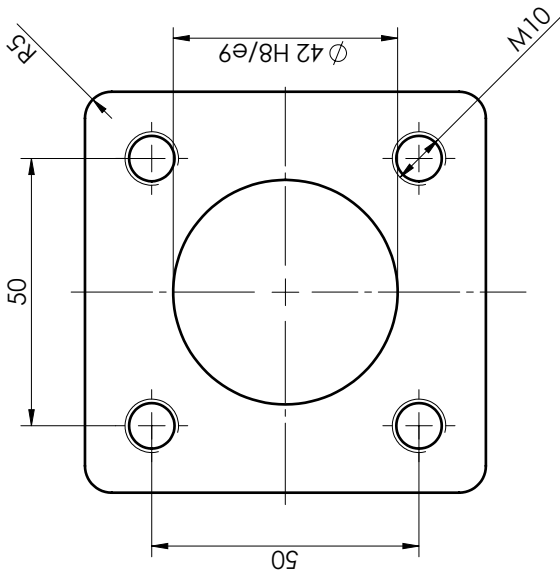


9	1	ISO 4762 M5 x 8 --- 8N			
8	1	Segerring_DIN472			
7	1	WDR_tetning			
6	1	kulelagerTopp			
5	2	weldRing			
4	1	Styringsaksel flens			
3	1	lagermutter			
2	1	styreaksling			
1	1	lagerhus			
Pos., Ant.	Tittel/benevning/dim.		Materiale	Vekt	Art. nr./ref.
Dato: 01.05.16		Konstr./Tegnet: M.A.	Målestokk: 1:5	NMBU	
		Projeksjon:			
Thorvald II			Erstatning for: Erstatlet av:		
Sammenstilling lagerhus			A1		
Henvising:			Beregning:		

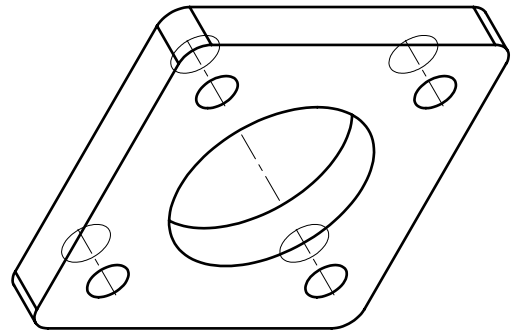


Dato: 01.05.16	Konstr./Tegnet: M.A.	Projeksjon:	Målestokk: 1:1	NMBU
Toleranse: ISO 2768-1 - medium				
Thorvald II				Erstatning for: Erstatning av:
Styringsaksel				A2
Henvising:				Beregning:

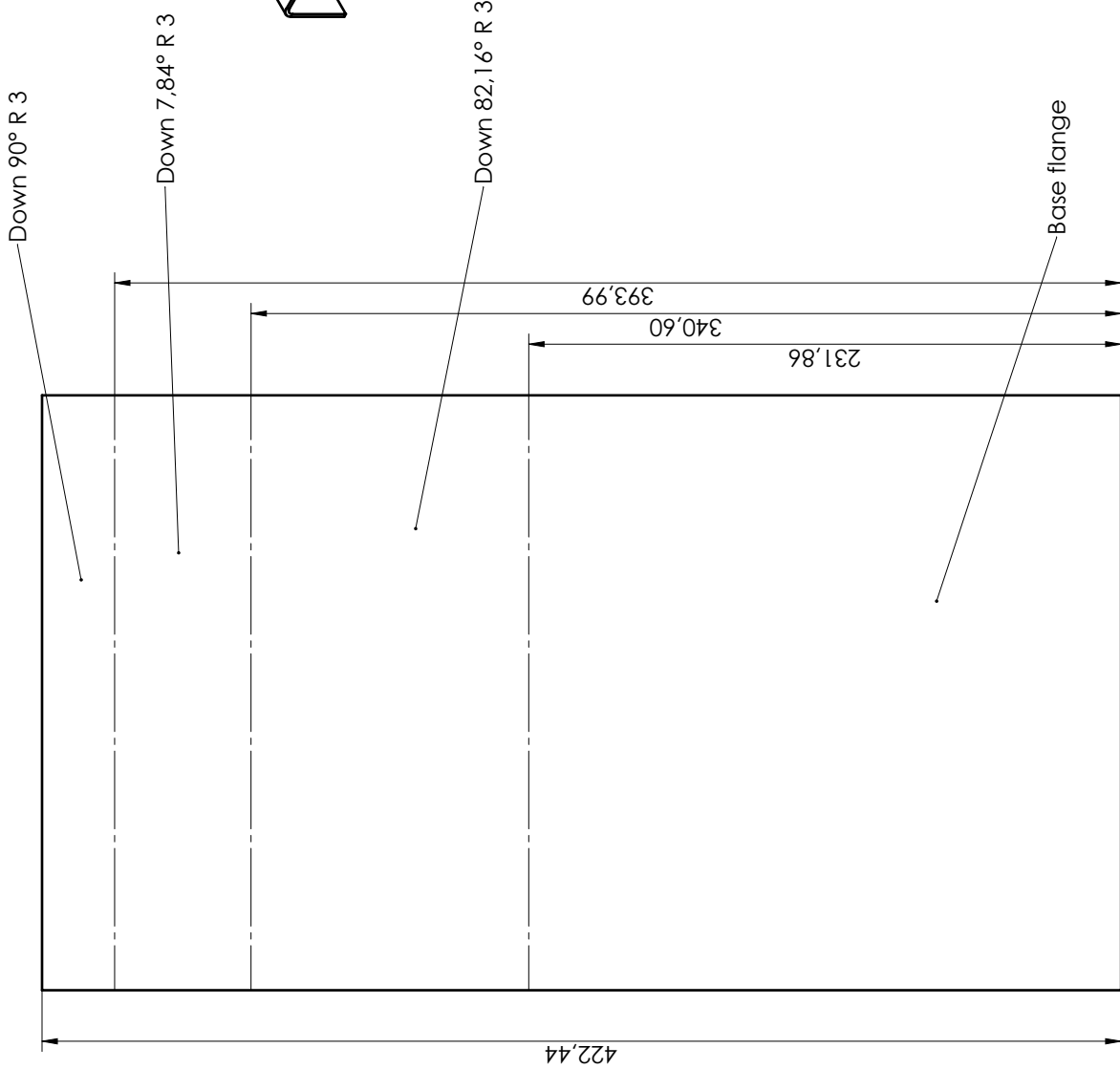
SECTION F-F
SCALE 1:1



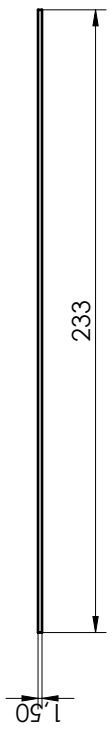
Toleranse: ISO 2768-1 - medium

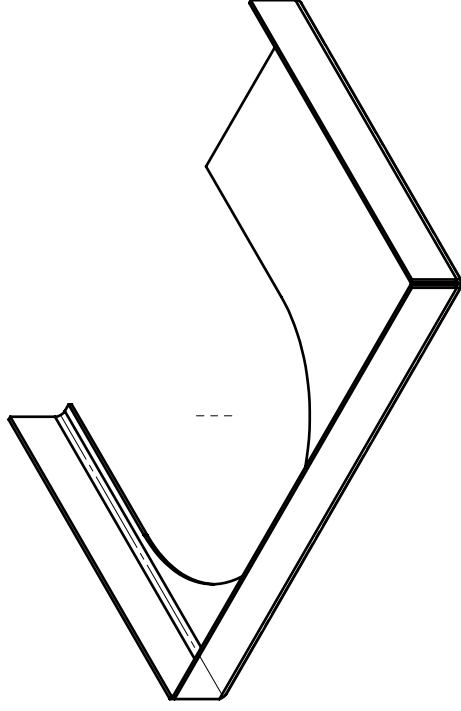
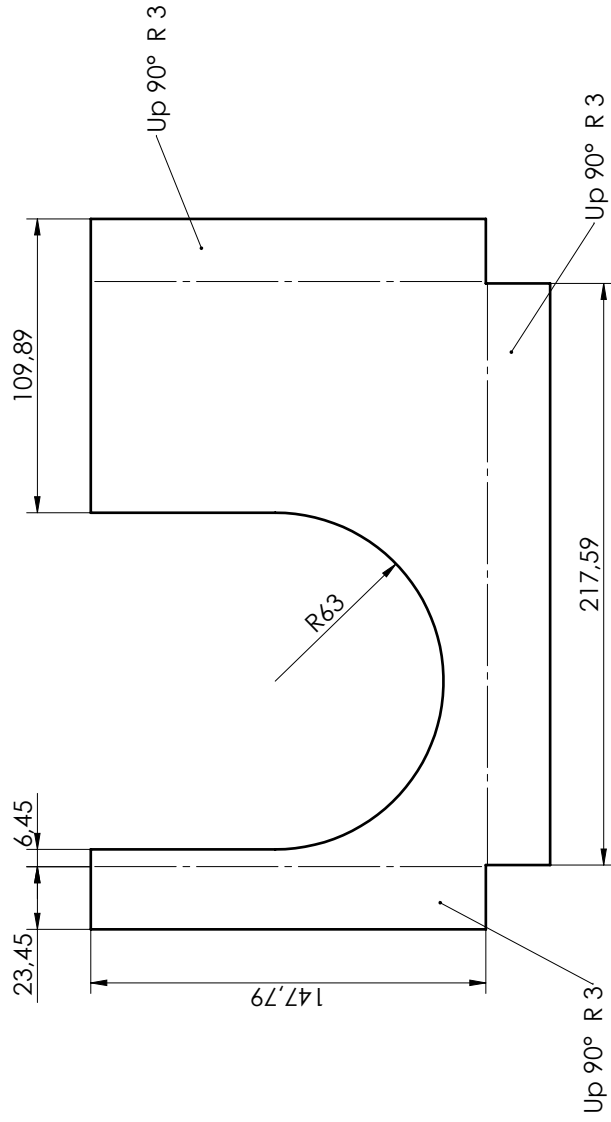
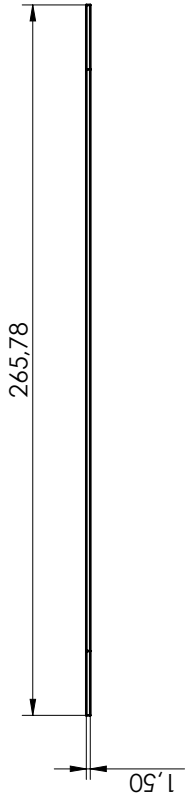


Dato: 20.04.16	Konstr./Tegnet: M.A.	Projeksjon:	Målestokk: 1:1	NMBU
Toleranse: ISO 2768-1 - medium			Erstatning for: Erstatning av:	
Thorvald II				A1
Styringsaksel - flens				
Henvising:				Beregning:

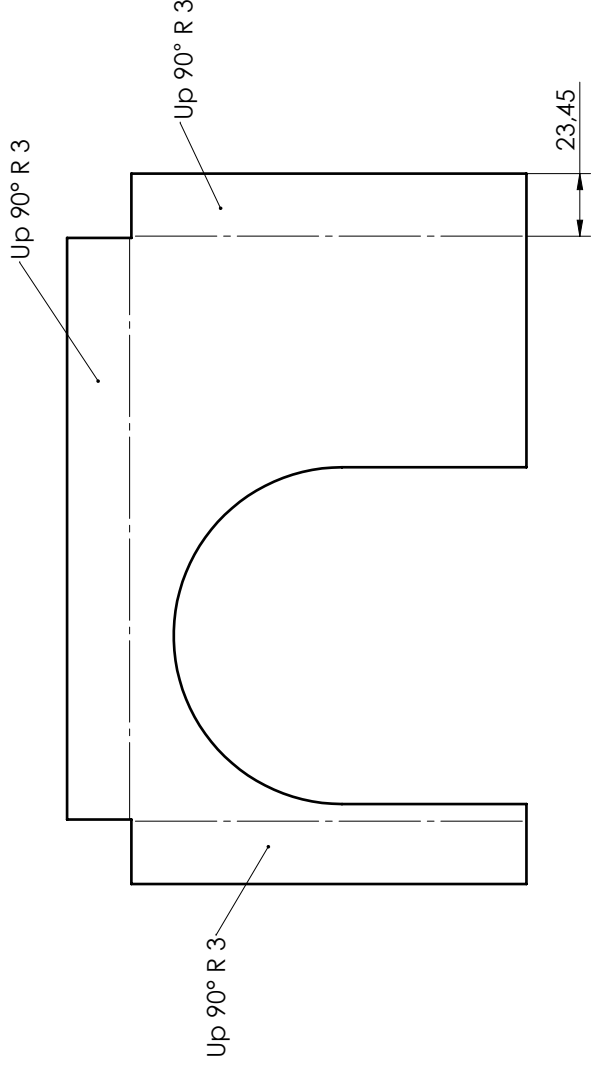
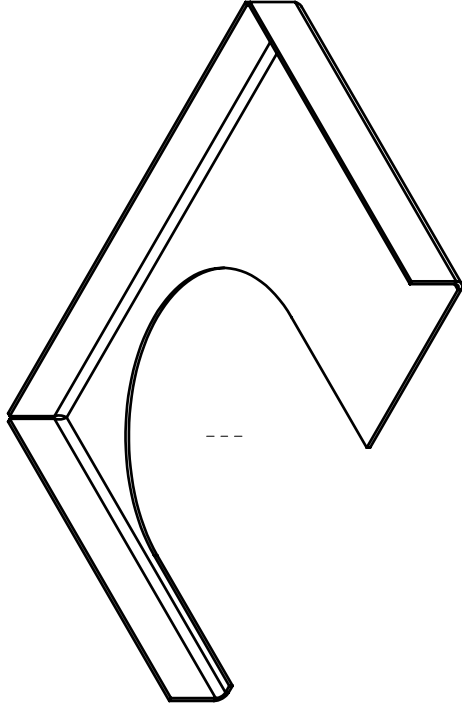


Dato: 27.04.16	Konstr./Tegnet: M.A.	Projeksjon:	Målestokk: 1:2	NMBU
Toleranse: ISO 2768-1 - medium			Erstatning for: Erstatlet av:	A1
Thorvald II towerCoverBend				
Henvising:				Beregning:



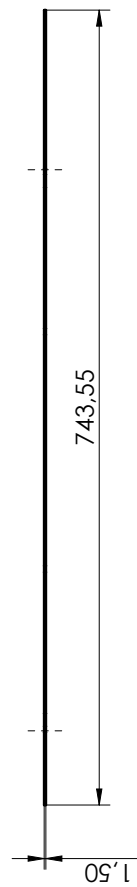
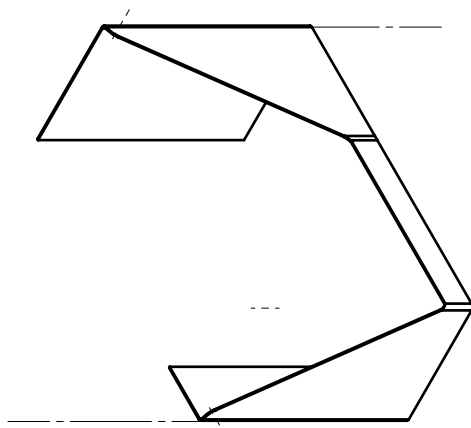
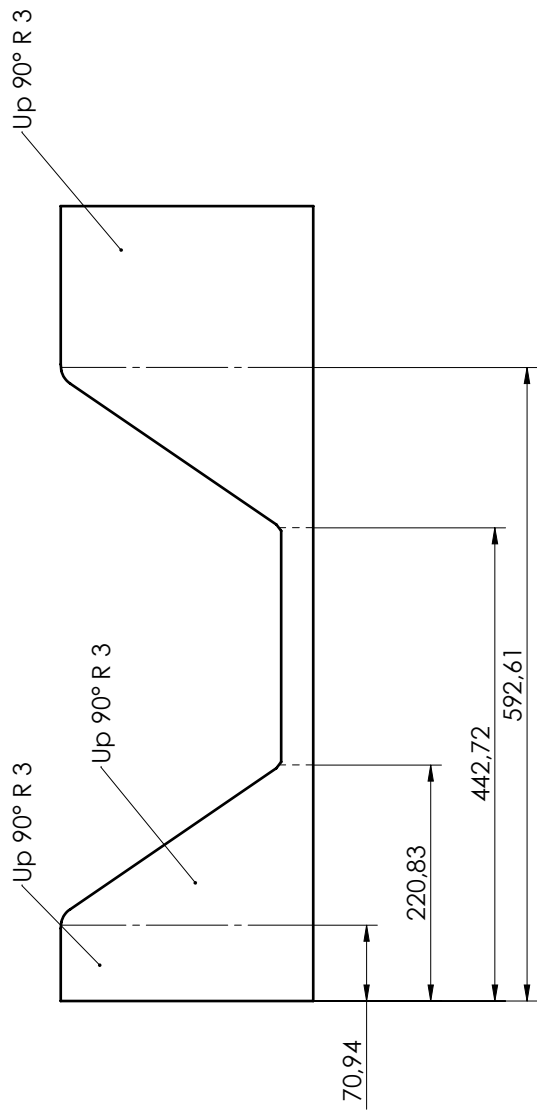



Dato: 27.04.16	Konstr./Tegnet: M.A.	Projeksjon:	Målestokk: 1:2	NMBU
Toleranse: ISO 2768-1 - m medium				
Thorvald II				Erstatning for: Erstatlet av:
towerCoverBottom				A1
Henvisning:			Beregning:	

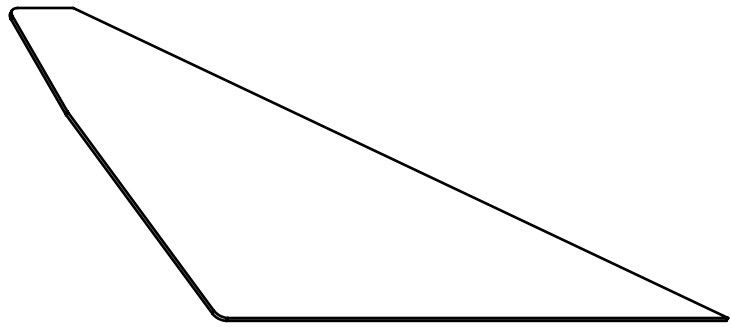
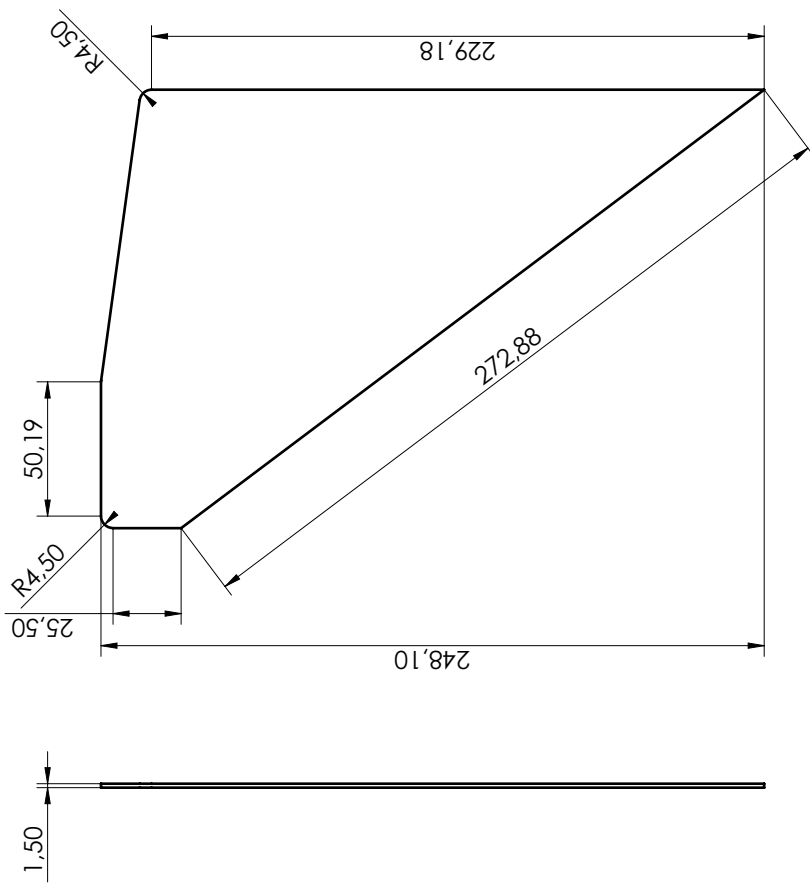


Identisk til towerCoverBottomA1 med knekk motsatt vei

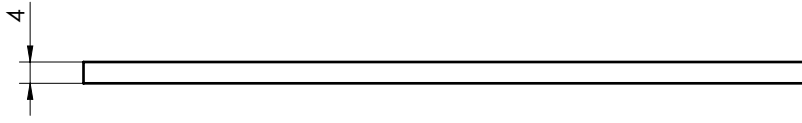
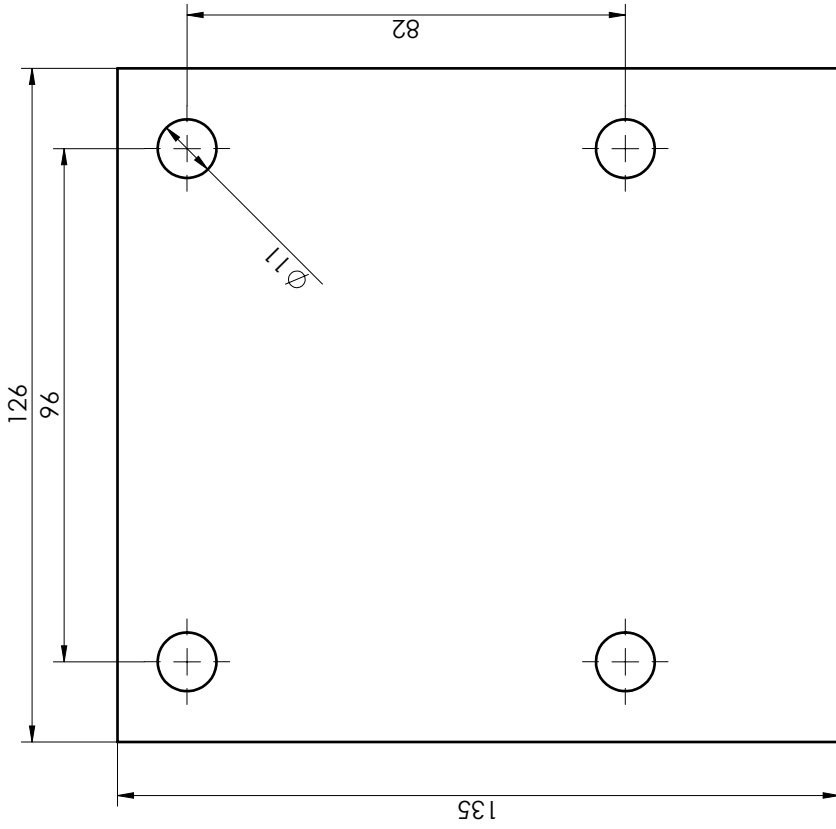
Dato: 01.05.16	Konstr./Tegnet: M.A.	Projeksjon:	Målestokk: 1:1	NMBU
Toleranse: ISO 2768-1 - medium			Erstatning for:	Erstatning av:
Thorvald II			A1	
towerCoverBottomMirror				
Henvisning:			Beregning:	



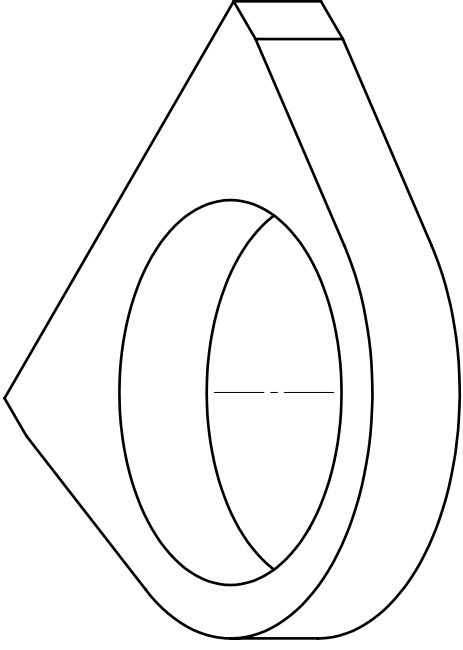
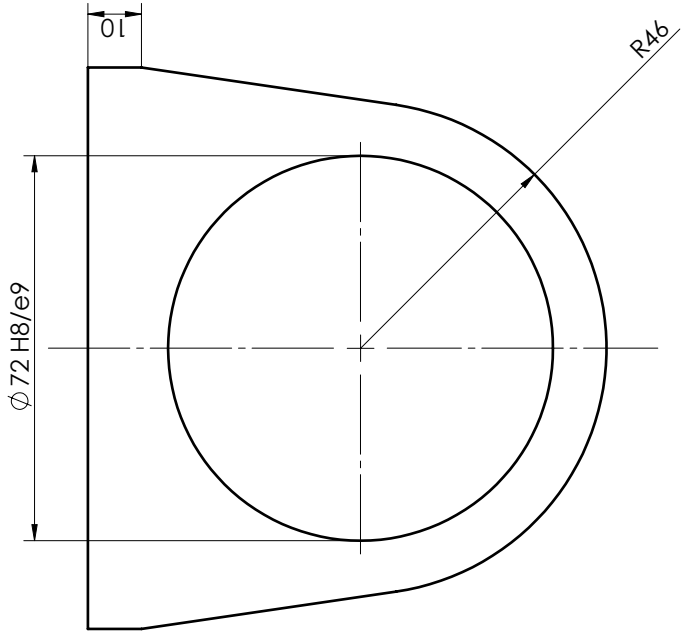
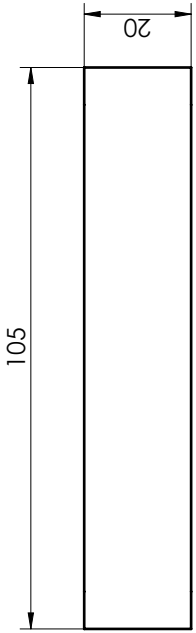
Dato: 27.04.16	Konstr./Tegnet: M.A.	Projeksjon: 	Målestokk: 1:5	NMMBU
Toleranse: ISO 2768-1 - mEDIUM		Erstatning for: Erstatlet av:		
Thorvald II		A1		
towerCoverLower		Beregning:		
Henviing:				



Dato: 27.04.16	Konstr./Tegnet: M.A.	Projeksjon:	Målestokk: 1:2	NMBU
Toleranse: ISO 2768-1 - medium		Erstatning for: Erstatlet av:		
Thorvald II		A1		
towerCoverSide		Beregning:		
Henviing:				



Dato: 27.04.16	Konstr./Tegnet: M.A.	Projeksjon:	Målestokk: 1:1	NMBU
Toleranse: ISO 2768-1 - medium				
Thorvald II towerWall				A1
Henvising:			Beregning:	



Dato: 20.04.16	Konstr./Tegnet: M.A.	Projeksjon:	Målestokk: 1:1	NMBU	
Toleranse: ISO 2768-1 - medium				Erstatning for: Erstatlet av:	
Thorvald II				A1	
weldRing					
Henvising:			Beregning:		



Norges miljø- og
biovitenskapelige
universitet

Postboks 5003
NO-1432 Ås
67 23 00 00
www.nmbu.no